



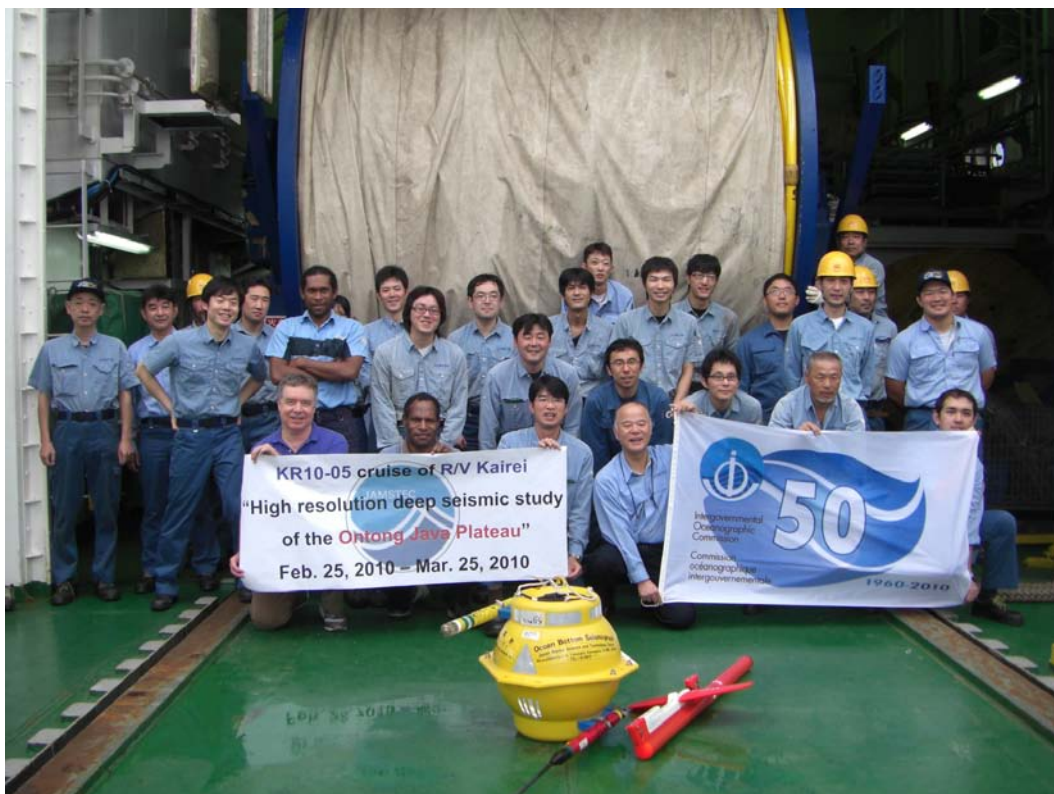
Cruise Report

R/V Kairei KR10-05

High resolution deep seismic study

of the Ontong Java Plateau

Feb. 25, 2010 – Mar. 26, 2010



Japan Agency for Marine-Earth Science and Technology

(JAMSTEC)

Shipboard science party contact details

Dr. Seiichi Miura

Institute for Research on Earth Evolution (IFREE)

Japan Agency for Marine-Earth Science and Technology (JAMSTEC)

Mr. Naoto Noguchi

Institute for Research on Earth Evolution (IFREE)

Japan Agency for Marine-Earth Science and Technology (JAMSTEC)

Prof. Millard F. Coffin

National Oceanography Center, Southampton

University of Southampton Waterfront Campus

Mr. Simon A. Kawagle

Division of Geoscience

University of Papua New Guinea

Mr. Ronald T. Verave
Geophysical Mapping Branch
Mineral Resources Authority

Marine Technician List

Masayuki Toizumi	Nippon Marine Enterprises,Ltd.	Chief Marine Technician
Kaoru Tsukuda	Nippon Marine Enterprises,Ltd.	Marine Technician
Yuki Ohwatari	Nippon Marine Enterprises,Ltd.	Marine Technician
Morifumi Takaesu	Nippon Marine Enterprises,Ltd.	Marine Technician
Yuta Watarai	Nippon Marine Enterprises,Ltd.	Marine Technician
Takuya Maekawa	Nippon Marine Enterprises,Ltd.	Marine Technician
Mitsuteru Kuno	Nippon Marine Enterprises,Ltd.	Marine Technician
Ryo Miura	Nippon Marine Enterprises,Ltd.	Marine Technician
Atsushi Isogai	Nippon Marine Enterprises,Ltd.	Marine Technician
Kyoko Tanaka	Nippon Marine Enterprises,Ltd.	Marine Technician
Taro Shirai	Nippon Marine Enterprises,Ltd.	Marine Technician

R/V *Kairei* Crew List

職名	氏名	Position	NAME
船長	田中 等	Captain	TANAKA HITOSHI
一航士	木村 直人	Chief Officer	KIMURA NAOTO
二航士	足立 龍生	2nd Officer	ADACHI TATSUO
三航士	山口 諒	3rd Officer	YAMAGUCHI RYO
次三航士	高田 宰人	Jr. 3rd Officer	TAKATA SAITO
機関長	梶西喜代徳	Chief Engineer	KAJINISHI KIYONORI
一機士	大田 隆志	1st Engineer	OTA TAKASHI
二機士	加藤 兼三	2nd Engineer	KATO KENZO
三機士	山口 雄治	3rd Engineer	YAMAGUCHI KATSUTO
電子長	高橋 正始	Chief Electronics Operator	TAKAHASHI MASAMOTO
二電士	伊藤 英洋	2nd Electronics Operator	ITO HIDEHIRO
三電士	幡 三沙都	3rd Electronics Operator	HATA MISATO
甲板長	久木 康吉	Boatswain	KYUKI YASUYOSHI
甲板手	河村 好昭	Able Seaman	KAWAMURA YOSHIAKI
甲板手	久保田隆夫	Able Seaman	KUBOTA TAKAO
甲板手	大端 正則	Able Seaman	OHATA MASANORI
甲板手	村田 海人	Able Seaman	MURATA KAITO
甲板員	中田 秀明	Sailor	NAKATA HIDEAKI
甲板員	三浦 俊	Sailor	MIURA SHUN
操機長	北野 勝	No.1 Oiler	KITANO MASARU
操機手	橋本 知幸	Oiler	HASHIMOTO TOMOYUKI
操機手	東川 雄二	Oiler	HIGASHIGAWA YUJI
機関員	植木 史博	Assistant Oiler	UEKI FUMIHIRO
機関員	中原 祐貴	Assistant Oiler	NAKAHARA YUKI
司厨長	松本 勇夫	Chief Steward	MATSUMOTO ISAO
司厨手	竹村 龍栄	Steward	TAKEMURA RYUEI
司厨手	和田 透	Steward	WADA TORU
司厨手	久保田秀樹	Steward	KUBOTA HIDEKI
司厨員	中野 瑞紀	Steward	NAKANO MIZUKI

Project proponents

Name of lead proponent: Dr. Yoshio Fukao

Institution: Japan Agency for Marine-Earth Science and Technology

Department/Position: Institute for Research Earth Evolution/Program Director

Research team of JAMSTEC

Name	Institution	Position	Task
Yoshio Fukao	JAMSTEC	Program Director	Project Leader
Yoshiyuki Tatsumi	JAMSTEC	Program Director	Vice Project Leader
Shuichi Kodaira	JAMSTEC	Group Leader	Lithosphere structure imaging
Daisuke Suetsugu	JAMSTEC	Group Leader	Deep mantle structure imaging
Naohiko Ohkouchi	JAMSTEC	Group Leader	Paleoenvironmental Study
Katsuhiko Suzuki	JAMSTEC	Group Leader	Isotopic Geochemical Study
Narumi Takahashi	JAMSTEC	Sub Group Leader	Lithosphere structure imaging
Ayako Nakanishi	JAMSTEC	Scientist	Lithosphere structure imaging
Koichiro Obana	JAMSTEC	Scientist	Lithosphere structure imaging
Yuka Kaiho	JAMSTEC	Principal Technical Scientist	Lithosphere structure imaging
Seiichi Miura	JAMSTEC	Technical Scientist	Lithosphere structure imaging
Gou Fujie	JAMSTEC	Technical Scientist	Lithosphere structure imaging
Tetsuo No	JAMSTEC	Technical Scientist	Lithosphere structure imaging
Takeshi Sato	JAMSTEC	Technical Scientist	Lithosphere structure imaging
Mikiya Yamashita	JAMSTEC	Technical Scientist	Lithosphere structure imaging
Kaoru Takizawa	JAMSTEC	Technical Scientist	Lithosphere structure imaging
Tsutomu Takahashi	JAMSTEC	Postdoctoral Scientist	Lithosphere structure imaging
Hiroko Sugioka	JAMSTEC	Senior Technical Scientist	Deep mantle structure imaging
Kenji Shimizu	JAMSTEC	Scientist	Petrological Study
Jun-ichiro Kuroda	JAMSTEC	Scientist	Paleoenvironmental Study
Takatoshi Yanagisawa	JAMSTEC	Scientist	Mantle Dynamics

Acknowledgments

Mar. 25, 2010

To Captain Hitoshi Tanaka,

We are deeply grateful to you and your excellent crew of C/O Naoto Kimura, C/E Kiyonori Kajinishi, 1/E Takashi Ota, C/EO Masamoto Takahashi, C/S Isao Matsumoto, and the rest of the officers and crew, as well as Chief Masayuki Toizumi and the rest of the skilled Marine Technician team, for your powerful contributions to the success of this cruise that has provided fruitful new data. We fully appreciate having had this precious opportunity. All of us would like to sail with you again in the future.

Sincerely yours,

Dr. Seiichi Miura

Mr. Naoto Noguchi

Institute for Research on Earth Evolution

Japan Agency for Marine-Earth and Technology

三浦 誠一
野口 直人

Prof. Millard F. Coffin

National Oceanography Center, Southampton

University of Southampton and Natural Environmental Research Council

United Kingdom

Will Coffin

Mr. Simon A. Kawagle

Division of Geoscience

University of Papua New Guinea

Papua New Guinea

Simon A. Kawagle

Mr. Ronald T. Verave

Geophysical Mapping Branch

Mineral Resource Authority, PNG

Papua New Guinea

Ronald T. Verave

Ship track of this cruise

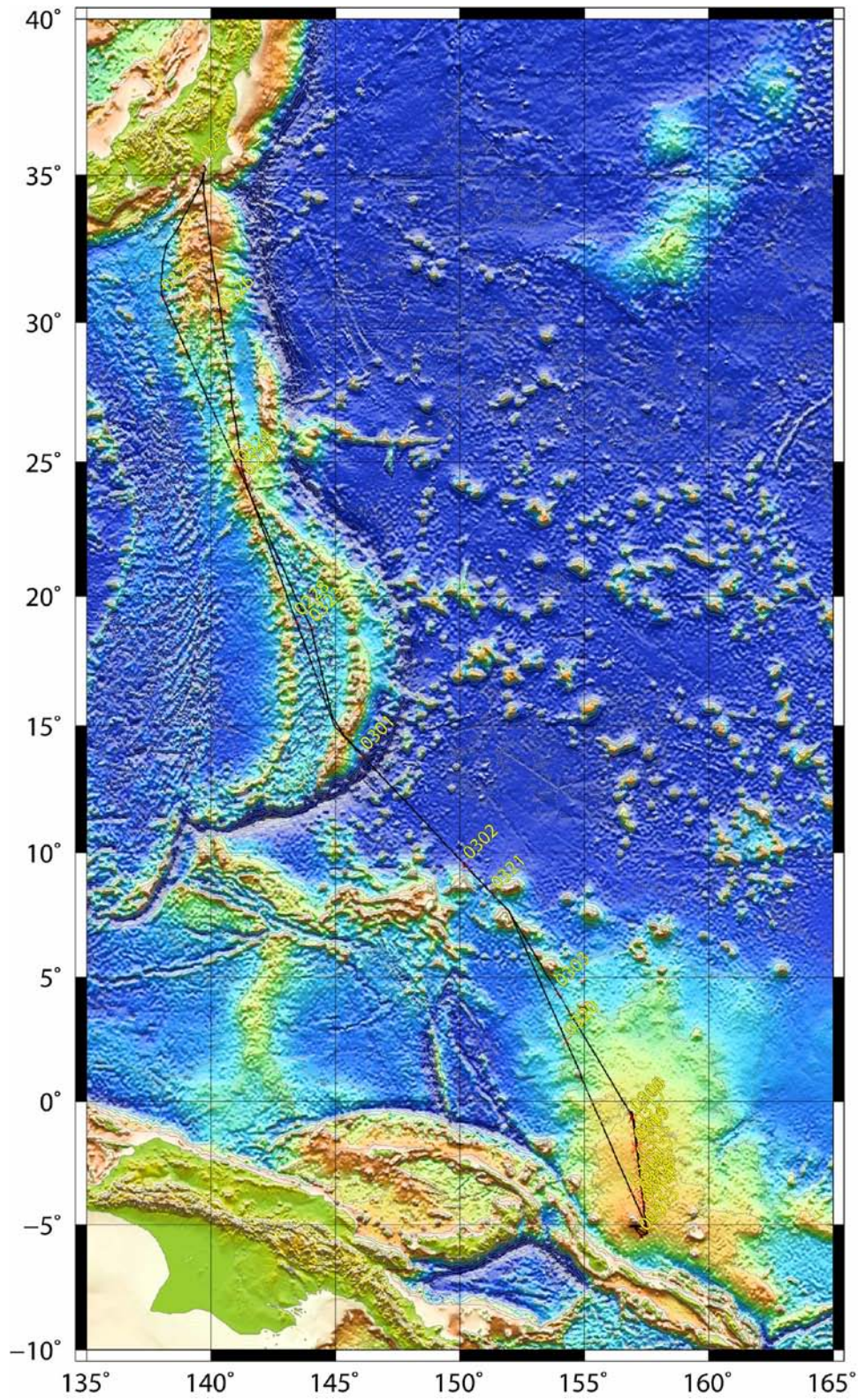


Table of Contents

Shipboard science party contact details	i
Marine Technician List	iii
R/V <i>Kairei</i> Crew List	iv
Project proponents	v
Acknowledgements	vi
Ship track	vii
Table of Contents	viii
Executive Summary	1
Objectives and geological background	2
Outline of research cruise	6
Cruise narrative	9
Crustal structure of the Ontong Java Plateau (OJP)	15
Life at the Edge: Super Eruptions cause Earth Crises	20
The Geological Framework of Papua New Guinea (abstract)	21
Airgun array	22
Multichannel Seismic Reflection (MCS) system	24
Ocean Bottom Seismographs (OBS)	31

Global Positioning System (GPS)	37
SeaBeam	42
Shipboard Three-Component Magnetometer	48
Gravity meter	52
Expendable Bathythermographs (XBT)	55
Notice on use	56
Appendix: The Geological Framework of Papua New Guinea: an overview	

Executive Summary

This cruise was aimed at acquiring seismic data, including wide-angle reflection and refraction using ocean bottom seismometers (OBS), near-vertical reflection using multi-channel reflection seismic (MCS), as well as geophysical - gravity, magnetic and bathymetry - data, to understand the origin of the Ontong Java Plateau (OJP). A NNW-SSE seismic line 600 km long was run on the main OJP. During the cruise, 100 OBSs were deployed every 5 km along the seismic line, and a large volume airgun array was fired at 200 m (from SSE to NNW) and 50 m (from NNW to SSE) intervals for primarily OBS and MCS data, respectively, although data were recorded by all systems in both directions. This cruise is the first dense OBS survey on the OJP. The fully interpreted should contribute to understanding the origin of the OJP. Moreover, scientific insights gained and the data acquired during this cruise support the Integrated Ocean Drilling Program (IODP) drilling proposal addressing the origin of the OJP (IODP proposal 623).

Objectives and geological background

The primary objective of the Ontong Java Plateau (OJP) seismic study is to test hypotheses for the origin of the OJP, i.e., plume, bolide impact, or plate tectonic, on the basis of crust and uppermost mantle structure imaged by seismic refraction and reflection data.

The Early Cretaceous Ontong Java Plateau and neighboring ocean basin flood basalts in the western Pacific constitute the most voluminous Large Igneous Province (LIP) on Earth. OJP-related volcanism may have repaved as much as 1% of Earth's surface. Since the late 1980s, the predominant hypothesis for the origin of LIPs has been the plume head model. The OJP is the largest documented flood basalt province, covering an area (including flood basalts in the Nauru, East Mariana, and possibly Pigafetta Basins) of $>4 \times 10^6$ km², about half the size of the contiguous USA, and a maximum crustal thickness of more than 30 km. Despite its size, several key characteristics expected from a plume head origin are not present in the case of the OJP. However, while alternatives to plume head models for the OJP are receiving increased attention, they cannot be evaluated adequately with existing samples and data. Three general hypotheses for OJP formation are addressed here: (i) surfacing plume head, (ii) large bolide impact, and (iii) eclogite-rich upper mantle beneath a superfast spreading ridge.

Surfacing Plume Head: Surfacing of a bulbous head from a new mantle plume ascending from deep in the mantle can (theoretically) produce the huge volumes of melt required to generate a flood basalt province in 1-5 Myr. The lithosphere may be thinned by thermal or mechanical erosion from the plume, and/or by external plate stresses. Following the plume head stage, melting is theorized to continue at much reduced rates in a narrow "tail"; in oceanic areas, prolonged plume-tail volcanism is postulated to produce major island and seamount chains. Most models of plume formation predict lower mantle-derived plume heads to be well mixed, entraining relatively little non-plume mantle during their ascent, and to produce magmas significantly more homogeneous than those from plume tails. This is consistent with the isotopic and incompatible-element homogeneity of the voluminous Kwaimbaita magma type and the distribution of this magma type across the plateau and surrounding basins. The ocean-island-like isotopic signature, the evidence for high-degree partial melting, and the apparently rapid formation of most of the OJP are also consistent with predictions of this type of model. However, significant discrepancies exist between observations and

model that include lack of significant uplift during emplacement, lack of significant post-eruptive subsidence, lack of any associated post-plateau seamount chain, an anomalous mantle root, and basalt timing and composition.

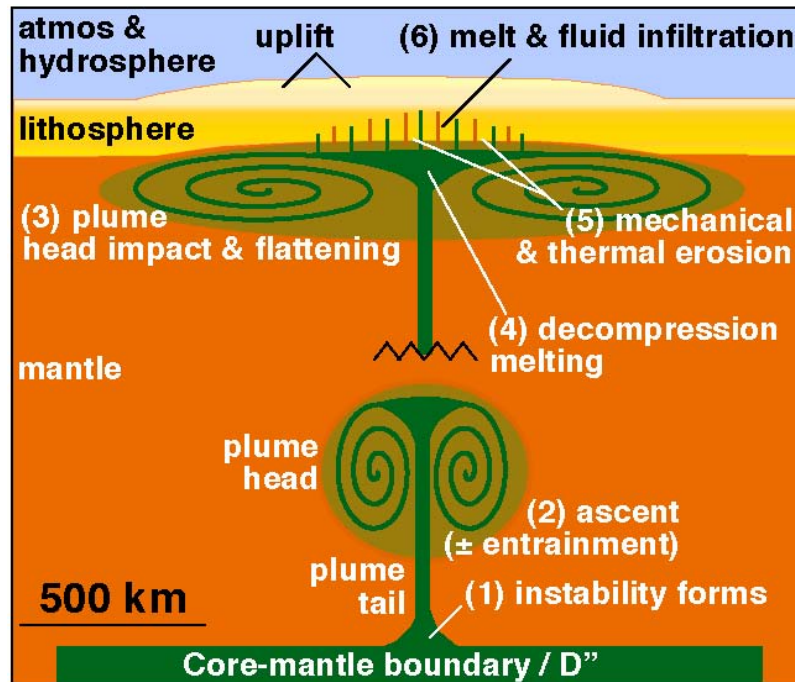


Fig. 1 Surfacing plume head model

Bolide impact: This model proposes that very large impacting bolide penetrates and destroys the entire lithosphere and uppermost asthenosphere in the vicinity of the impact. Instantaneous decompression of the upper mantle causes large-scale melting and regional physical-chemical changes in the upper mantle, the former resulting in formation of the OJP and perhaps accounting for the root of “replacement mantle” that has not yet equilibrated with the surrounding asthenosphere. Large degrees of nearly instantaneous mantle melting would homogenize resulting magmas. Emplacement of the OJP would be geologically instantaneous, and the signature of the impact would be recorded in proximal and/or global Lower Aptian sediments. This model is consistent with apparently rapid emplacement of most of the OJP at ~122 Ma, the isotopic and incompatible-element homogeneity of the voluminous Kwaimbaita magma type and its distribution across and beyond the plateau, the lack of a linked hotspot trail, possibly with the mantle root, and perhaps with the limited uplift and subsidence. Discrepancies exist between observations and model predictions here, too, although a lack of relevant samples, data and extensive numerical impact modeling of large impacts currently

precludes a full testing of this hypothesis.

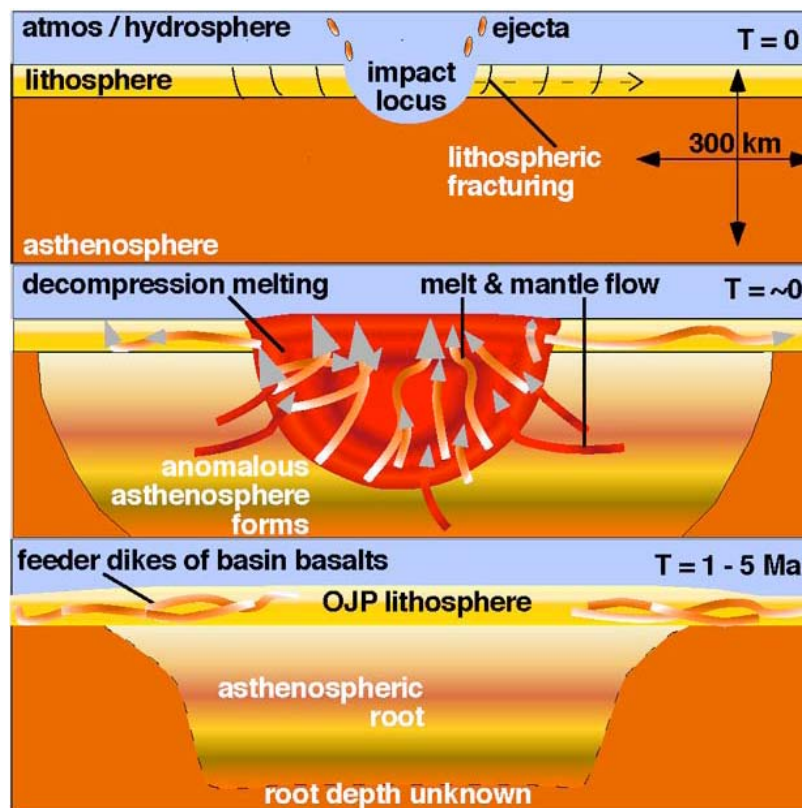


Fig. 2 Bolide impact model.

Upper mantle origin: This model proposed the OJP formed near a fast-spreading (~ 15 cm/yr) ridge as old subducted oceanic crustal fragments (eclogite) were entrained by strong passive asthenospheric upwelling. The entrained eclogite-rich mantle would melt to at least 50% on average. The depleted, relatively low-density residuum would remain beneath the plateau. This model predicts a slight age progression across the plateau perpendicular to the axis of seafloor spreading. Melting of dense eclogitic mantle could explain the submarine formation of the OJP. Subsequent delamination of any remaining fertile shallow mantle could account for minor magmatism at ~ 90 Ma (and possibly ~ 62 Ma) and the abnormal subsidence history of the OJP. As with the other models, however, observations argue against some aspects of this model, i.e., seafloor spreading history, basalt and cumulate composition, and the anomalous mantle root. There has been long debate about which model described above is most applicable to the formation of the OJP. We believe that detailed crust and uppermost mantle imaging is the most fundamental data to address this issue. Recent results of JAMSTEC's seismic studies in seismogenic zone and subduction factory studies have provided remarkable

data to address similar issues. We are therefore strongly believe that seismic surveys using JAMSTEC's seismic instrument will provide important data to solve outstanding issues concerning the origin of the OJP.

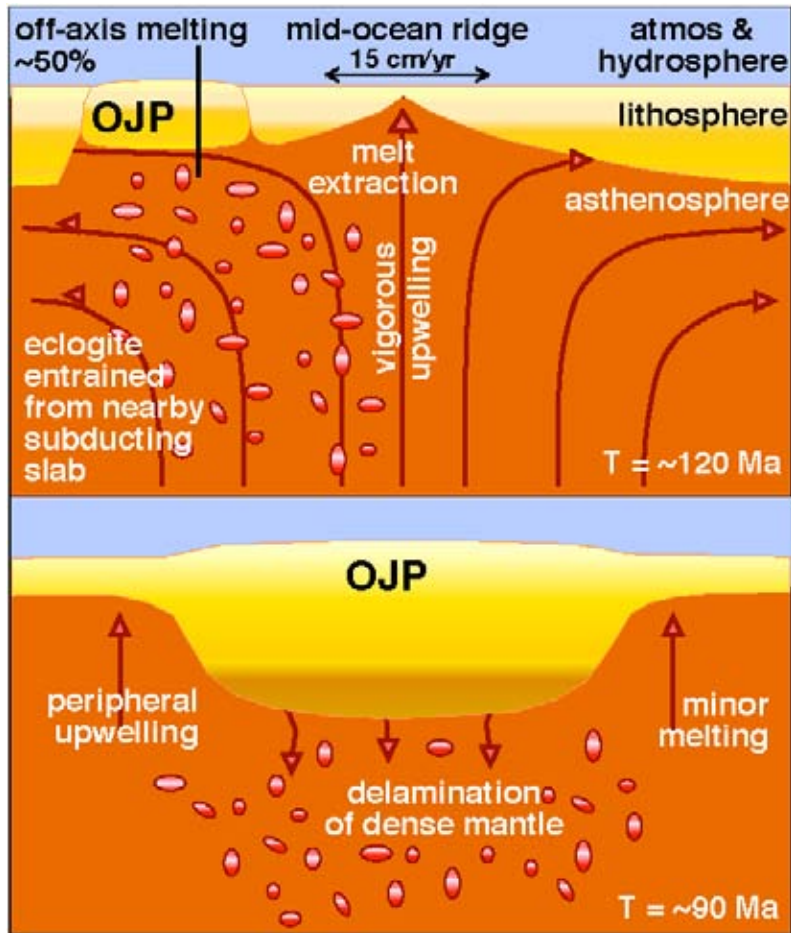


Fig. 3 Formation of the OJP at a fast spreading ridge

Outline of research cruise

Cruise number: KR10-05

Ship name: R/V Kairei

Chief scientist: Seiichi Miura [JAMSTEC]

Representative of Science Party: Yoshio Fukao [JAMSTEC]

Title of Proposal: High resolution deep seismic study in the Ontong Java Plateau

Research Area: Ontong Java area, southwest Pacific.

Cruise period, Port call: 2010/2/25-3/26, Yokosuka to Yokosuka

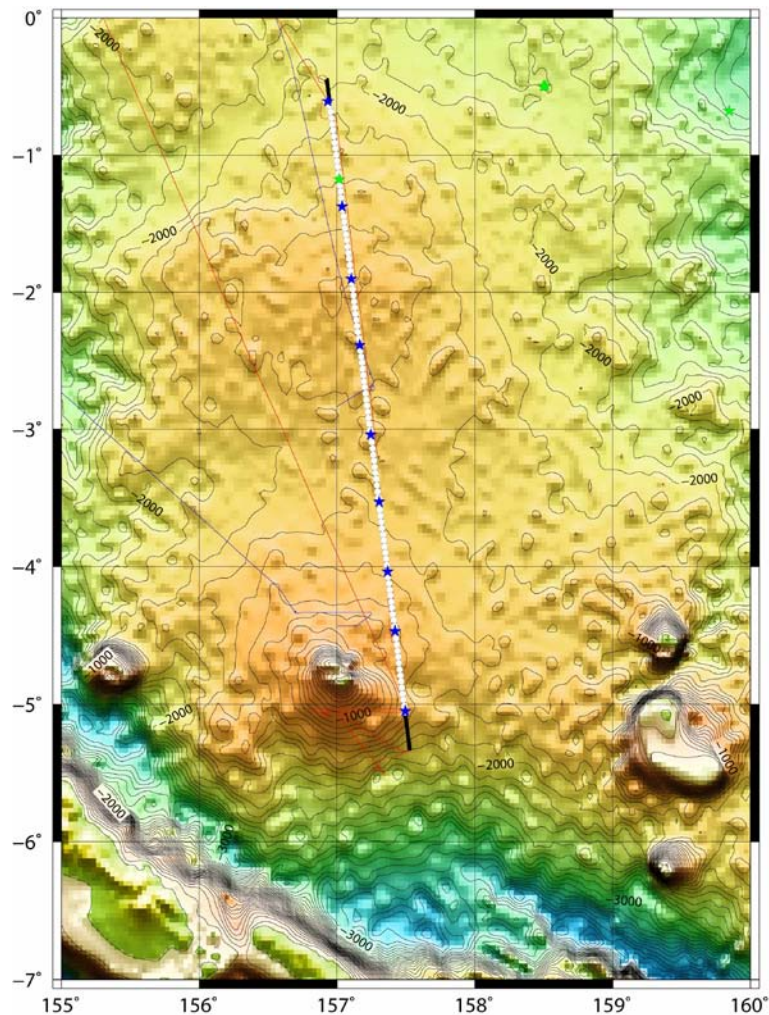


Fig. 1: Seismic line (black) and OBS (white circle) location of this cruise on bathymetric map of ETOPO2. Ship tracks of this cruise and KR05-01 are also indicated by red and blue lines, respectively. Blue stars are XBT locations. Green stars are drilled holes.

Date		
2010/2/25	Thu	Departure from JAMSTEC
2010/2/26	Fri	Transit
2010/2/27	Sat	Transit
2010/2/28	Sun	Transit
2010/3/1	Mon	Transit
2010/3/2	Tue	Transit
2010/3/3	Wed	Transit
2010/3/4	Thu	OBS deployment
2010/3/5	Fri	OBS deployment
2010/3/6	Sat	OBS deployment
2010/3/7	Sun	Airgun shooting for OBS
2010/3/8	Mon	Airgun shooting for OBS
2010/3/9	Tue	Airgun shooting for OBS
2010/3/10	Wed	Airgun shooting for OBS, MCS
2010/3/11	Thu	Airgun shooting for MCS
2010/3/12	Fri	Airgun shooting for MCS
2010/3/13	Sat	Airgun shooting for MCS
2010/3/14	Sun	OBS retrieval
2010/3/15	Mon	OBS retrieval
2010/3/16	Tue	OBS retrieval
2010/3/17	Wed	OBS retrieval
2010/3/18	Thu	OBS retrieval
2010/3/19	Fri	OBS retrieval
2010/3/20	Sat	Transit
2010/3/21	Sun	Transit
2010/3/22	Mon	Transit
2010/3/23	Tue	Transit
2010/3/24	Wed	Transit
2010/3/25	Thu	Transit
2010/3/26	Fri	Arrival to JAMSTEC

Table: Daily activity of this cruise

Seismic survey of OBS: one hundred OBS with 5-km interval on 600-km seismic line

Seismic survey of MCS: 444-ch hydrophone streamer with 12.5-m group interval

XBT: nine XBT were deployed on the seismic line

Bathymetric, magnetics and gravity observation: continuous observation during the cruise

Data shearing and contribution of shipboard scientists

MCS and OBS data would be processed and interpreted by Research team of JAMSTEC, including Dr. Miura and Mr. Noguchi. Mr. Simon Kawagle and Mr. Ronald Verave will bring the acquired data to their institute of PNG, and can use the data within PNG science community. Prof. Mike Coffin will contribute to advise on interpretation, discussion, development of the manuscripts, and future planning of survey.

Cruise narrative

Feb. 20:

Prof. Coffin departed from Heathrow Airport, U. K. to Narita, Japan.

Feb. 21:

Prof. Coffin arrived at Narita and stayed in a hotel in Shinjuku, Tokyo.

Feb. 22:

Prof. Coffin visited the Ocean Research Institute, University of Tokyo.

Feb. 23:

Mr. Kawagle and Mr. Verave departed from Port Moresby to Narita via Cairns. Mr. Chiba, chief of administrative division, went to meet them at Narita Airport and advise them on transportation for the following day. The PNG participants stayed at the Narita Airport Rest House. Prof. Coffin visited the Ocean Research Institute, University of Tokyo.

Feb. 24:

Mr. Kawagle and Mr. Verave traveled by bus from Narita Terminal 2 to Yokohama City Air Terminal (YCAT). Dr. Miura picked them up and proceeded to JAMSTEC Headquarters. The PNG participants visited the guesthouse of JAMSTEC and left their luggage in their rooms. They also went to Shinkai-tei, the cafeteria of JAMSTEC, to reserve breakfast for the following morning. After that, they visited R/V *Kairei* to view their cabins and to see the seismic system. A short tour of JAMSTEC was arranged for them to introduce JAMSTEC and to see high pressure experiments and ROVs. Prof. Coffin was met by Ms. Ozawa at the JAMSTEC gate, and they took his luggage to his cabin on R/V. *Kairei*. A special seminar given by Prof. Coffin was held in the seminar room of JAMSTEC. All shipboard scientists of this cruise and related people enjoyed a welcoming party at the “elle shante” in Oppama. The PNG participants stayed at the guesthouse of JAMSTEC. Prof. Coffin stayed in the hotel in Shinjuku.

Feb. 25:

All shipboard scientists were on board by 9 a. m. We took commemorative photos with a special flag of the “50th anniversary of IOC”, in front of the ship name “*KAIREF*” and on the top deck. Since the PNG participants needed to purchase daily necessities for the

cruise, Dr. Komatsu, an administrative staff member, drove them in his car to shop briefly before the departure. R/V *Kairei* departed the pier of JAMSTEC at 10 a.m. on schedule. Because of thick fog, R/V *Kairei* dropped anchor at the Yokosuka Port and remained there from 10:25 to 12:35. Guidance for daily life and safety on board was provided from 11:00. After weighing anchor, R/V *Kairei* began the cruise to the Ontong Java Plateau (OJP). There was a ceremony for a safe and successful cruise (KONPIRA) from 16:40.

Feb. 26:

R/V *Kairei* took a southerly course along Izu Islands due to rough seas. The ship sailed along the Shichito-Io seamounts.

Feb. 27:

The ship sailed along the West Mariana Ridge, a counterpart of the Mariana Arc.

Feb. 28:

The ship sailed across the Mariana Trough to Guam.

Mar. 1:

The ship sailed from the Mariana Trench to the Caroline Islands.

Mar. 2:

The ship sailed among the Caroline Islands to the northwest of the OJP. Air charge tests of the airguns and air lines were conducted to check the airguns.

Mar. 3:

The ship sailed over the northwestern portion of the OJP. Timing settings for OBS recording were made.

Mar. 4:

R/V *Kairei* arrived at the survey area at 9:00. At first, we conducted a seawater temperature measurement using an expendable bathy thermograph (XBT) at 9:05. After that, OBS deployment started at 9:43. OBSs from Site001 to Site025 were deployed. During the survey, Dr. Miura and Mr. Noguchi split watch times into day (6:00-18:00) and night (18:00-6:00) shifts, respectively. Prof. Coffin, Mr. Kawagle and Mr. Verave were all on the daytime watch.

Mar. 5:

OBS deployment continued from Site026 to Site065. The second XBT was launched at 8:11.

Mar. 6:

OBSs were deployed from Site066 to Site100. During OBS deployments, three XBT were launched. After the deployment, we undertook a bathymetric survey along westbound line from Site100 for about three hours starting at 23:51.

Mar. 7:

The bathymetric survey finished at 3:03. After that, R/V *Kairei* sailed southeast to the MCS deployment point. At first, starboard and port paravanes were deployed from 6:11 to 6:43. Airgun sub-arrays were deployed from 7:27 to 9:06. Streamer deployment started at 9:36. During streamer deployment, the No. 2 airgun sub-array was temporarily retrieved, because currents carried the streamer cable close to the sub-array. Streamer deployment finished at 13:30. No. 2 sub-array deployment followed from 13:40 to 14:05. After full deployment of the MCS system, test shooting and a “soft start” approach were undertaken. The first shooting along the seismic line was from 14:57 to 15:25. Since the depth of the lead-in cable was not properly set to 21-m, the towing length of lead-in cable was adjusted from 15:33 to 15:47. Finally, airgun shooting on the seismic line was restarted from 16:01 at a 200 m shot interval for the OBSs.

Mar. 8:

Airgun shooting northbound continued.

Mar. 9:

Airgun shooting northbound continued.

Mar. 10:

Airgun shooting northbound finished at 2:38, and the ship turn 180°. Airgun shooting southbound started at 5:49 at a 50 m shot interval for MCS. Airgun firing stopped because of the first air leakage of the No. 3 sub-array at 10:10. To repair the air leakage, the ship circled for retrieval, the airgun was replaced, and the No. 3 sub-array was re-deployed. The airgun array was ready to shoot at 14:40, and shooting restarted at 15:38 when the ship was back on the line and the MCS system properly configured.

Mar. 11:

A second air leakage occurred at 2:52, followed by stopping firing of the leaking airgun at 2:59. Despite the air leakage, shooting for MCS continued without repairs, because ship time for shooting the line was limited and a high priority was to acquire MCS data along the southernmost part of the line. Moreover, MCS data below the seafloor was not seriously affected by the air leakage.

Mar. 12:

Airgun shooting for MCS continued. A ship tour was conducted for the shipboard scientists from 10:00 to 11:15 by C/O Naoto Kimura. The tour involved visiting the bridge, the after bridge, the Kaiko cable winch, the bow, the emergency electric generator, the acoustic transducer, the sewage tank, the engine room, the compressor room, and the rudder room. A third air leakage occurred around 14:30 in the No.2 sub-array. Airgun shooting continued without repairs.

Mar. 13:

Airgun shooting finished at 13:09. Retrieval of the MCS system including airguns, paravanes, and the streamer with tail buoy was conducted from 13:20 to 18:10. A bathymetric survey parallel to and contiguous with the survey of Mar. 6-7 was conducted from 20:17.

Mar. 14:

The bathymetric survey finished at 1:34. The OBS at Site100 was retrieved from 03:07 to 03:58. Because of strong winds and high waves related to a cyclone, OBS retrieval was conducted intermittently. Five OBSs at Site100, 88, 87, 86, and 83 were retrieved. The ship steamed north to portions of the line less affected by the cyclone.

Mar. 15:

The ship continued to steam north, and because the wind speed was lower than that of the previous day, OBS retrieval restarted at 6:17 from Site058. Nineteen OBSs were retrieved this day.

Mar. 16:

OBS retrieval continued from Site039 to Site009, as the sea conditions was favorable.

Mar. 17:

OBSs from Site008 to Site001 were retrieved. Subsequently, the ship transited from Site001 to Site059. OBSs from Site 059 southward had not been retrieved due to the high winds and waves of Mar. 14-15 associated with the cyclone. During the transit, a bathymetric survey was conducted on a line two miles east of the line previously conducted. OBS retrieval restarted at Site059 at 17:34, and continued until Site064 before midnight.

Mar. 18:

OBS retrieval continued from Site065 to Site093.

Mar. 19:

OBS retrieval continued from Site094 to Site099. OBS retrieval finished at 4:21. The transit to JAMSTEC in Yokosuka started at 4:30.

Mar. 20:

Transit to JAMSTEC.

We took a group photo at the deck in front of the streamer winch, with the flag for 50th anniversary of Intergovernmental Oceanographic Commission (IOC).

Mar. 21:

Transit to JAMSTEC.

Mar. 22:

Transit to JAMSTEC.

Mar. 23:

Transit to JAMSTEC.

Mar. 24:

Transit to JAMSTEC.

We held a shipboard seminar from 9:00 to 10:45 in the Research Room of R/V *Kairei*. The presenters were Seiichi Miura, Millard F. Coffin, and Simon A. Kawagle.

Mar. 25:

Transit to JAMSTEC.

Mar. 26:

Arrival at JAMSTEC at 9:00. Prof. Coffin, Mr. Kawagle, and Mr. Verave traveled to Yokohama by train. They stayed at hotels close to Yokohama station.

Mar. 27:

Prof. Coffin departed Japan on a flight to Heathrow, UK. Mr Kawagle and Mr. Verave left Japan on a flight to Port Moresby, PNG.

Crustal structure of the OJP

The Ontong Java Plateau (OJP), one of largest oceanic plateau on Earth (Coffin and Eldholm, 1994), is located at the margin of the Pacific Plate where it is colliding with the Solomon Island Arc. The shallow water depths of the OJP suggest that its crustal thickness is greater than that of normal oceanic crust. However, only a few surveys have been conducted to investigate the entire crust, and none of these were of an extent or scale to address the problem comprehensively.

One example is a seismic study from the 1970s published by Furumoto et al. (1976). They conducted a two-ship refraction survey on the OJP with explosive sources and a short hydrophone. They showed a crustal thickness from 35 to 42 km (Fig. 1). However, the maximum offset distance of the survey was about 140 km, which is thought to be insufficient to detect refracted waves from the uppermost mantle beneath the OJP. Moreover, their phase interpretations might have been based on later reflection phases, which was mentioned by Gladchenko et al. (1997).

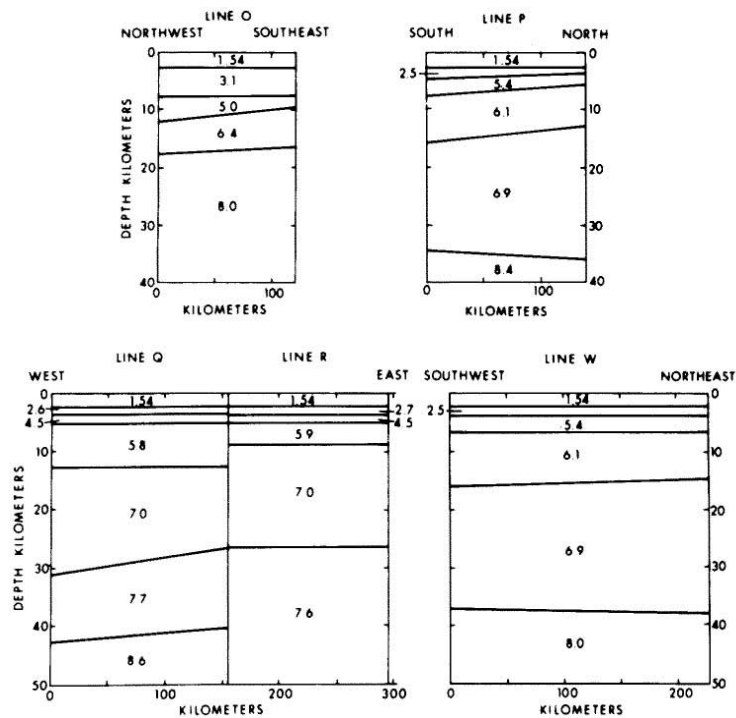


Fig. 1: Crustal structures by Furumoto et al. (1976)

Reinterpretation of the seismic data of Furumoto et al. (1976) combined with gravity modeling was presented by Gladchenko et al (1997). They showed that the crustal thickness of the OJP is about 32 km in the central part, and decreases toward the edge

of the plateau (Fig. 2).

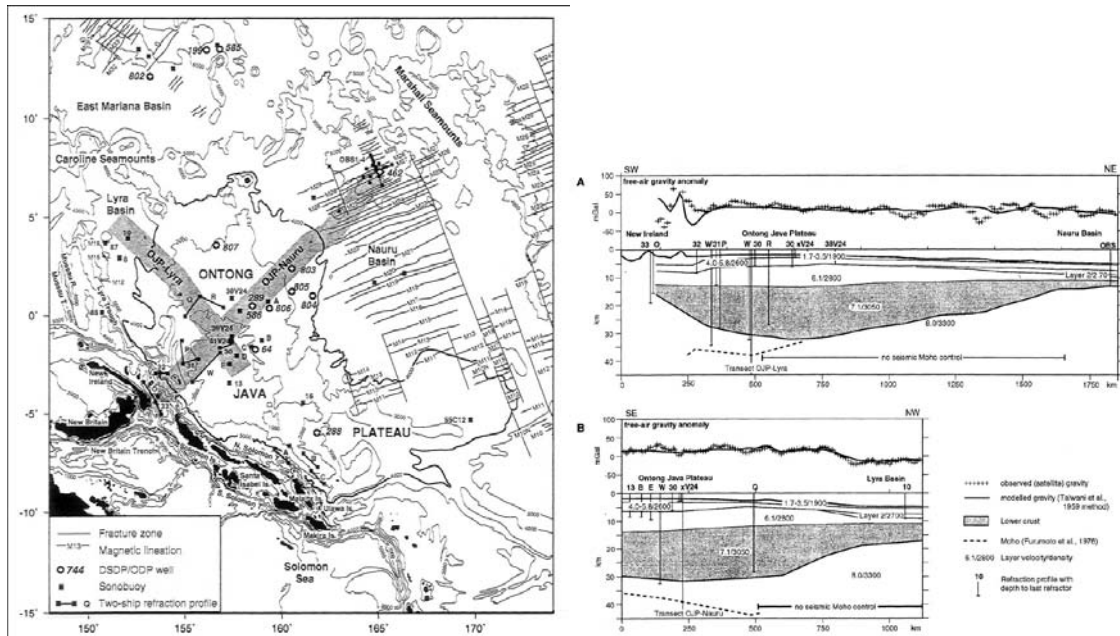


Fig. 2: Location map and crustal structures (Gladchenko et al., 1997)

Seismic surveys around the OJP have been conducted at least four times since the 1990s which have involved the Japanese science community: EW9511, KH98-1, KR05-01, and KR06-16 cruises (Fig. 3).

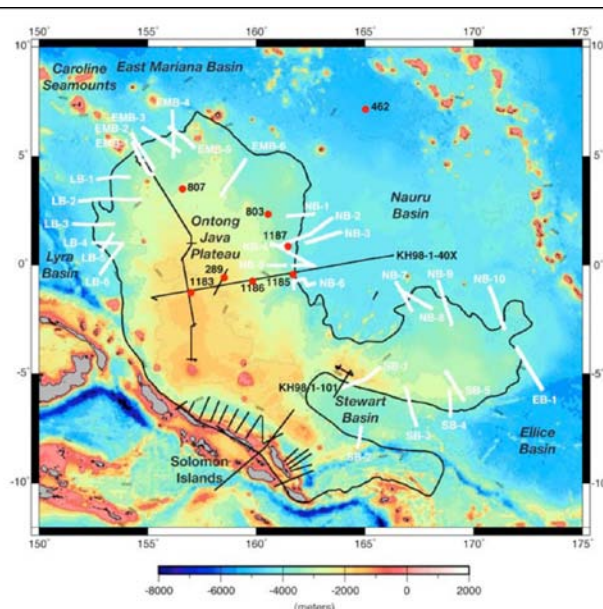


Fig. 3: Seismic survey tracks across the Ontong Java Plateau (IODP proposal 623, Neal et al.)

The EW9511 cruise addressed the collision of the OJP with the Solomon Island Arc,

which includes the southern edge of the OJP. During EW9511, eighteen ocean bottom seismometers were deployed on a seismic transect from the OJP to the India-Australia Plate. The crustal thickness of the OJP at the southern edge is 33 km, including a 15 km-thick high velocity lower crust (Miura et al., 2004). The upper part of the OJP is being accreted to the Solomon Island Arc as the Malaita Accretionary Prism, and the lower part of the OJP is interpreted as subducting beneath the Solomon Island Arc, suggested by seismicity (Fig. 4).

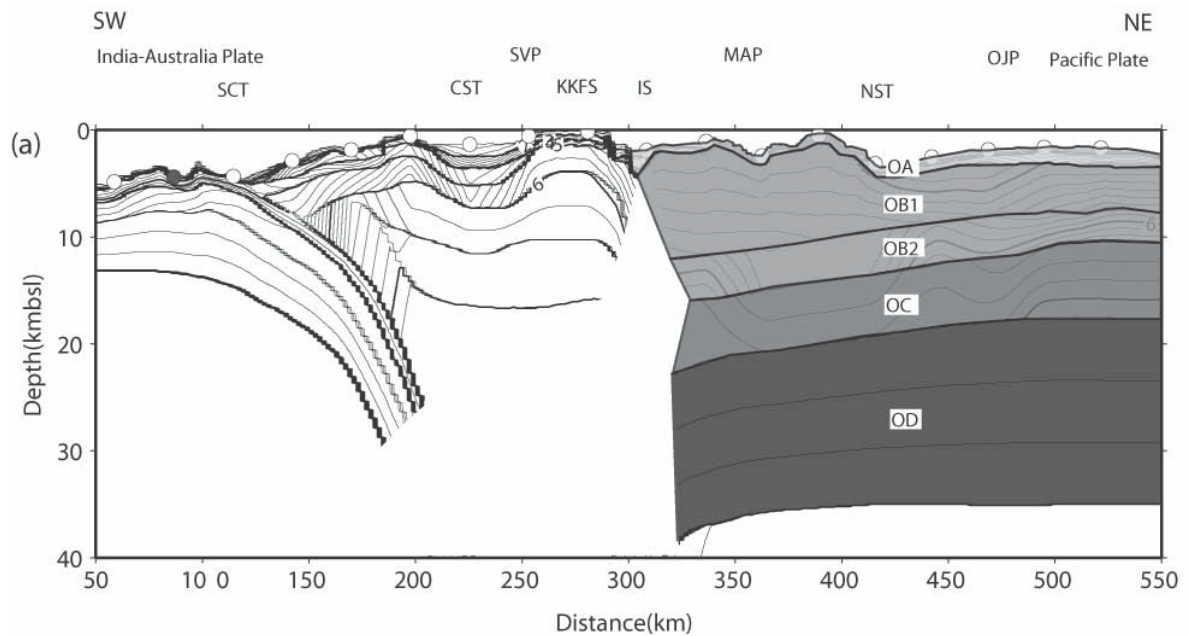


Fig. 4: Crustal structure of the OJP and Solomon Island Arc (Miura et al., 2004)

The KH98-1 cruise was targeted to acquire data from the central OJP into the Nauru Basin east of the OJP (Mochizuki et al., 2005; Inoue et al., 2008). They show seismic profiles on the main OJP and into the Nauru Basin. Mochizuki et al. (2005) combined the MCS data with sonobuoy data and gravity modeling, showing discrepancies in crustal thickness between the actual water depth and that predicted by age-depth modeling. Inoue et al. (2008) analysed intrabasement reflections on the main OJP, and developed a model of alternating massive and pillow lava flows for their origin.

The KR05-01 and KR06-16 cruises were conducted to acquire the reflection profiles in the vicinity of proposed drill sites by the IODP drilling proposal 623. The KR05-01 was mainly conducted in the middle part of the OJP (Inoue et al., 2008), and the KR06-16 was conducted in Lyla basin, which is a western marginal basin.

A Rayleigh-wave tomography study of broad-band seismic data was presented by

Richardson et al. (2000). They show that the depth variation of the Moho beneath the OJP averages 33 km and reaches a maximum of 38 km (Fig. 5). Moreover, they discovered a low-velocity root extending to 300 km beneath the OJP, suggesting the existence of a root associated with formation of the OJP.

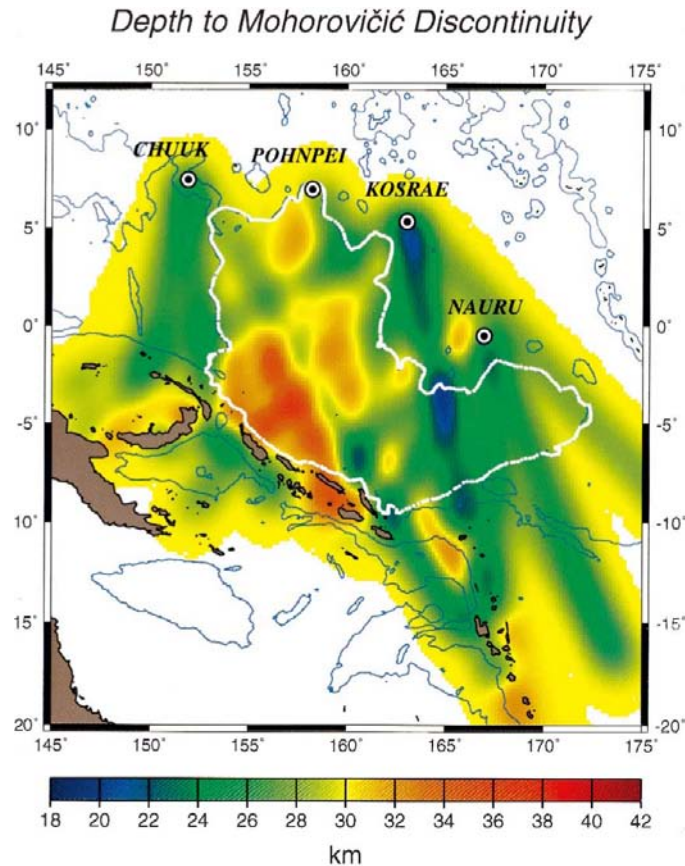


Fig. 7. Map of crustal thicknesses obtained in the three-dimensional inversion.

Fig. 5: Map of crustal thicknesses (Richardson et al., 2000)

References:

- Coffin, M. F., and Eldholm, O., 1994. Large Igneous Provinces: Crustal structure, dimensions, and external consequences. *Rev. Geophys.*, 32, 1-36.
- Furumoto, A. S., Webb, J. P., Odegard, M. E., and Hussong, D. M., 1976. Seismic studies on the Ontong Java Plateau, 1970. *Tectonophysics*, 34, 71-90.
- Gladchenko, T. P., Coffin, M. F., and Eldholm, O., 1997. Crustal structure of the Ontong Java Plateau: Modeling of new gravity and existing seismic data. *J. Geophys. Res.*, 102, 22711-22729.
- Inoue, H., Coffin, M.F., Nakamura, Y., Mochizuki, K., and Kroenke, L.W., 2008.

- Intrabasement reflections of the Ontong Java Plateau: implications for plateau construction. *Geochem. Geophys. Geosyst.*, 9, Q04014, doi:10.1029/2007GC001780.
- Miura, S., Suyehiro, K., Shinohara, M., Takahashi, N., Araki, E. and Taira, A., 2004. Seismological structure and implications of collision between the Ontong Java Plateau and Solomon Island Arc from ocean bottom seismometer-airgun data. *Tectonophysics*, 389, 191-220.
- Mochizuki, K., Coffin, M. F., Eldholm, O., Taira, A., 2005. Massive Early Cretaceous volcanic activity in the Nauru Basin related to emplacement of the Ontong Java Plateau. *Geochem. Geophys. Geosyst.*, 6, Q10003, doi:10.1029/2004GC000867
- Neal, C. R., Coffin, M., Mahoney, J.J., Tatsumi, Y., Kroenke, L., Abrams, L., Bralower, T., Fitton, J.G., Ingle, S.P., Inoue, H., Ito, G., Jenkyns, H., Keszthelyi, L., Kodaira, S., Koppers, A., Miura, S., Mochizuki, K., Nakanishi, M., Ohkouchi, N., Ravizza, G., Russo, R., Saito, S., Shen, Y., Saunders, A., Tejada, M., Wallace, P., 2007. Origin of the Ontong Java Plateau: Plume, Bolide, or Plate Tectonic? IODP Proposal 623-Full4
- Richardson, P., Okal, E. A., and Van der Lee, S., 2000. Rayleigh-wave tomography of the Ontong-Java Plateau. *Phys. Earth Planet. Inter.*, 118, 29-51.

*Life at the Edge: Super Eruptions cause Earth Crises

The formation of large igneous provinces (LIPs)—continental flood basalts, ‘volcanic’ margins, and oceanic plateaus—may impact the atmosphere, oceans, and biosphere by rapidly releasing huge amounts of particulates, magmatic volatiles (CO₂, SO₂, Cl, F, etc.), and potentially volatiles (CO₂, CH₄, SO₂, etc.) from intruded sediments (e.g., carbonates, organic-rich shales, evaporites). A key factor affecting the magnitude of volatile release is whether eruptions are subaerial or marine; hydrostatic pressure inhibits vesiculation and degassing of relatively soluble volatile components (H₂O, S, Cl, F) in deep water submarine eruptions, although low solubility components (CO₂, noble gases) are mostly degassed even at abyssal depths. Directly or indirectly, such injections may cause changes in the atmosphere/ocean system that can lead to perturbations of atmosphere/ocean chemistry, circulation, ecology, and biological productivity. These changes can be global in extent, particularly if environmental conditions were at or near a threshold state or tipping point. LIPs may have been responsible for some of the most dramatic and rapid changes in the global environment. For example, between ~145 and ~50 Ma, the global ocean was characterized by chemical and isotopic variations (especially in C and Sr isotope ratios, trace metal concentrations, and biocalcification), relatively high temperatures, high relative sea level, episodic deposition of black shales (oceanic anoxic events), high production of hydrocarbons, mass extinctions of marine organisms, and radiations of marine flora and fauna. Temporal correlations between the intense pulses of igneous activity associated with LIP formation and environmental changes suggest more than pure coincidence. The 1783-84 eruption of Laki on Iceland provides the only historical record of the type of volcanism that constructs transient LIPs. Although Laki produced a basaltic lava flow representing only ~1% of the volume of a typical transient LIP flow (10³ km³), the eruption’s environmental impact resulted in the deaths of 75% of Iceland’s livestock and 25% of its inhabitants. During Cenozoic time, peak eruption of the North Atlantic LIP at ~56 Ma coincided with the Paleocene-Eocene thermal maximum, when numerous deep-sea benthic foraminifera became extinct and there was a major turnover in terrestrial mammals. Late Cretaceous oceanic anoxic event 2 (OAE-2) coincided with the formation of the Caribbean and possibly Madagascar flood basalts at ~94 Ma, and in Early Cretaceous time, formation of the Ontong Java, Manihiki, and Hikurangi plateaus at ~122 Ma in the Pacific coincided with oceanic anoxic event 1a (OAE-1a). Eruption of the Siberian flood basalts at ~250 Ma (Permian-Triassic boundary) coincided with the largest extinction of plants and animals in the geological record; 90% of all species became extinct at that time.

*: This is the abstract of the special seminar presented by Prof. Millard F. Coffin at JAMSTEC in Feb. 24, 2010, which is the day before departure.

THE GEOLOGICAL FRAMEWORK OF PAPUA NEW GUINEA – AN OVERVIEW

R.T. Verave & S.A. Kawagle

ABSTRACT

Papua New Guinea (PNG) has a complex geology, which is due its tectonic setting. The region is sandwiched in between two major opposing tectonic plates – Indo-Australian Plate to the south-southwest and the Pacific Plate to the east-northeast, which converges obliquely. Nevertheless, the geological framework is best described as a series of geological terranes or discrete geological regions, which are commonly separated by geological elements. The typical tectonic setting also gives rise to a complex seismicity pattern, and contributing significantly to the style of mineralisation found in the region.

Most of mainland PNG is underlain by the Australian Craton. The rest of the material that make up the landmass is of Late Cretaceous age or younger metamorphosed and unmetamorphosed island arc volcanic rocks that had collided with the Craton. Material from obducted oceanic crust and igneous intrusive and volcanic rocks also contribute a significant percent of the total rock volume.

The initial collision and accretion of volcanic arc with the Craton was the Irian Jaya arc in Late Cretaceous; which has resulted in the emplacement of ophiolites. This was followed by East Papua volcanic arc with the Owen Stanley Terrane in the Paleocene. Subsequent collisions and accretion included Sepik (Salumei) arc in the Late Eocene-Oligocene, Finisterre arc in Early Miocene, and Bismarck volcanic arc in Pliocene. These volcanic arcs developed above north-dipping subduction zones.

Other developments either contemporaneously with the collisions or as separate events include opening and closing of small oceans basin, suturing of terranes to the Craton, and the obduction of oceanic crust onto the Craton. The latest collision event resulted in formation of major fold and thrust belts and other fault systems on mainland PNG, magmatism and its associated mineralisation, and volcanic activities.

The jamming of the Kilinailau Trench by the Ontong Java Plateau in mid-Miocene, initiated development of the New Britain Trench, and hence a northward-dipping subduction zone in the Pliocene. At present, the Solomon Sea Plate is doubly subducting beneath New Britain, New Ireland and Bougainville at the New Britain Trench. The South Bismarck Plate is subducting beneath the PNG mainland at the New Guinea Trench. The Manus and Woodlark Basins are active spreading centres.

Airgun array



Fig.1: APG airgun on deck

Airgun array of R/V Kairei has been upgraded since 2008 with multi-channel seismic reflection system (MCS). Airgun model is annular port airgun (APG) of BOLT Inc., shaping cylindrical chambers, housings, and shells containing air and electric junctions (Fig. 1). The array has four sub-arrays of 1950 cu. in. consisting to eight airguns from 100 cu. in. to 600 cu. in. Therefore total volume of the array is 7800 cu. in. The distances between airguns are small about 1 m, which is favorable to form airgun clusters generating effective source output.

Towing depth of airguns for this cruise was 10 m to acquire deep penetration signals down to Moho. Shooting intervals for OBS and MCS were respectively 200 m and 50 m. The numbers of shootings were respectively 2663 and 10973 including overlapped shot points caused by turn around for the air leakage repair mentioned later. The reason of sparse shooting for OBS is that large time interval can prevent noises of previous shots on OBS profiles.

Before the acquisitions for seismic data, we conducted a “soft start” approach, which is a starter for airgun shootings increasing charge volumes from small number of airguns to large ones. This approach is preferable not only for airguns and MCS, but also for environment especially marine mammals. No marine mammals were observed

during the airgun shootings.

During airgun shooting for data acquisition, there were three air leakages of the airgun array. The first air leakage was caused by broken of air seals in a 600 cu. in. chamber of No.3 sub-array, which was replaced to new one, with turning around the ship. The second and third leakages were not repaired during the survey because of time limitation. After the retrieval of airguns on deck after the survey, the airguns were investigated to cause of air leakages. The second air leakage was No. 1 sub-array caused by two failures of an air hose in a shield next to a 600 cu. in. airgun (Fig. 2) and of an air hose between termination housing of umbilical cable and the first airgun (Fig. 3). The third air leakage was No. 2 sub-array caused by a damaged air hose at the end of the sub-array rubbed by a cable connector (Fig. 4).

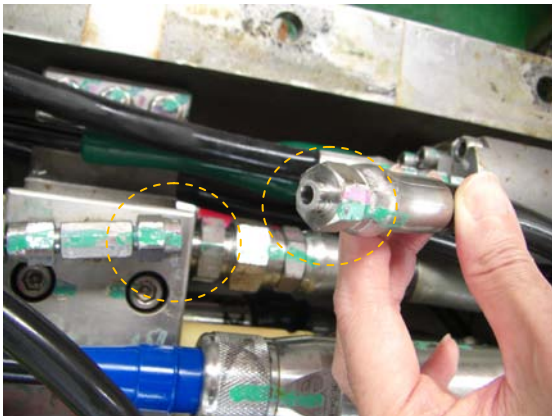


Fig. 2: Air hose failure in a shield



Fig. 3: Air hose failure ahead of the airguns



Fig. 4: Damaged air hose rubbed by connector

Multi-channel seismic reflection system (MCS)

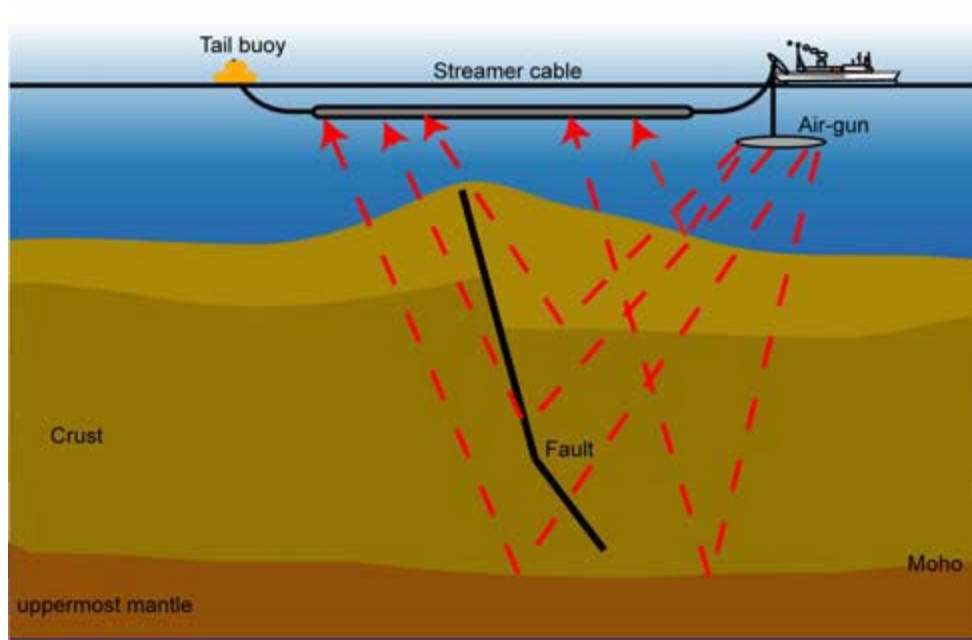


Fig. 1: Outline of MCS survey

The multi-channel seismic reflection system (MCS) consists of an airgun array, a streamer cable containing hydrophones and terminated with a tail buoy, a navigation system with global positioning system (GPS) receivers, and a shipboard control system that records the data (Fig. 1). Separate sections in this document describe the airgun array and GPS; therefore, explanations of these are excluded from this section.

The streamer cable is a Sercel Sentinel Digital Streamer, with a 12.5-m group interval consisting of 8 hydrophones, and a total of 444 channels (Fig. 2). The sensitivity of each hydrophone is $-194.1 \text{ dB re } 1 \text{ V/uPa} \pm 1.0 \text{ dB}$ at 20° Celsius , which is equivalent to 19.72 V/Bar . Two channel units have an individual 24 bit A/D converter of the delta-sigma type. Recorded data is compressed by a module called a LAUM, which is a data compressor, data router, and power supplier. LAUMs are located every 60 channels in the streamer. Total lengths of the streamer cable used during this cruise are 5851 m with a 149 m lead-in cable, and 5881 m with a 179 m lead-in cable length, both including active sections, stretch sections, and towing lead-in cable. The towing depth of the cable was controlled at 21-m by 21 depth controllers called “birds”. Each “bird” has a depth sensor and a compass sensing its three dimensional location underwater (Fig. 3). The tail buoy has a GPS unit to locate the end of the streamer (Fig. 4).



Fig. 2: Streamer cable

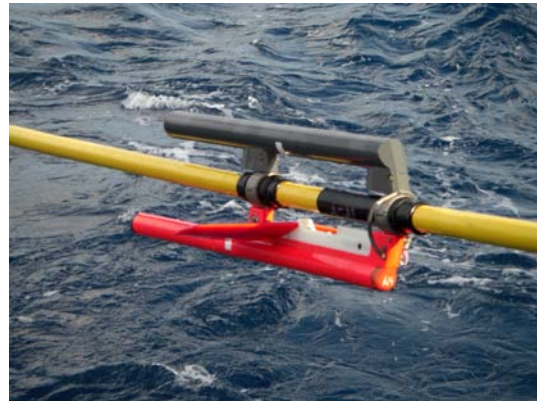


Fig. 3: Depth controller "bird"



Fig. 4: Tail buoy

The shipboard MCS systems consists of four main groups: navigation control, airgun control, streamer control, and other navigation (Fig. 5). The navigation control group SPECTRA is a system name for navigation software on three workstations and an interface unit (Power RTNu). SPECTRA defines coordinate axes, seismic lines, and shot points. Shot times are calculated by SPECTRA using the defined coordinates and position information of the ship and airgun sub-arrays. Then SPECTRA generates System Start signals 200 ms prior to the target point of a shot (Fig. 6) that are sent to airgun control and streamer control groups. SPECTRA records shot times and locations, and geometry information for the airguns, streamer, and ship. The airgun control group DigiSHOT controls and monitors all airguns. Air pressure, array depth, and near field wave forms are also monitored. As noted above, the System Start signals are sent to DigiSHOT from SPECTRA 200 ms before the target point of a shot (Fig. 6). Then DigiSHOT sends a Shot Trigger signal to the airguns. Each airgun sends a Time Break

signal back to DigiSHOT. The Clock Time Break signals are sent to the Master Clock and True Time, which are shot time recorders in GPS time with milli-second accuracy for OBS data processing. The streamer control group Seal System consists of software on workstations, quality control software, interface units, a power supply for the hydrophone streamer, a recording buffer disk, Network Access Storage (NAS) disks, and tape drives (3590E). The Seal System receives System Start signals from SPECTRA, and sends a Recording Start signal to each LAUM in the hydrophone streamer. The hydrophone data are collected by the LAUMs and sent back via the hydrophone streamer to shipboard units for recording on a buffer disk. After buffering, the data are recorded on NAS disks and 3590E tapes in SEG-D format. The other Navigation group consists of differential GPS (DGPS) of the MCS system (StarFire), relative GPS (RGPS) of the airgun sub-arrays and tail buoy (BuoyLink), depths and compass readings of the birds, and navigation information of R/V *Kairei* as DGPS of SkyFix XP, gyro compass, SOJ (SENA Original JAMSTEC), and radar. The navigation information is sent to SPECTRA and recorded in geometry file format “P2/91”. The navigation data for each shot time are written in a different format, “P1/91”, which are geometry data applied to seismic data recorded by the Seal System.

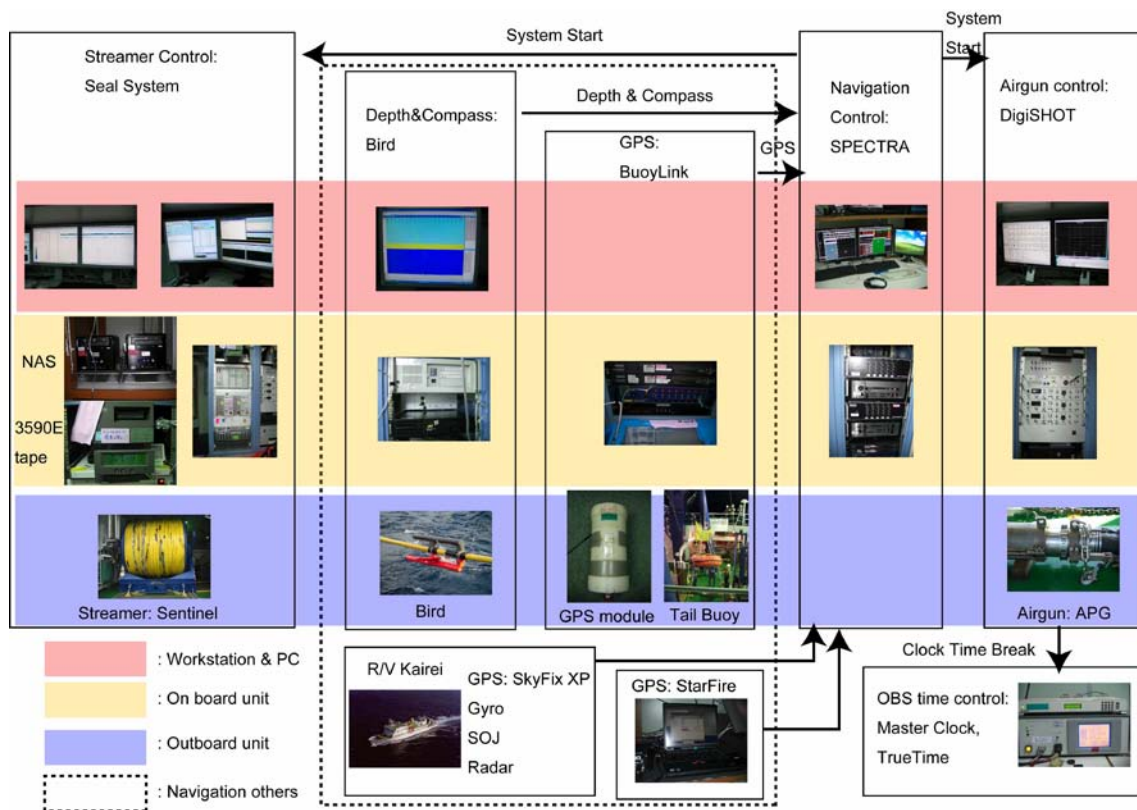


Fig. 5: MCS system of R/V *Kairei*

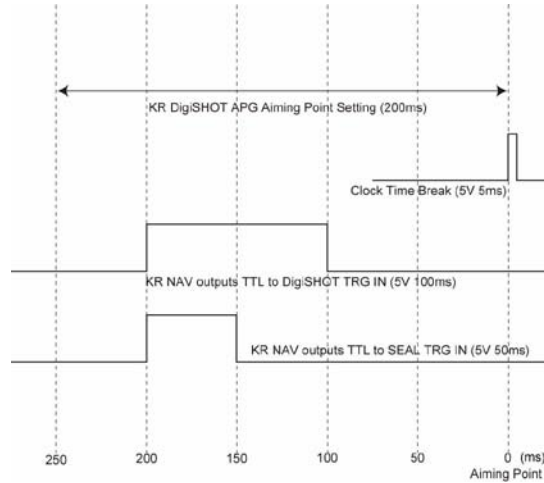


Fig. 6: System time configuration

During this cruise focusing on the central OJP, MCS data were acquired on a seismic line extending from 5°16.9753'S and 157°31.2514'E in the south to 0°4.3610'N and 156°51.6932'E in the north. On the seismic line, shooting at a 200 m interval was conducted firstly northbound for OBS to minimize previous shot noise on the OBS data (LineNSobs_0, LineNSobs_1). Shooting at a 50 m interval was conducted secondly southbound for MCS to improve the signal to noise (S/N) ratio (LineNSmcs_0, LineNSmcs_1). Detailed line information is shown in Table 1. Because of insufficient time, the northernmost 60 km of the planned line was canceled. Sample rates were 2 ms for all lines. Data lengths for 200-m and 50-m intervals were 25 s and 18 s, respectively.

Table1: Line list

NO.	LINE NAME	UKOOA P1/90 P2/91	DATE (UTC)	TIME (UTC)	F.S.P.	S.P. POSITION		Depth (m)	NUMBER OF SHOT FGSP - LGSP	LENGTH FGSP - LGSP (m)	DIRECTION (°)	Mode
					F.G.S.P. L.G.S.P. L.S.P.	Lat.	Lon.					
1	LineNSobs_0	LineNSobs_0.0.p190 LineNSobs_0.0.p291	07/03/2010	04:57:54	921	5 18.99137S	157 31.82820E	1894	16	3000	352.789	Distance (200m)
			07/03/2010	05:01:31	929	5 18.78867S	157 31.70218E	1898				
			07/03/2010	05:25:12	989	5 17.20108S	157 31.28133E	1821				
			07/03/2010	05:25:12	989	5 17.20108S	157 31.28133E	1821				
2	LineNSobs_1	LineNSobs_1.0.p190 LineNSobs_1.0.p291	07/03/2010	06:01:21	1077	5 14.83228S	157 30.98484E	1780	2645	528800	352.789	Distance (200m)
			07/03/2010	06:04:20	1085	5 14.61640S	157 30.96297E	1776				
			09/03/2010	16:38:17	11661	0 29.88518S	156 55.89741E	2005				
			09/03/2010	16:38:17	11661	0 29.88518S	156 55.89741E	2005				
3	LineNSmcs_0	LineNSmcs_0.0.p190 LineNSmcs_0.0.p291	09/03/2010	19:49:02	11780	0 26.86635S	156 55.51418E	2018	450	22450	172.958	Distance (50m)
			09/03/2010	20:39:00	11672	0 29.77230S	156 55.88108E	2009				
			10/03/2010	00:00:35	11223	0 41.85940S	156 57.36420E	1919				
			10/03/2010	00:10:38	11206	0 42.31545S	156 57.43203E	1928				
4	LineNSmcs_1	LineNSmcs_1.0.p190 LineNSmcs_1.0.p291	10/03/2010	05:38:25	11280	0 40.32420S	156 57.19121E	1914	10358	517850	172.958	Distance (50m)
			10/03/2010	05:55:32	11238	0 41.45535S	156 57.31601E	1915				
			13/03/2010	03:09:32	881	5 20.29531S	157 31.63757E	1905				
			13/03/2010	03:09:32	881	5 20.29531S	157 31.63757E	1905				
								Total	13469	1072100		

The configuration of the source and receiver are shown in Figs. 7 and 8. The depths of source and receiver were 10 m and 21 m, respectively, optimized for low frequency, deep penetrating signals. Minimum offset was changed during acquisition because the towing length of the lead-in cable was increased to keep the streamer depth at its target depth.

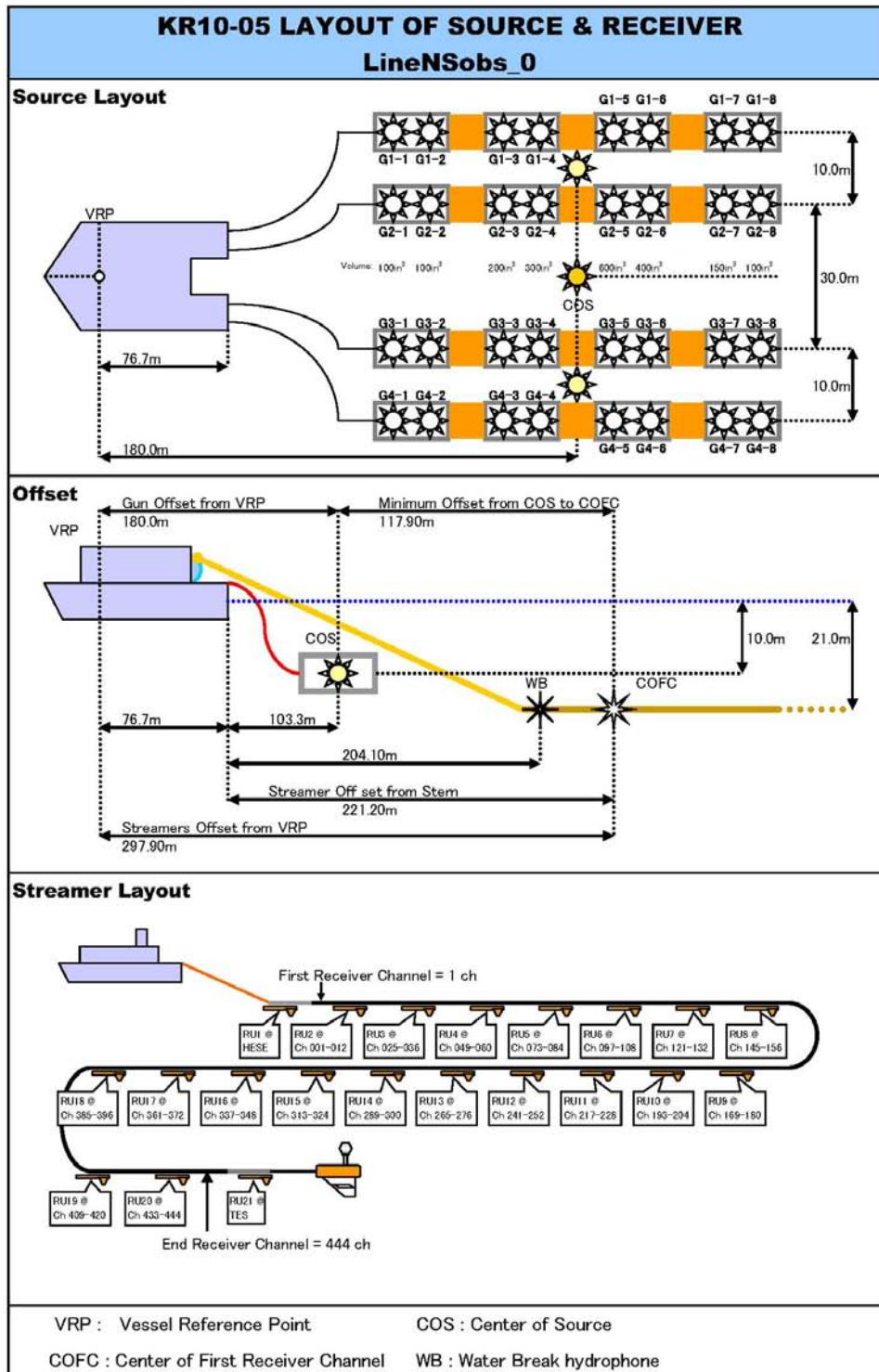


Fig. 7: Configuration of source and receiver for LineNSobs_0

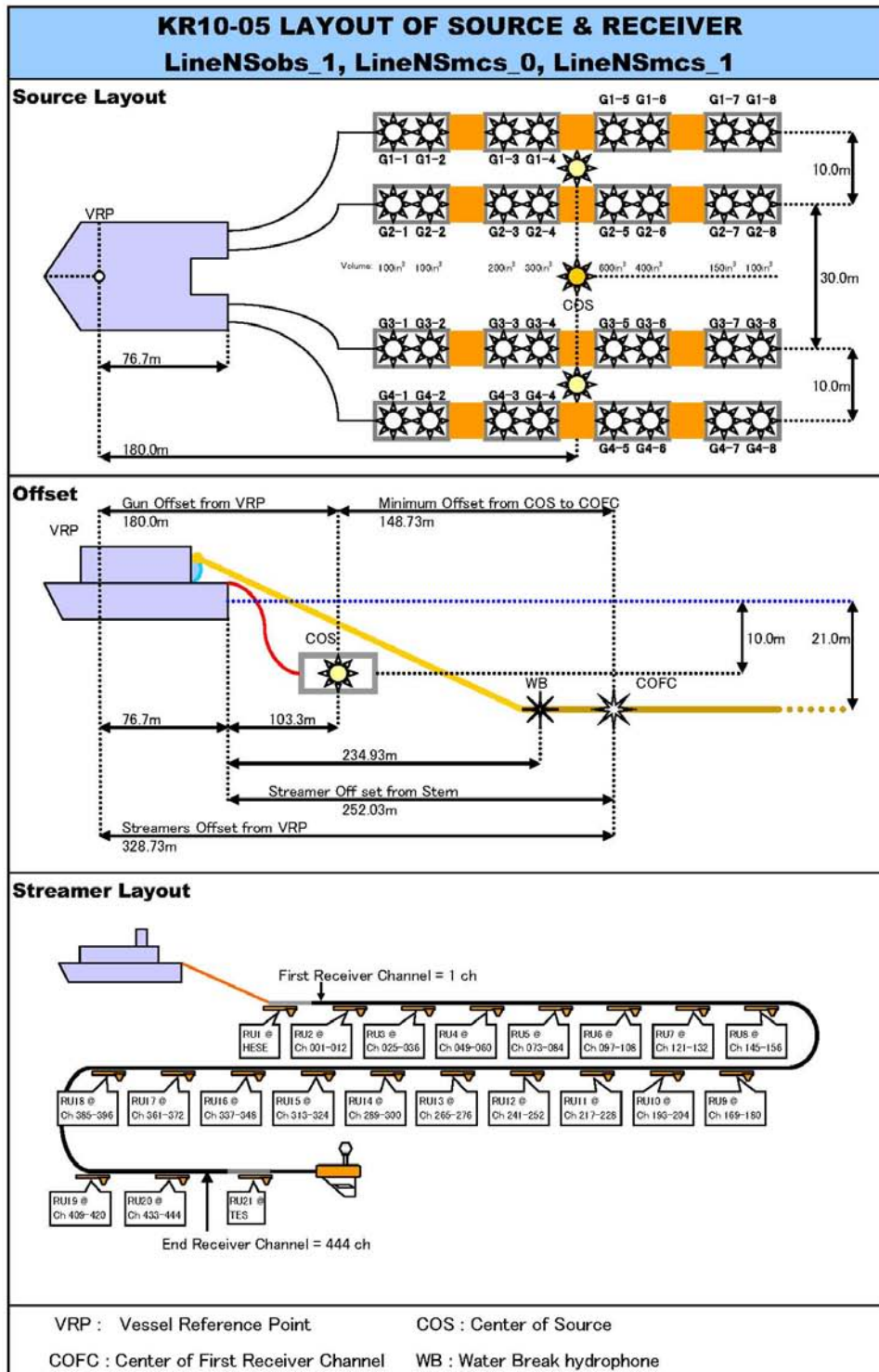


Fig. 8: Configuration of source and receiver of LineNSobs_1, LineNSmcs_0
LineNSmcs_1

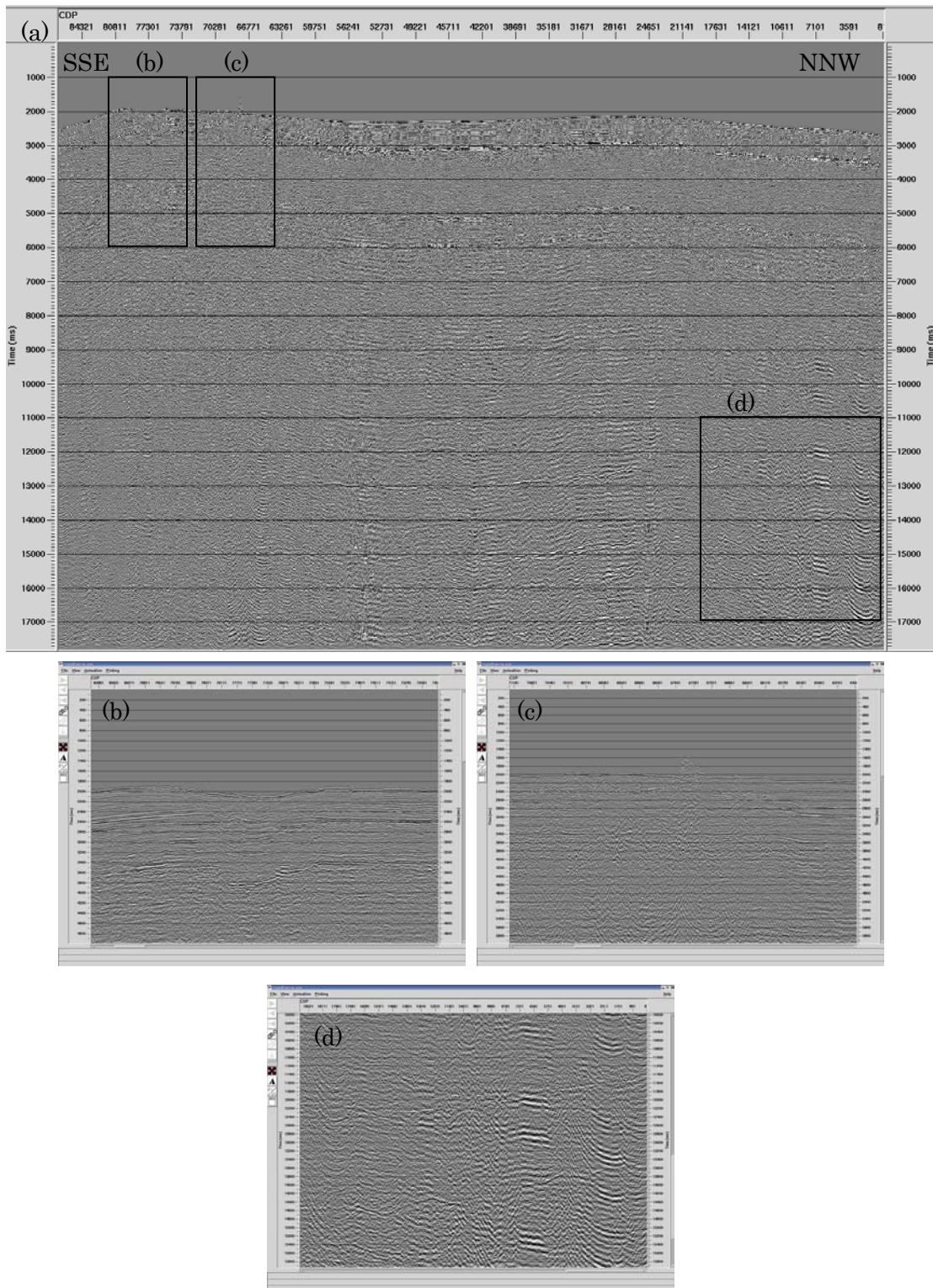


Fig. 9: MCS profiles for LineNSmcs

Ocean Bottom Seismometers (OBS)



Fig. 1: Deployment of an OBS

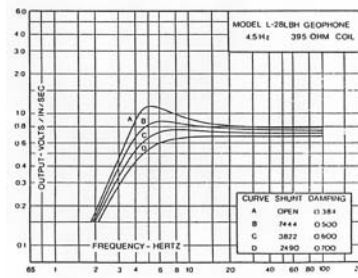
During this cruise, we deployed 100 OBSs to acquire wide-angle reflection and refraction data, and thereby reveal the whole crustal structure of the OJP. JAMSTEC's OBS is model POBS-150 of Katsujima-seisakusho (Fig. 1), which is a modified version of the Ocean Research Institute (ORI), University of Tokyo's model (Shinohara et al., 1993), originally developed by Kanazawa (1986).

Electrical devices including a rechargeable battery, data recorder with an internal clock and a hard disk drive, and geophones with a gimbal system are stored inside a 19-inch glass sphere. The battery longevity is three to four weeks with the following recording parameters: 4 channels, 16 bit A/D conversion, and 100 Hz sampling. Since the deployment period for this cruise was about two weeks, we applied a sampling rate of 250 Hz to acquire high frequency signals.

Each OBS has three component geophones (Mark Products L-28LBH) with a gimbal case to adjust inclination of the sensors (Fig. 2). The effective frequency is higher than 4.5 Hz (Fig. 3).



Fig. 2: OBS sensors in glass sphere



今回の使用するカーブはDです (ダンピング 0.70)
 ダンピング低抗 2490オーム
 感度 0.69V/IN/S

Fig. 3: Frequency response of geophone

Moreover, a hydrophone (Benthos AQ-18 or HITEC HTI-99-DY) is mounted outside of the glass sphere.

Deployment of the OBS is by free-fall from the sea surface to sea bottom; each OBS has iron weight of about 40 kg attached underneath that causes it to sink. Descent speed is about 85 m/min. During the descent, the OBS position is calculated by the ship's Acoustic Navigation System (ANS) based on travel times of acoustic communications between the OBS's and ship's transponders. Retrieval of the OBS starts with release of the iron weight by an acoustic signal from the ship, which takes about 15-20 minutes. Once the weight is released and left behind on the seafloor, the buoyancy of air inside the glass sphere causes the OBS to ascend at a speed of about 65 m/min. When the OBS arrives at the sea surface, a radio beacon is activated to generate radio signals with call signs. For nighttime retrievals, a flashing light is also activated. Such equipment enables locating the OBS over a wide area.

The OBS transponder comes in two types: STD-303 of Kaiyo Denshi Inc. (KDC: Fig. 4) and System Giken Kogyo Inc. (SGK: Fig. 5). The KDC type has a separated transponder consisting of a transducer and a transponder pipe. The SGK type is monocoque structure that includes both a transducer and a pipe containing electrical parts.



Fig. 4: OBS with KDC transponder



Fig. 5: OBS with SGK transponder

The accuracy of the internal clock is about 10^{-6} , which is equivalent to a 0.6 s error in a week. Therefore, the internal clock of each OBS drifts from standard time over the time interval of a deployment. To adjust for drift, we measure the drift before deployment and after retrieval, and estimate the drift during deployment with a linear calculation (Fig. 6).

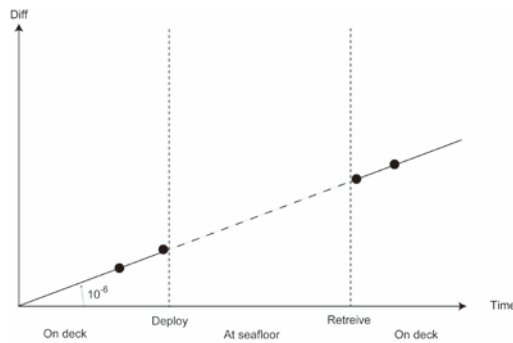


Fig. 6: Time shift and calibration of OBS clock

The OBSs were deployed at a 5 km spacing, about one every 40 minutes depending on ship speed, from the northernmost Site001 to the southernmost Site100 between Mar. 4 and Mar. 6. Recording start time was initially set at 19:30 on Mar. 6, but had to be changed because of delays in original deployment plans caused by contrary currents. Details of the OBS deployment with locations are shown in Table 1.

Airgun shooting at 200 m and 50 m intervals were conducted from Mar. 7-Mar. 10 and Mar. 10-Mar. 13, respectively. Each OBS recorded the airgun signals of wide-angle reflections and refractions arising from the OJP's internal structure (Fig. 7).

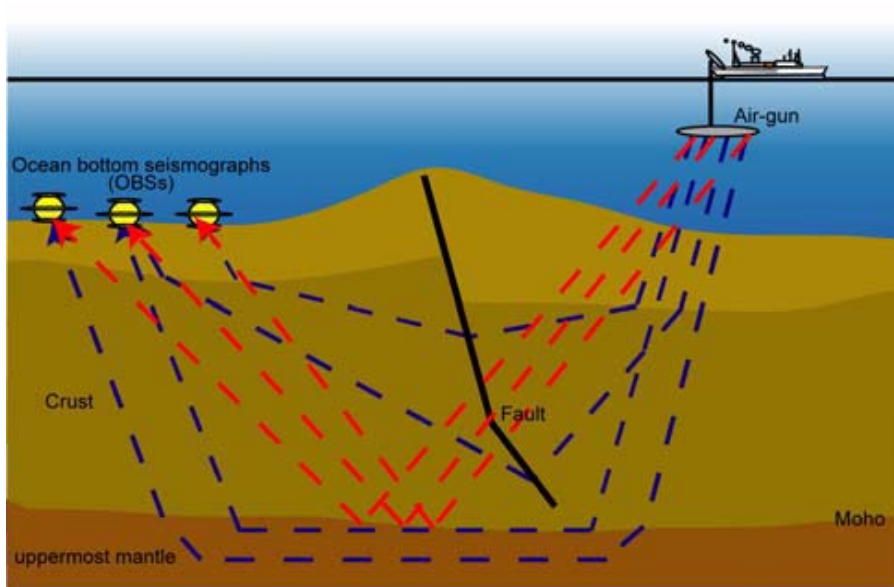


Fig. 7: Outline of OBS survey

Following airgun shooting, OBSs were retrieved from Mar. 14 to Mar. 18. Details of OBS retrieval are also shown in Table 1. During the transit to JAMSTEC, the glass spheres were opened to retrieve the HDDs and transfer the OBS data to external storage. The OBS data stored externally were processed and output to receiver gathers in the time-distance domain. Figure 8 shows examples of OBS data in the time-distance domain.

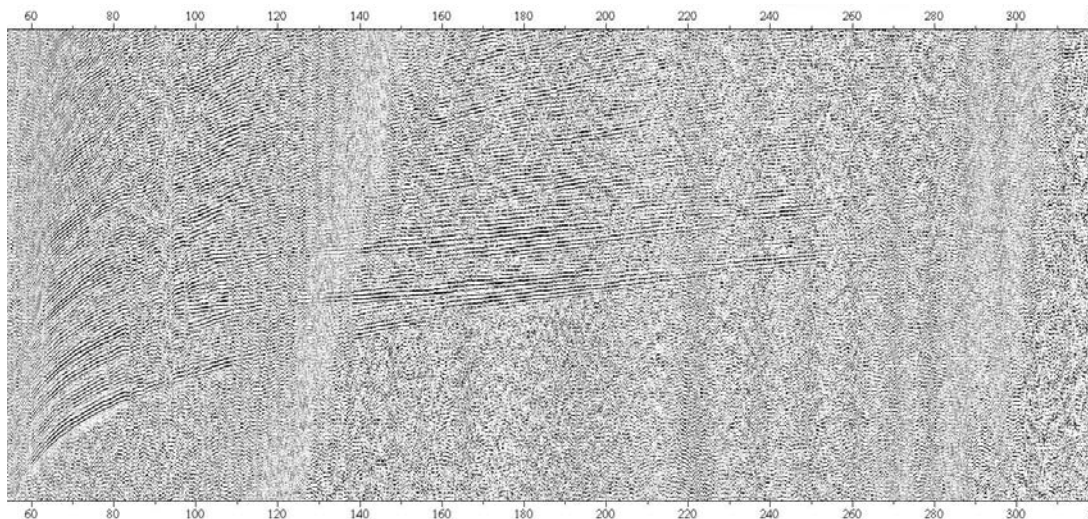


Fig. 8: Examples of OBS data in the time-distance domain (Site100). Vertical component, with band-pass filter and auto gain control (AGC) are applied.

GPS (Global Positioning System)

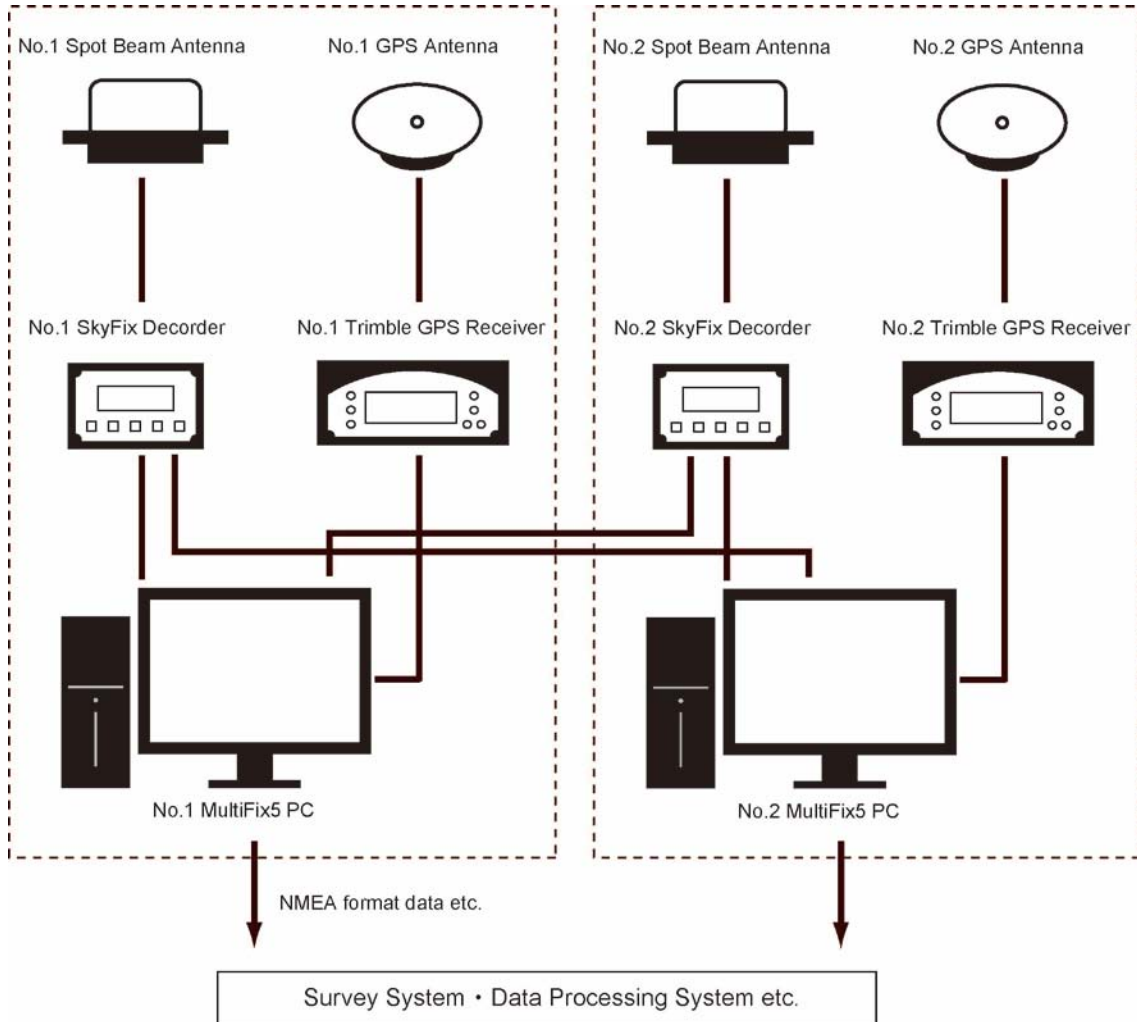
Outline of system

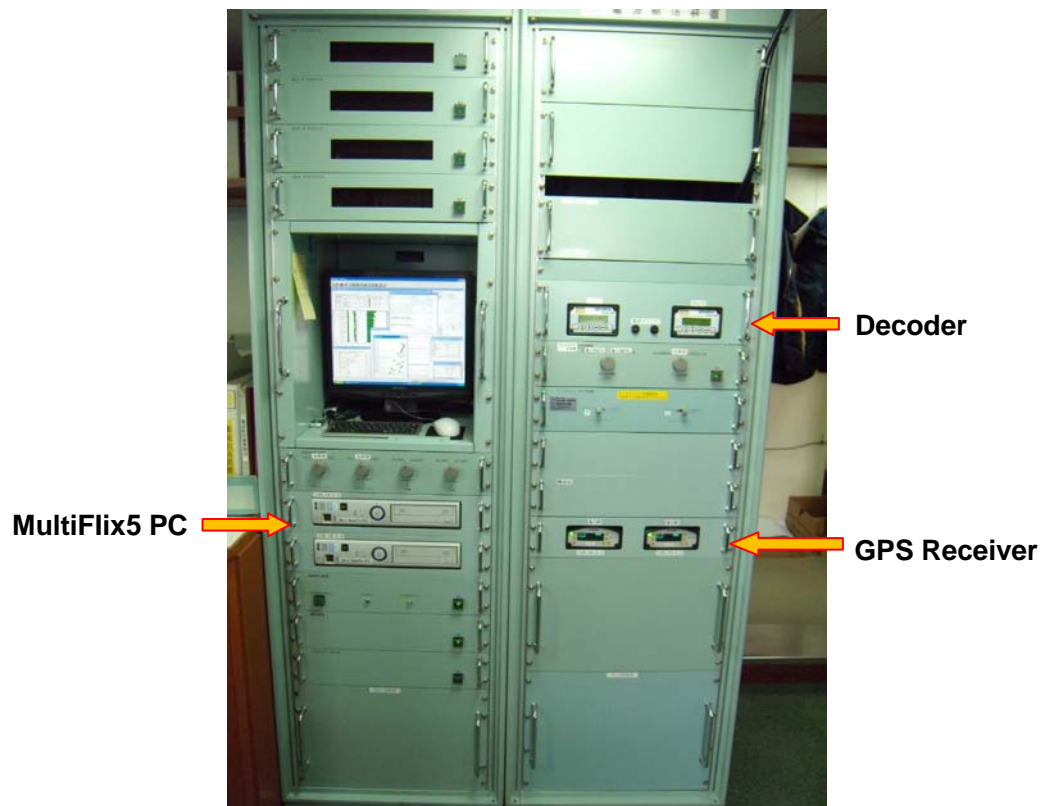
R/V "*KAIREI*" has two independent GPS antennas. The GPS antennas are mounted on the highest open deck on the ship, and receive signals from several satellites (ideally, more than five for precise and accurate navigation). As the ship moves, its location requires correction, using signals from a fixed base point. These correction data are sent by "Spot Beam*1" to an instrument called "SkyFix-XP (Fugro)" on the *KAIREI*. SkyFix-XP (Decimetric Differential GPS) corrects the errors from the satellite (clock, orbit, ionospheric delay, tropospheric delay, multipath), which are generated in the existing Differential-GPS (D-GPS), by using Precise Point Positioning (PPP) technology. In addition, "MultiFix5 software (Fugro)" determines more precise positions. Major specifications are shown below.

- 1) High-precision calculation of positioning (Horizontal: 10cm, Vertical: 20cm (95%))
- 2) Almost worldwide covered area which is independent of distance from the base point
- 3) Correction of GPS satellite errors (clock, orbit, ionospheric delay, tropospheric delay, multipath)
- 4) Double satellite beam (Spot Beam system)
- 5) Display based on UKOOA (United Kingdom Offshore Operators Association) standard and quality control by output signals

*1 "Spot Beam" is a new (high power) satellite system that is an alternative to "INMARSAT (low power)". This system became operational in Jan. 2010.

System configuration of GPS is shown below. Two basic systems are operated in parallel for improved reliability.

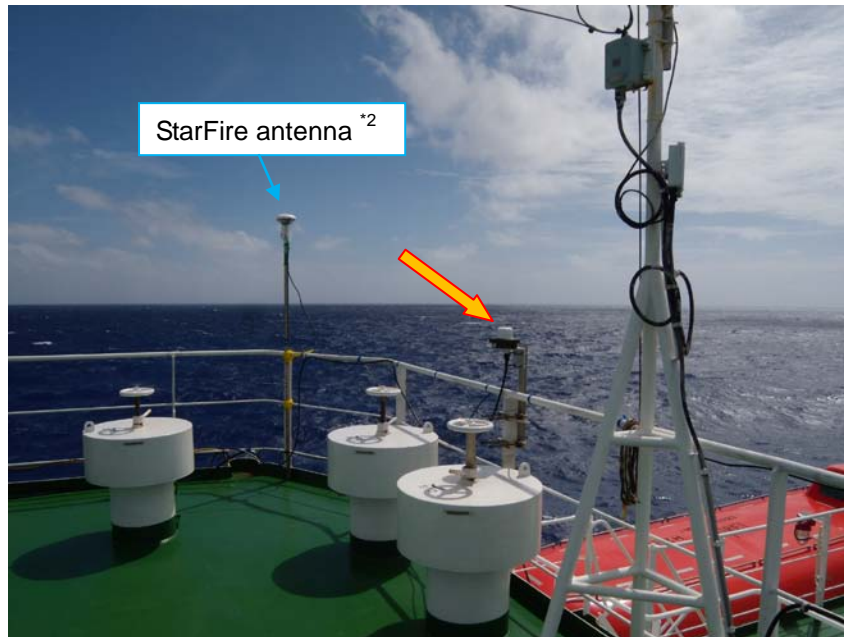




SkyFix-XP system

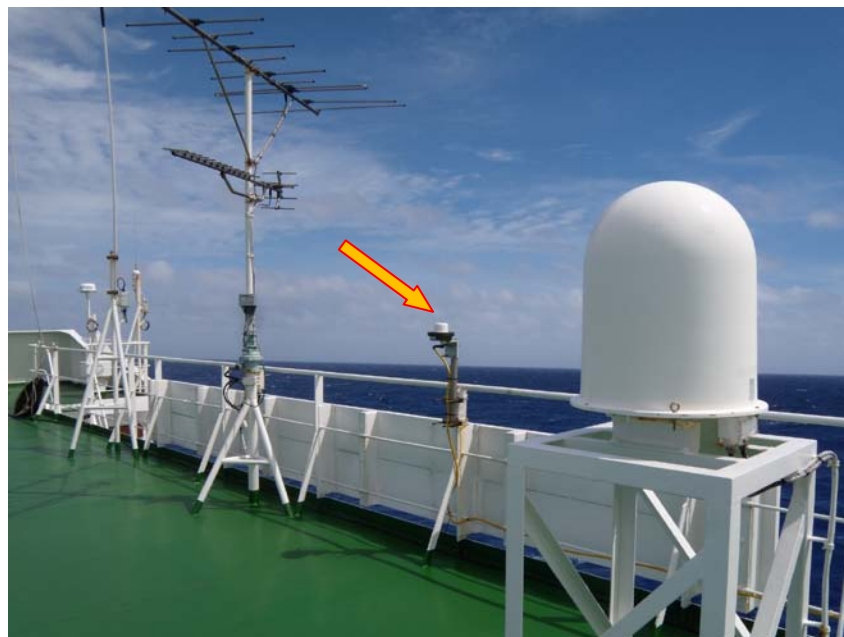


GPS antennas



Spot Beam antenna

*2 "StarFire" is another GPS system for MCS navigation data



Spot Beam antenna

Data acquisition

Several types of output data format are available. For example, NMEA (National Marine Electronic Association) GGA is used for MCS navigation. In the case of a 1 s sampling interval, when *KAIKEI* is traveling at 15 kts, the distance traveled between fixes is about 7.7 m, and at 5 kts (MCS survey speed) the distance is about 2.6 m.

SeaBeam

Outline of system

Bathymetric data are collected by the SEA BEAM 2112 (Sea Beam Instruments). The SEA BEAM 2112 is a multi-beam survey system that generates data, and produces wide-swath contour maps and side scan images. It transmits sonar signals from projectors mounted along the keel of the ship. The sonar signals travel through the sea water to the seafloor and they are reflected off the bottom. Hydrophones mounted across the bottom of the ship receive the reflected sonar signals. The system electronics process the signals, and based on the travel time of the received signals and intensities of the signal waves, calculate the bottom depth and other characteristics such as S/N ratio for echoes received across the swath. Positioning of depths on the seafloor is based on GPS and ship motion input. The data are logged to the hard disk for post processing which allows for additional analysis. Plotters and a side scan graphic recorder are also included with the system for data recording and display.

Hardware and Software overview

The hardware system consists of two main subsystems, transmitter and receiver respectively. Fig. 1 shows a basic diagram of the system. The basic 12 kHz projector array is a 14-foot long linear array positioned fore and aft along the ship's keel. It forms a downward projected acoustic beam for which the maximum response is in a plane perpendicular to its axis. The beam angle is narrow, 2° in the fore/aft direction. The receiver array detects and processes the returning echoes through stabilized multiple narrow athwartship beams in a fan shape. The hydrophone array has a flat shape in the case of R/V "*KAIRET*", although the standard SEA BEAM 2000 series system has a V-shaped array (Fig. 1). The system synthesizes $2^\circ \times 2^\circ$ narrow beams at an interval of 1° , and the swath width varies from 120° at depths from 1500 m to 4500 m, to 100° from 4500 m to 8500 m and deeper than 8500 m, as shown in Fig. 2. The transmit interval of the sonar signal ping interval increases with water depth; for example, the interval is about 20 s at 6500 m. Thus, the horizontal resolution of the bathymetry data depends on the depth and ship's speed. The accuracy of the depth measurement is reported at 0.5% of the depth.

The software which controls the system is called Sea View. It employs the Lynx Operating System. Indy Work Stations (SGI) are used for operation. The obtained raw

data includes data records of each ping (bathymetry, side scan image, position, etc.), nautical information and correction parameters such as water velocity structure. Post processing consists of editing data (deletion of bad data, correction of position, etc.), making grid data files and various maps. The software used is Sea View and GMT

Major specification of the SeaBeam system

Measurement Depth		50~11000m
Swath Width	~4500m	120°
	~6000m	100°
	~11000m	90°
Transmission Beam Angle		2° (-3dB)
Receiving Beam Angle		2° (-3dB)
Pulse Length		3~20 ms
Frequency		12 kHz
Pulse Width		3~20 ms
Sampling Interval		1.33 ms or 2.67 ms
Roll Angle		±20°
Pitch Angle		±7.5°
Vessel Speed		0~30 kt

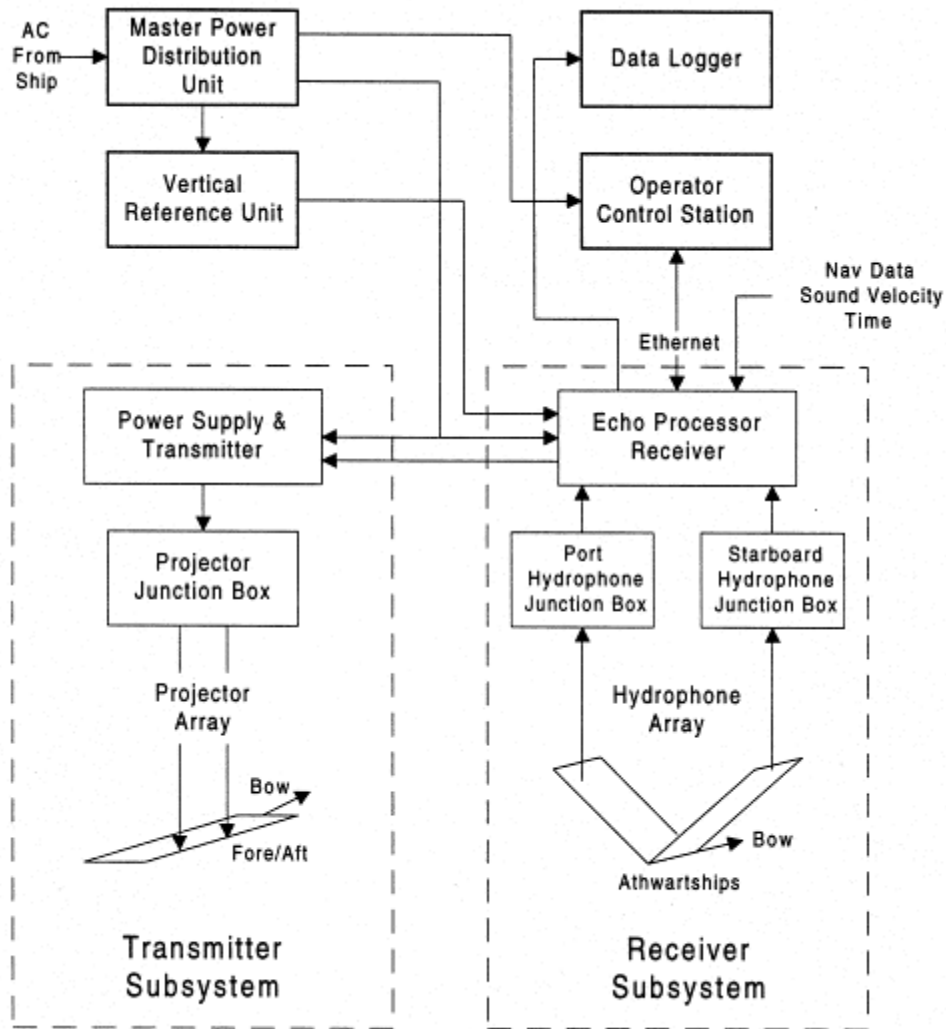


Fig.1. Basic diagram of the SeaBeam system

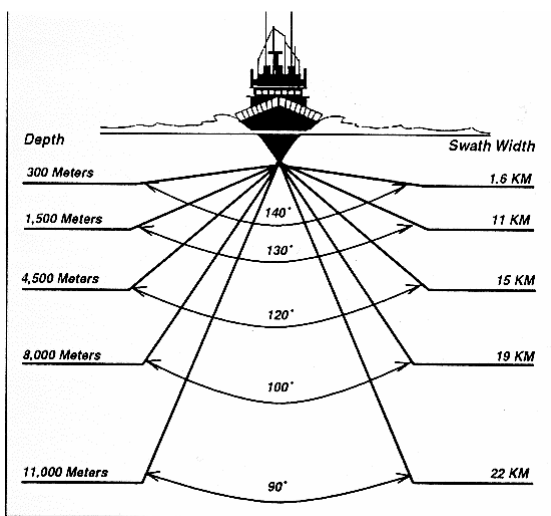


Fig.2. Relation of swath width to depth



SeaBeam system & Work stations

Data acquisition

Bathymetric surveys were carried out during most of the cruise, except during the retrieval of OBSs. In particular, the radio officers edited three lines of the data, the MCS survey line and two short transit lines (transit from the end of OBS deployment to airgun shooting for OBSs, and transit from the MCS survey to OBS retrieval). During the two short transits, we acquired bathymetric data south of Tauu Atoll. Bathymetric maps produced from the new data are shown below (Figs. 3-5).

KR1005

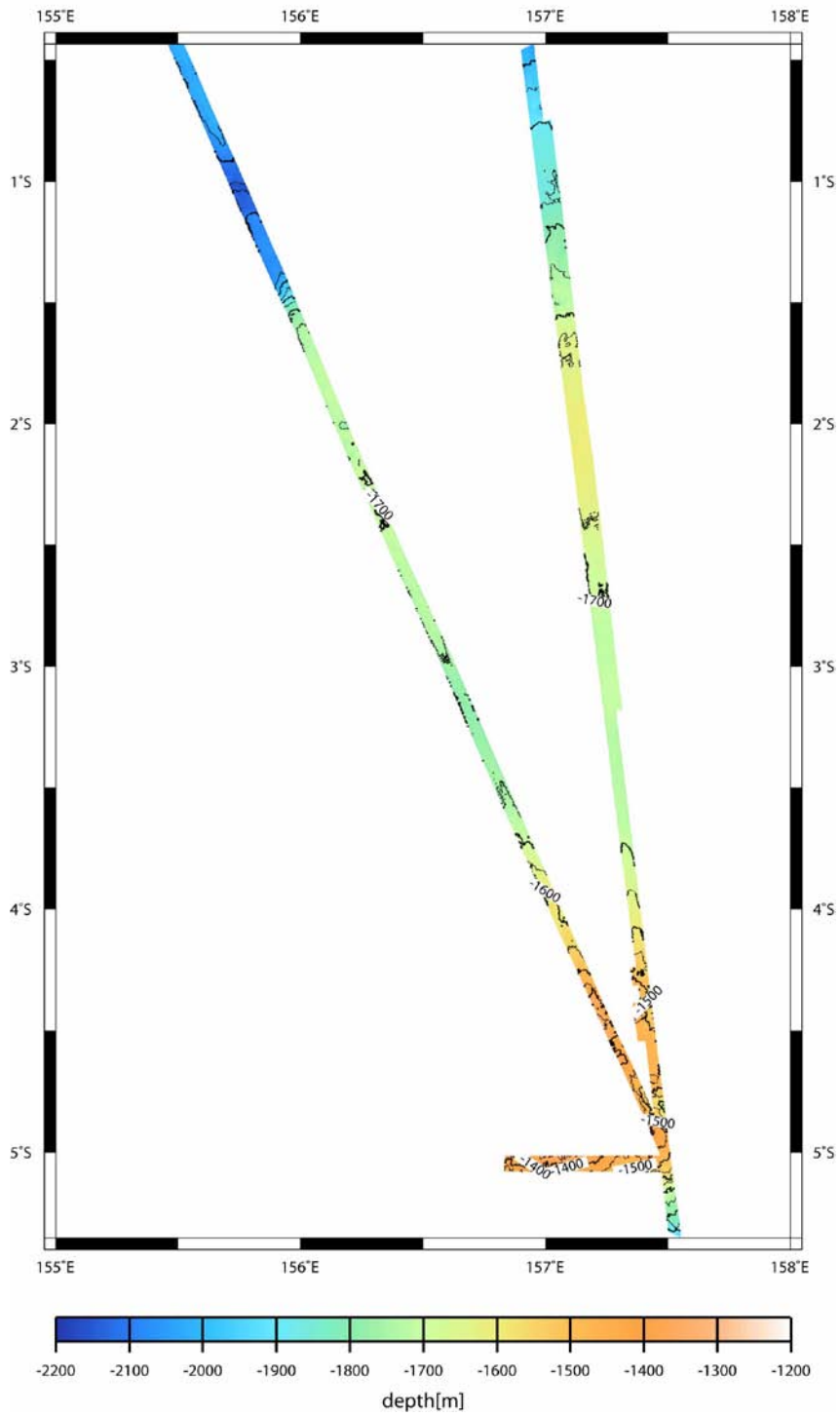


Fig. 3: SeaBeam data acquired during this cruise on the OJP

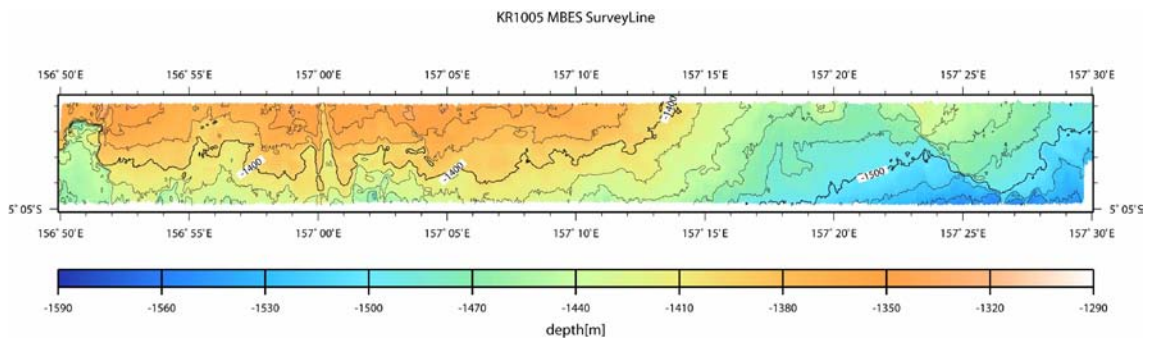


Fig. 4: SeaBeam data from the southern flank of Tauu Atoll

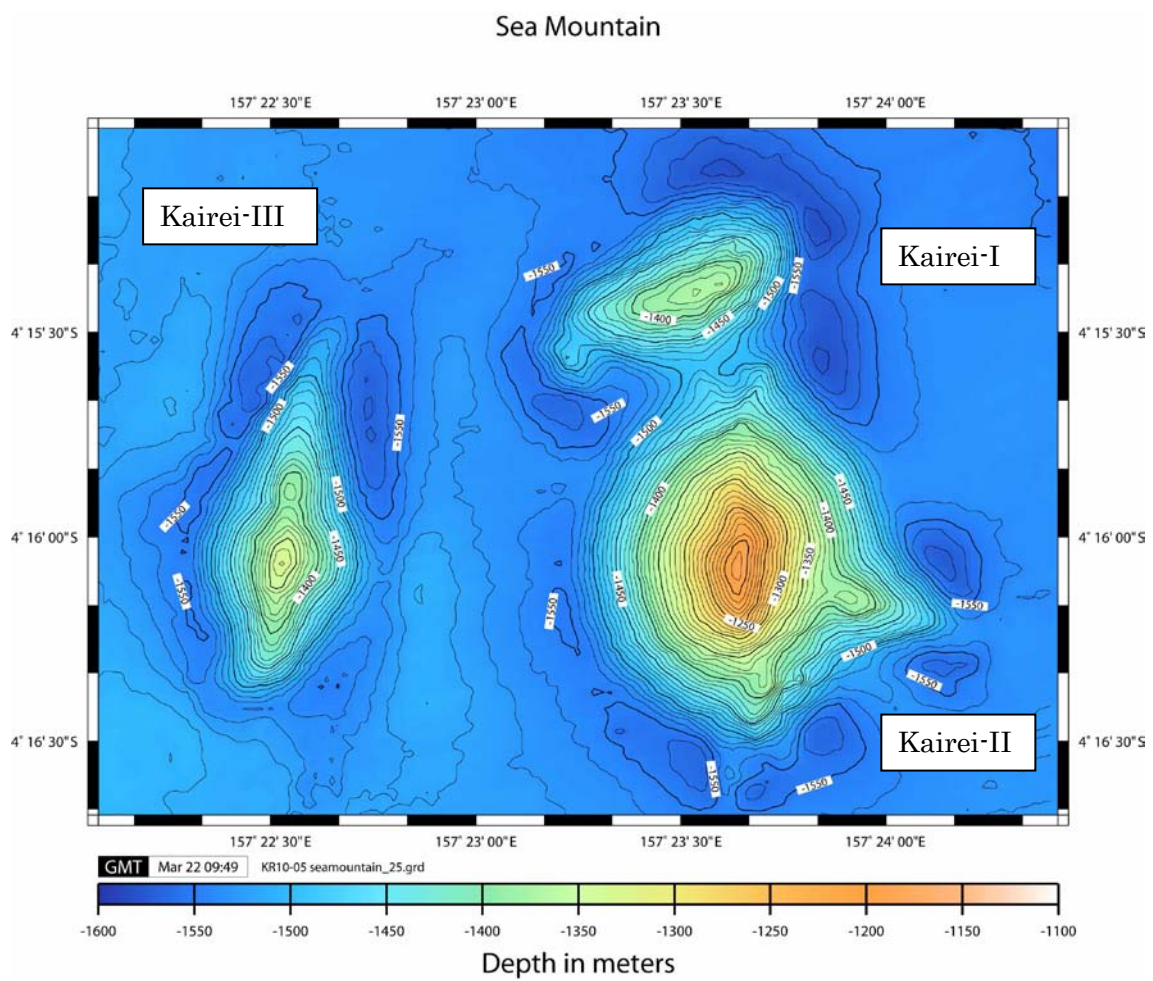


Fig. 5: SeaBeam data showing seamounts discovered during this cruise near Site082

Shipboard Three-Component Magnetometer

Outline of system

A shipboard three-component magnetometer system (Tierra Tecnica SFG1214) on R/V “*KAIRET*” was used for magnetic field measurements. Three-axes flux-gate sensors with ring-cored coils were fixed about 2 m above the deck above the bridge. Outputs of the sensors were digitized by a 20-bit A/D converter (1 nT/LSB), and sampled at 8 times per second. Ship's heading data were also sampled at 8Hz, which were transmitted directly from a gyro compass for navigation in the bridge. Roll and pitch data of 8 Hz are provided from an attitude sensor (TVM-4) installed on the floor of the gravity meter room. Ship's position (GPS) and speed data are taken from the LAN every second. Data are logged on a personal computer. The data are stored on the internal hard disk drive of a PC in ASCII format, and transferred to a workstation for processing using FTP.

Hardware overview

The three-component Magnetometer consists of three major units. The system configuration is shown in Fig.1.

a. Magnetic sensor:

Flux-gate magnetic sensors with ring-cored coils are configured orthogonally to measure the three components of the Earth's magnetic field. The sensors are fixed on the open deck above the bridge to reduce artificial noise and effects of magnetic structures.

b. Measurement unit:

The measurement unit converts the signal of the magnetic sensor into the magnetic field value. At the same time, it reads the data from the gyro compass and attitude sensor. Outputs of the sensors are sampled at 8 times per second, which are transmitted to the data recording unit.

c. Data recording unit

The data recording unit edits the data that are transmitted from the measurement unit, the navigation data (time, latitude, longitude, vessel speed etc.) and the absolute magnetic field value, and outputs the data to the shipboard LAN.

Attitude sensor:

The attitude sensor is a strapped down system which combines accelerometer and fiber

gyro. Roll and Pitch data are provided and transmitted to the measurement unit.

Major specifications of 3-componet magnetometer

Magnetic Sensor	System	Flux-gate sensor with ring-cored coils
	Number of components	Orthogonal 3 components
	Orthogonal Degree	$\leq \pm 2$ min
	Cable Length	50 m
	Size, Weight	ϕ 280×130H (mm), 5 kg
Measurement Unit	Measurement Range	± 100000 nT
	Resolution	1 nT
	Noise	0.5 nT
	Temperature Stability	0.5 T/°C
	Absolute Accuracy and Linearity	< 100 nT
	AD converter	20 bit
	Conversion Rate	8 times/sec
	Digital Input	RS232C 3ports
	Size, Weight	480W×150H×430D (mm), 4kg
Data Recording Unit	Recording Media	Hard disk drive
Attitude Sensor	Measurement Item	Roll angle, Pitch Angle
	Measurement Range	$\pm 45^\circ$
	Accuracy	$\pm 0.2^\circ$ ($< 30^\circ$)
	Resolution	0.0055°/LSB
	Output	RS422 compliance
	Size, Weight	ϕ 320×180H (mm), 5kg
Others	Power Supply	Single Phase AC100V, 50/60Hz
	Power Consumption	350VA

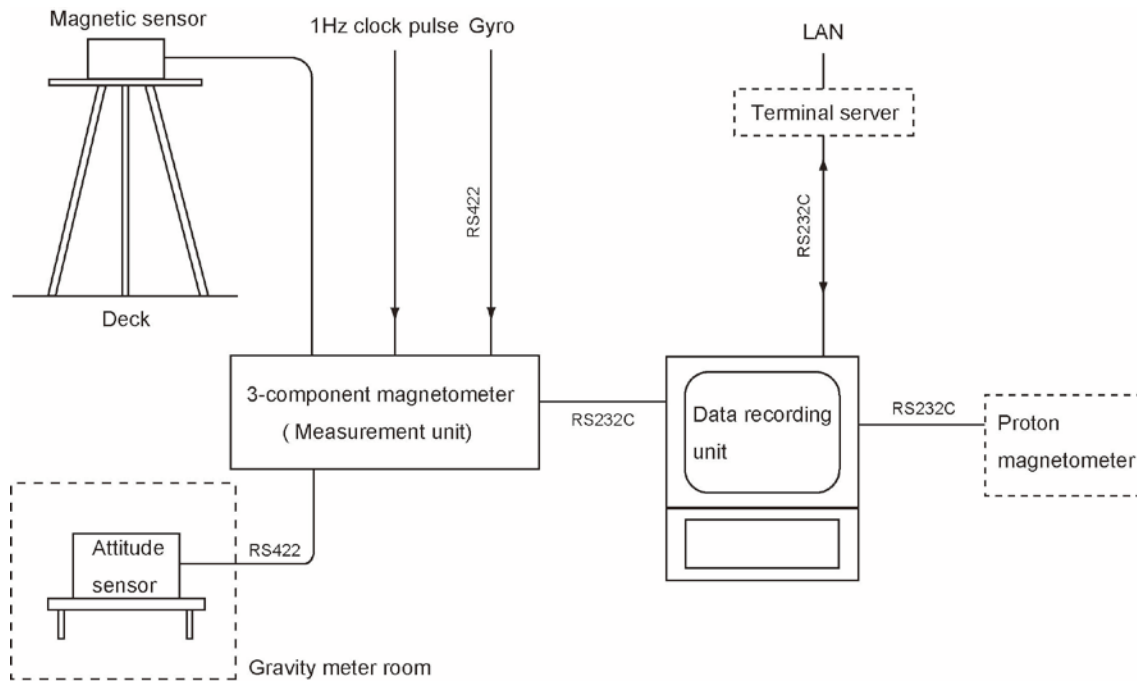
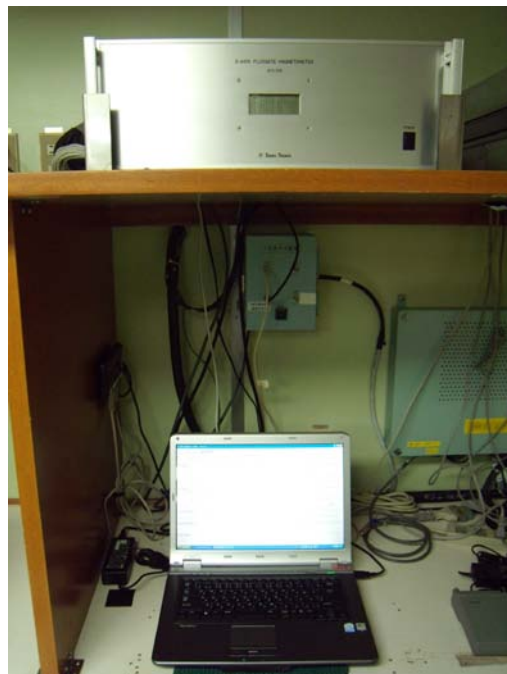


Fig.1. System configuration of 3-component magnetometer



Magnetic sensor (Deck)



Measurement unit (upper) & Data recording unit (lower)
(Geophysics laboratory)



Attitude sensor (Gravity meter room)

Data acquisition

Three components of magnetic field data were recorded from the departure to the arrival date at the JAMSTEC pier in Yokosuka (2010/2/25 to 2010/3/26). The measurement interval is 1/8 second. The resolution of the magnetic measurement is 1 nT.

Gravity meter

Outline of System

Shipboard gravity measurements are made using a BODENSEEWERK KSS31 marine gravity meter system. This system is installed in the gravity meter room and consists of two main components, a platform containing a gyro and a gravity sensor, and an electronic circuit to determine gravity. An on-line data filter for "Sea State 4" was selected, which enabled us to obtain good gravity data with smooth variations. According to the documents provided by the manufacturer, the filter should cause a delay of 123 seconds. The gravity data were logged every minute throughout the cruise. Shipboard gravity is tied to absolute gravity at the pier and Marine Technology Research Building at JAMSTEC.

The system incorporates ship's position, speed, and heading through the ship's LAN, performing the Etovös correction*¹ on-line. Free-air gravity anomaly*² data presented in this report are based on the on-line Etovös corrected gravity without drift correction. Readjustment of time differences between filtered gravity and ship's speed and heading might be required for onshore data processing.

*1 Etovös correction

Gravity is a resultant force of terrestrial gravitation and centrifugal acceleration; therefore observed shipboard gravity contains an error caused by centrifugal acceleration. For example, if a ship travels from west to east, the influence of centrifugal acceleration is greater than if the ship were stationary. In this case, observed gravity is less than actual gravity. This phenomenon is called the "Etovös Effect". A positive correction for the Etovös Effect is required when a ship runs west to east, and a negative correction is required when a ship runs east to west.

*2 Free-air gravity anomaly

The free-air gravity anomaly is derived from the altitude of an observation position which is relative to the geoid. In the case of a land gravity survey, this anomaly depends on topography. However, in the case of shipboard gravity, the sea surface is an equipotential surface approximately equivalent to the geoid, because the difference between the sea surface and geoid is not significant (<10 m).

Major specifications of Gravity meter

Accuracy on Profile	Vertical Acceleration	DYNAMIC* (mgal RMS)	EFFECTIVE** (mgal RMS)
	<15,000	0.5	0.2
	15,000 - 80,000	1	0.4
	80,000 - 20,0000	2	0.8
Accuracy during Turn	Vertical Acceleration	DYNAMIC*** (mgal RMS)	EFFECTIVE*** (mgal RMS)
	15,000 - 80,000	2.5	1
Drift Rate (mgal/month)	<3		
Measuring Range (mgal)	10,000		
Scale Factor Calibration (standard)	<0.5%		
Platform Freedom	Pitch	±40°	
	Roll	±40°	
Environmental Conditions	Temperature	+10°C up to +35°C	
	Temperature Gradient	<2°C/hour	
Response Time	Definition	$t = 1/2\pi fc$ fc = corner frequency	
	Gravity Sensor	$\tau = 36$ s (low pass filter 1 st order)	
	Selectable Filter	$\tau = 5.2$ to 75 s (Bessel filter 4 th order)	
Data Interface	Analogue Output for Signal Monitor	2 to 6 channels	
	Digital Data Interface	Standard V24 or RS232C serial data transmission	
Power Supply	All Systems	220V, 50 Hz, single phase or 110V, 60 Hz, single phase (transformer) or 240V, 50-60 Hz, single phase (transformer)	
Weight and Size	Platform, Sensor and Gyro	72kg, 68×53×53 (cm ³)	

	Gravity Measurement Electronic Circuit (19inch rack)	200kg, 55×65×183 (cm ³)
--	---	-------------------------------------

* Accuracy without applying data reduction

** Accuracy applying data reduction procedures

*** Depending on accuracy of navigation data



Gravity meter system rack



Gyro & Sensor

Data acquisition

Gravity data were recorded from the departure to the arrival date at the JAMSTEC pier (2010/2/25 to 2010/3/26). These data were sampled every minute, so when *KAIREI* was traveling at 15 kts, the distance traveled between fixes is about 463 m, and at 5 kts (MCS survey speed) about 154 m. Shipboard gravity data must be corrected using absolute gravity data from land. For KR10-05, the shipboard gravity data were corrected using absolute gravity values obtained at the pier and Marine Technology Research Building at JAMSTEC.

XBT (eXpendable Bathy Thermograph)

An XBT is a measurement system for seawater temperatures, using a probe with a temperature sensor (T-5 probe, Tsurumiseiki Inc.; Fig. 1) wired to the digital converter (TS-MK130, Tsurumiseiki Inc.; Fig. 2) and the computer in the ship's laboratory (Fig. 3). A probe is dropped from the stern of the ship. During descent of a probe, seawater temperature is measured continuously. Maximum depth of the T-5 probe is 1830 m, which is equivalent to 291 s in time. Depth of a probe is calculated by time, because the descent speed is constant. From the temperature data, a vertical profile of sound speed is calculated. The sound speed information is used for sound speed corrections of the Seabeam bathymetric survey data. During this cruise, nine XBT measurements were conducted for correcting the sound speed across equatorial currents (Table 1).



Fig. 1 Probe deployment



Fig.2: Digital converter



Fig. 3: Computer for XBT

Table 1: Conducted Details

No.	Date	Time (JST+1)	Lat.	Lon.
XBT1	2010. 3. 4	9:05:00	0-36.3811 S	156-55.9185 E
XBT2	2010. 3. 5	8:10:30	2-23.2122 S	157-09.8380 E
XBT3	2010. 3. 6	0:06:47	3-31.7245 S	157-18.2937 E
XBT4	2010. 3. 6	7:46:00	4-02.1534 S	157-22.0016 E
XBT5	2010. 3. 6	15:01:01	4-28.1981 S	157-25.2102 E
XBT6	2010. 3. 6	23:03:55	5-03.1327 S	157-29.5895 E
XBT7	2010. 3. 15	10:32:59	3-02.3293 S	157-14.6962 E
XBT8	2010. 3. 16	7:57:01	1-54.1912 S	157-06.2208 E
XBT9	2010. 3. 16	16:55:30	1-22.6109 S	157-02.2573 E

Notice on use:

This cruise report comprises preliminary documentation as of the end of the cruise. It may not be corrected even if changes in content are found after publication. It may also be changed without notice. Data in the cruise report may be raw or not processed. Please ask the PI(s) for the latest information before using. Users of data or results of this cruise are requested to submit their results to Data Integration and Analysis Group (DIAG), JAMSTEC.

THE GEOLOGICAL FRAMEWORK OF PAPUA NEW GUINEA – AN OVERVIEW

Ronald Verave

Geological Survey Division, Mineral Resource Authority, Papua New Guinea

Simon A. Kawagle

Earth Sciences Division, University of Papua New Guinea, Papua New Guinea

ABSTRACT

Papua New Guinea (PNG) has a complex geology, which is due its tectonic setting. The region is sandwiched in between two major opposing tectonic plates – Indo-Australian Plate to the south-southwest and the Pacific Plate to the east-northeast, which converges obliquely. Nevertheless, the geological framework is best described as a series of geological terranes or discrete geological regions, which are commonly separated by geological elements. The typical tectonic setting also gives rise to a complex seismicity pattern, and contributing significantly to the style of mineralisation found in the region.

Most of mainland PNG is underlain by the Australian Craton. The rest of the material that make up the landmass is of Late Cretaceous age or younger metamorphosed and unmetamorphosed island arc volcanic rocks that had collided with the Craton. Material from obducted oceanic crust and igneous intrusive and volcanic rocks also contribute a significant percent of the total rock volume.

The initial collision and accretion of volcanic arc with the Craton was the Irian Jaya arc in Late Cretaceous; which has resulted in the emplacement of ophiolites. This was followed by East Papua volcanic arc with the Owen Stanley Terrane in the Paleocene. Subsequent collisions and accretion included Sepik (Salumei) arc in the Late Eocene-Oligocene, Finisterre arc in Early Miocene, and Bismarck volcanic arc in Pliocene. These volcanic arcs developed above north-dipping subduction zones.

Other developments either contemporaneously with the collisions or as separate events include opening and closing of small oceans basin, suturing of terranes to the Craton, and the obduction of oceanic crust onto the Craton. The latest collision event resulted in formation of major fold and thrust belts and other fault systems on mainland PNG, magmatism and its associated mineralisation, and volcanic activities.

The jamming of the Kilinailau Trench by the Ontong Java Plateau in mid-Miocene, initiated development of the New Britain Trench, and hence a northward-dipping subduction zone in the Pliocene. At present, the Solomon Sea Plate is doubly subducting beneath New Britain, New Ireland and Bougainville at the New Britain Trench. The South Bismarck Plate is subducting beneath the PNG mainland at the New Guinea Trench. The Manus and Woodlark Basins are active spreading centres.

1.0 INTRODUCTION

Papua New Guinea (PNG) is located north of Australia and east of Indonesia. It has a central mountain range that runs the length of the country, and is bounded to the north by lesser mountain ranges and plains, and to the south by a broad plain. The Sepik River drains the north side of the central range, and the Fly River drains the south.

Beyond the southern plains a broad, shallow shelf extends to the Australian coast. Other shorelines are steeper, and some are bounded by deep sea trenches. Small ocean basins lie to the northeast and

southeast and a great submarine plateau, Ontong Java Plateau, lies to the extreme northeast, beyond the islands of the Bismarck Archipelago. Smaller submarine plateaus lie south of the eastern part of PNG.

The PNG region is regarded as an area of complex tectonic setting. The complexity is largely related to its position on the Pacific 'Rim of Fire', the interactive plate boundary between the continental Indo-Australian Plate to the south-southwest and the oceanic Pacific Plate to the north-northeast (Figs. 1 & 2). This tectonic boundary occurs as a complex arrangement of active subduction zones and associated island arcs extending as a crustal-scale suture, east and south through the Solomon Islands, Vanuatu and Fiji to New Zealand, and west into Indonesia and on to the Philippines and Japan. The boundary and arcs have not always had the current configuration, and changes in the tectonic setting through time have provided complex overprinting relationships that are reflected in the geology.

Figure 1 shows PNG's location in the 'Pacific Rim of Fire'. Figure 2 shows the geology of New Guinea region. The western part of New Guinea (Indonesia) is underlain by Pre-Cambrian basement, and the eastern part (Papua New Guinea), Palaeozoic basement.

Over many millions of years, PNG has undergone uplift and deformation as a result of collision(s) (e.g. Davies & Smith, 1974; Johnson & Jaques, 1980) of up to 100mm per year (Tregoning et al., 2000; Hall, 2002; Hill & Hall, 2002), between the northward moving Indo-Australian Plate and north-westward moving Pacific Plate. This is one of the fastest plate movements on Earth and projection of this motion back through geological time provides an indication of the degree of shortening inherent in the description of PNG as a classic terrane of craton – island arc collision (up to 100km per million years).

Due to the complexity of the region's geology, many divergent opinions and interpretations are expressed in prints that deal with the subject. This paper aims to present an overview of the geological framework of PNG as understood by many workers.

2.0 GEOLOGICAL FRAMEWORK

PNG (and including the island of New Guinea) is at an interface between the northward-moving Australian Plate and the west-northwest-moving Pacific Plate. The resultant motion is convergence at a rate of over 100 mm/yr on an azimuth close to 070°.

Convergence has led to a succession of collisions of the Australian Craton with the micro-continents and volcanic islands of the Pacific and with fragments of the Craton that had been separated from the Craton and then docked again. While the southern half of the island was always part of the Australian continent, the northern part has been added by successive collisions. In geological terms, the southern part is autochthonous and the northern part allochthonous, being made up of accreted terranes.

The boundary between the Pacific and Australian plates is marked by a number of microplates. Those offshore are bounded by spreading ridges, deep sea trenches, and transform faults (see later), and those onshore by thrust, extensional, and strikeslip faults and folds. Earthquakes are located on the microplate boundaries. Volcanic activity is associated with the deep sea trenches and spreading ridges.

PNG's geological framework can be best described as comprising a series of geological terranes or discrete geological regions. These terranes are commonly separated by geological elements, structures such as faults, fold belts and thrust belts, lineaments, basins and trenches. The terminology used to describe the individual terranes reflects the increased understanding of plate tectonic theory, as applied to the PNG region over the past 40 years.

The components that broadly define the tectonic setting of PNG include:

- The Australian Craton, which underlies the Fly Platform and much of PNG as a rigid continental block extending to the south.

- The New Guinea Orogen, represented by the mountainous spine of PNG, formed as a collision zone and can be divided into the Western (Highlands and Ramu-Sepik regions) and Eastern (Papuan Peninsula and Islands) orogens. It is a composite terrane of metamorphosed sediments that have undergone fold-thrust belt deformation, island arc magmatic extrusive and intrusive rocks, and obducted oceanic crust.
- The Melanesian Arc comprises a series of now-dismembered island arcs which lie to the north of the New Guinea Orogen, within the segmented oceanic Pacific Plate margin.
- The Caroline and Pacific Plates, which have been subducted into the Manus and Kilinailau Trenches respectively, are locally obducted onto the Orogen.

In the following section, the terranes and their bounding geological elements are briefly discussed. It starts from south to north in the western part of the country, and then central, followed by the eastern part, and finally ends up with the islands to the east and northeast of the mainland.

3.0 TERRANES AND GEOLOGICAL ELEMENTS

3.1 Southwest-north western portion

Fly Platform

The Fly Platform is a broad, low-lying, relatively level region south of the central cordillera in southwestern PNG (Figs. 3 & 4). Its basement is crystalline rocks of the Palaeozoic Australian Craton (Indo-Australian Plate) that is overlain by a thick succession of sub-horizontal, largely undeformed Triassic to uppermost Tertiary marine sedimentary rocks of near-shore and shelf facies (Dow, 1977; Struckmeyer, 1993). These are covered by a thick veneer of Quaternary sediments comprising coarse molasses derived from the rising central cordillera in the north, fining southwards.

The platform is essentially unaffected by the Cainozoic deformation that is apparent in terranes to the north. A slight uplift and southward tilting north of the Fly River resulted in shallow incision of the present day streams.

Figure 3 shows the geological framework of PNG and include the geological terranes and their bounding geological elements discussed in this paper. Figure 4 shows only the geological terranes. The Aure Deformation Zone has been formerly referred to as Aure Fold Belt (AFB) as indicated in Figure 2.

Papuan Thrust (north-western part)

The Papuan Thrust occurs as a partly mapped, partly inferred co-linear series of shallow north-dipping thrust planes along the edge of the foothills of the Southern Highlands. It is thought to represent the basal thrust separating overlying deformed Papuan Fold Belt sediments from the underlying, minimally deformed sediments of the Fly Platform (Rogerson et al., 1987a). The thrust is inferred to continue south of mainland PNG, offshore and underlying of the Eastern Fold Belt, in eastern PNG (see later).

Papuan Fold Belt

The Papuan fold belt (Figs. 3 & 4) is an elongate southeast-trending geological terrane dominated by a thick succession of folded and thrust-faulted Upper Triassic to uppermost Tertiary (Hill, 1991) marine sedimentary rocks, occupying the southern fall of the central cordillera in the western mainland and merging in the southeast into the Aure Deformation Zone. The thickness of the entire sequence within the Fold Belt is estimated to be 2000m of Cretaceous sandstone, overlain by 1000m of Miocene to Quaternary limestone, sandstone and shale (Davies, 1992). The Papuan Fold Belt hosts significant mineral, oil and gas resources. The mineral resources are hosted within Miocene-Pliocene dioritic intrusive rocks. Jurassic shales play source rocks and Cretaceous sandstones, reservoirs to the oil and gas resources.

A major geographical feature of the Papuan Fold Belt is the Darai Plateau, which forms an extensive belt of karst limestone country developed on thrust blocks of Late Eocene to Late Miocene Darai Limestone. Quaternary stratovolcanoes surrounded by thick, widespread lahar outwash deposits rise 1500-2000m above the surrounding countryside. Volcanic activity is believed to have ceased, although fumarole hot springs occur and oral history across the region suggests a major eruption occurred in the Doma Peaks area several hundred years ago. Some craters deeply eroded, but many volcanic landforms are still well preserved. Extending southeast from the Mt Bosavi massif and bordering the Fly Platform, Quaternary volcanic centres including recent cones can be identified on aerial photographs.

New Guinea Thrust

The New Guinea Thrust (Fig. 3) is a corridor of arc-parallel structures that form a terrane boundary separating the Papuan Fold Belt from the region of intense deformation to the north, the New Guinea Thrust Belt. The Lagaip Fault is the most prominent structure in the western portion of the thrust (Davies, 1982). To the east, the thrust probably encompasses the Ambum and Kubor Faults (Davies, 1983), but is not easily traced east of Quaternary basalt cover in the Mt Hagen area (Dow, 1977; Smith, 1990). It continues west into West Papua as the Tahin Fault, in each case separating uncleaved from cleaved rocks (Davies, 1991).

New Guinea Thrust Belt

The New Guinea Thrust Belt (Figs. 3 & 4) occupies the northern section of the Western Orogen, and is separated from the Papuan Fold Belt to the south by the New Guinea Thrust, which includes the Lagaip Fault. The Belt is characterised by Upper Miocene foreland thrust deformation, represented by strongly cleaved, sub-horizontal to shallow north dipping stacked sheets and slices of regionally metamorphosed Mesozoic to Early Tertiary fine grained sediments. The latter are thought to be the deep water equivalents of the Papuan Fold Belt sedimentary succession to the south. Ophiolite slivers occur in late stage thrusts. The deformed sequence is overlain by volcanics and clastic sediments.

The New Guinea Thrust Belt is divisible into two zones:

- A northern zone of medium-grade metamorphic rocks of possible pre-Oligocene Tasman Orogen 'basement' origin, which crops out in low mountain ranges across the Sepik Plain. Intrusives of the Sepik Arc magmatic event (30-22 Ma, uppermost Oligocene to earliest Miocene) are exposed in the 'basement' country rocks (Dow, 1977; Rogerson et al., 1987b). Further to the east, another example is the Yuat Batholith (22.5-14.2 Ma), bounded by the Yuat Gorge and lower Lai River (Davies, 1982).
- A southern zone of predominantly low-grade regionally metamorphosed sedimentary rocks that occupies the northern flank of the central cordillera and hosts the Maramuni Arc magmatic activity. Maramuni Arc magmatic was much more extensive than that of the Sepik Arc and was active for some time after the commencement of thrusting. The Maramuni Arc was initially interpreted to have been emplaced in the 16-10 Ma time (extending from uppermost Early Miocene into early Late Miocene, but mostly Middle Miocene) (Davies, 1982; Davies et al., 1996; Rogerson et al., 1987b), but is now described as extending into the Pliocene (Findlay, 2003). Intrusions have a complex relationship with thrust planes, cutting across some, while being truncated by others.

The two zones are separated along the foot of the main cordillera by an east-west system of anastomosing low angle faults – the Fiak-Leonard Schultze Thrust system, which extends east to the Ramu-Markham Fault Zone. The northern boundary is locally obscured by thick Pliocene sediments that extend eastwards into the middle Ramu River area, covering the projected northwestern extension of the Ramu-Markham Fault Zone and any eastward extension of the higher grade metamorphics beyond the fault zone.

Late stage thrusts emplaced shallow dipping sheets and slices of obducted upper mantle and seafloor volcanics along the northern forefront of the central cordillera in the Late Miocene, forming three extensive ophiolite complexes – the Landslip Range Eocene seafloor volcanics and intercalated argillite in the west, the April Ultramafics in the centre, and the Marum Basic Belt in the east. These ophiolites were obducted at a different time to the Papuan Ultramafic Belt ophiolites of the Eastern Orogen.

Magma-derived gold and copper mineralisation developed in two periods within the terrane, an older Sepik event (30-22 Ma), and a younger ‘Maramuni’ event (17-10 Ma). East from Simbai, major uplift of the cordillera south of the Ramu River (the summit of Mt Wilhelm at 4509m in the Bismarck Range is PNG’s highest mountain) exposes Maramuni event intrusions of batholithic proportions in the Bismarck Intrusive Complex, Akuna Intrusive Complex, and the western margin of the Morobe Granodiorite. Obducted ophiolites along the forefront of the Bismarck Range, south of the Ramu River, expose large areas of upper mantle ultramafic rocks (the Marum Basic Belt), in which deep tropical weathering of dunite has produced the Ramu (Kurumbakari) Ni-Co lateritic deposit.

3.2 Central portion

Bewani Torricelli Terrane

The Bewani-Torricelli Terrane (Figs. 3 & 4) extends along the northwest coast of PNG from the western limit at the West Papua border through the Bewani, then Torricelli Mountain ranges. The Kairiru Island Group, located just offshore mid-way through the length of the belt, is included in this terrane. In the western sector, the terrane’s southern limit is defined by sediments of the Pliocene Aitape Trough. In the North Sepik region, widespread outcrop of Mesozoic metamorphics and intrusions, interpreted from gravity data, suggests that a continuous crystalline basement extends at depth across the Sepik Basin from the present coastline, south to the central cordillera.

The Bewani-Torricelli Mountains are dominated by Eocene seafloor volcanics and Late Oligocene island arc volcanics. This is coupled with widespread largely co-magmatic intrusions that return radiometric ages in the broad range of 73.2-17.3 Ma (Late Cretaceous to Early Miocene) (Davies, 1982; Rogerson et al., 1987b).

The Prince Alexander Mountains centred on a core of Jurassic metamorphic rocks and intrusions are tentatively included in this terrane. The mountains form a 100km long range splaying eastwards from the southern edge of the central Torricelli Mountains. A wide range of radiometric ages has been recorded for the intrusions, including Middle Jurassic, Early Cretaceous and uppermost Oligocene to Early Miocene (Rogerson et al., 1987b).

Finisterre Terrane

The Finisterre Terrane (Figs. 3 & 4) comprises the mountain belt that extends for at least 550km along the north coast of the New Guinea mainland from around the mouth of the Sepik River and eastwards through the Adelbert, Finisterre and Sarawaget Mountains. The latter comprise the Huon Peninsula where the belt reaches its widest dimension of 100km.

This terrane has traditionally been regarded as a classic example of an allochthonous terrane, formed at a great distance and accreted onto the north coast of PNG by subduction of the intervening lithosphere or strikeslip movement before the Early Miocene. The allochthonous status of the terrane is now in doubt. Recent mapping by the Geological Survey of Papua New Guinea (GSPNG) in the Finisterre Ranges indicate that the Finisterre Terrane is autochthonous (Findlay et al., 1997), probably developed from a chain of offshore volcanic islands in the Oligocene.

Interpretations of gravity and seismic data (Milsom et al., 2001) suggest that strikeslip movement on the Ramu-Markham Fault Zone is of Recent origin, and the Finisterre-Sarawaget Mountains (with their 4000m high summits and Pleistocene reef terraces up to 700m above sea level at the north-eastern corner of the Huon Peninsula) are an upthrust nappe on a shallow north dipping thrust plane,

which may represent a westward extension of the north dipping New Britain Trench along the Ramu-Markham Valley.

Ramu Markham Fault Zone

The Ramu-Markham Fault Zone (Fig. 3) has traditionally been regarded as a terrane boundary between the New Guinea Orogen and the Finisterre Terrane (Fig. 4), and so formerly defined part of the northern limit of the New Guinea Thrust Belt. It occupies the major topographic feature defined by the Ramu and Markham Valleys, but is not easily traced westward into the Sepik lowlands. Recent fieldwork by the GSPNG (Findlay, 2003) runs counter to previous interpretations and suggestions that no substantial accretion has occurred, and the Ramu-Markham Fault Zone is not a terrane boundary, although some major structures are present.

Aure Deformation Zone

The southern margin of the Papuan Fold Belt merges with the Aure Deformation Zone or Aure Fold Belt (Figs. 2-4) that extends from near Kerema on the Gulf coast, north to the contact with the Finisterre Terrane (Ramu-Markham Fault Zone) between Kainantu and Wau-Bulolo regions. This terrane comprises tight, commonly northerly trending sub-horizontal folds and parallel faults developed by east-west compression.

The Aure Deformation Zone is made up of thick sequence of rapidly deposited Late Oligocene to Miocene and Pliocene mostly clastic sediments, folded and faulted in response to westward movement of the East Papua Composite Terrane. It extends as far east as 146.8°E.

The deformation zone is interpreted to have developed as a northern branch of the Papuan Basin in the Middle Oligocene to Middle Miocene and was subsequently inverted. Thus, the intensity of folding decreases moving upward from the Early Miocene through the Middle Miocene and into overlying Quaternary sediments (Dow, 1977). This may reflect initial strong compression in response to westward foreland thrusting during formation of the Owen Stanley Thrust Belt. The latter trends north under the Finisterre nappe at its western extremity, reducing in intensity over time as the regional tectonics changed (Dow, 1977).

The Aure and Sunshine Faults occur towards the western and eastern margins of the Aure Deformation Zone, and the latter continues into the adjacent Owen Stanley Metamorphic Complex, delineating the northern buried margin of the Wau Basin (including the Bulolo Graben). These faults are assumed to reflect deep basement structures (Williamson & Hancock, 2005).

3.3 Eastern portion – Papuan Peninsula

Papuan Thrust (south-eastern part)

The north dipping Papuan Thrust (Fig. 3) is interpreted to continue offshore from the western part of the New Guinea Orogen where it is well documented, to the eastern part of the Orogen. This is interpreted to separate the underlying Papuan Plateau Palaeozoic crystalline basement from the overlying Cretaceous and younger Eastern Fold Belt rocks (Rogerson et al., 1987a).

Eastern Fold Belt

The Eastern Fold Belt (Figs. 3 & 4) is a narrow belt of folded sedimentary rocks along the south coast of the Papuan Peninsula. Cretaceous marine sediments, including neritic arenaceous limestone with deeper water carbonate, and terrestrial turbidite, deposited in an offshore continental rift environment, have been well dated from abundant planktonic foraminifera. Late Oligocene to Early Miocene tuffs may represent the onset of island arc volcanism elsewhere in the region, while younger bathyal turbidites and carbonates are also recognised (Pigram & Davies, 1987). These rocks were intensely folded and metamorphosed during the Oligocene to Mid-Late Miocene.

Gabbro, of the Early Eocene to Mid-Oligocene Sadowa Ultramafic Complex, occurs as thrust slices within the Eastern Fold Belt rocks in the Port Moresby area (Rogerson et al., 1987a). East of Port Moresby, on the Sogeri Plateau, these rocks are overlain by basalt and andesitic agglomerate of the Pliocene Astrolabe Agglomerates.

Bogoro Thrust

The Bogoro Thrust (Fig. 3) separates the Eastern Fold Belt from the overlying Owen Stanley Thrust Belt to the north. Near Port Moresby, the Bogoro Thrust places gabbro of the Sadowa Ultramafic Complex, over Eastern Fold Belt rocks. Further west, these rocks are thrust over Pliocene sediments at the margin of the Aure Deformation Zone.

Owen Stanley Thrust Belt

The Owen Stanley Thrust Belt (Figs. 3 & 4) developed as part of the accretionary wedge resulting from collision between the continental and oceanic plates possibly initiated as early as the Late Oligocene and continuing to the Pliocene (Pigram & Davies, 1987). Consequently, at the western margin, low-grade Cretaceous metamorphic rocks are in fault contact with Middle Miocene Yaveufa Formation west of Bulolo. The Owen Stanley Thrust Belt is older than the New Guinea Thrust Belt, and so previously metamorphosed and deformed rocks (Kaindi Schist) are intruded by Maramuni Arc volcanic rocks such as the 14.5-12 Ma Morobe Granodiorite (Pigram & Davies, 1987).

The Owen Stanley Thrust Belt comprises two main northwest-southeast trending linear rock units: the Owen Stanley Metamorphic Complex and the overlying Papuan Ultramafic Belt (Fig. 3). These rock units are separated by the Owen Stanley Fault System.

The Owen Stanley Metamorphic Complex originally developed as a thick pile of Cretaceous continent-derived fine-grained marine sediments deposited in the rifted margin of northern Australia, which was subsequently tectonised to form a 375 x 80km thrust up belt occupied by the Owen Stanley Ranges (rising to 4000m above sea level). Rock types include slate and phyllite of pelitic, psammitic and lesser volcanic origin, as well as marble, conglomerate and spilite (Pieters, 1978; Pigram & Davies, 1987).

Medium to high pressure regional metamorphism, associated with continent – ocean plate collision and subduction, transformed some of the Cretaceous sedimentary rocks and accounts for much of the variation in rock types (Pieters, 1978). Blue schist and granulite facies rocks occur at the northern margin close to the Owen Stanley Fault System contact with the overthrust Papuan Ultramafic Belt. Yet, Cretaceous rocks east of Wau-Bulolo are mid greenschist facies, possibly indicative of separate collision events (Davies et al., 1997).

The Papuan Ultramafic Belt occurs in the hanging wall of the Owen Stanley Fault System as a 400km long belt some 25-40km wide, lying along the north coast of the Papuan Peninsula and into the Papuan Islands as peridotite noted on Normanby and Fergusson Islands. Pieters (1978) subdivided a wedge of Jurassic to Cretaceous ocean floor rocks that have been obducted onto the Owen Stanley Metamorphic Complex into (roughly from top to bottom): (a) Lokanu Volcanics basalt (1000m or more); (b) high-level gabbro (1000m); (c) granular gabbro (3000-4000m); (d) cumulate gabbro (1000m); (e) cumulate ultramafics (up to 500m); and (f) tectonite ultramafic (4000-8000m).

Eocene tonalite intrudes into the Papuan Ultramafic Belt rocks that are elsewhere unconformably overlain by Middle Eocene volcanics (Pigram & Davies, 1987). This has provided an upper limit of emplacement as probable Oligocene age (Rogerson & Francis, 1983; Rogerson et al., 1987a).

Owen Stanley Fault System

The Owen Stanley Fault System (Fig. 3) crops out on the northeastern side of the main range separating the Owen Stanley Metamorphic Complex and Kutu Volcanics to the south, from the obducted Papuan Ultramafic Belt ophiolite further northeast. This complex fault system comprises

cusate thrust segments with southwest senses of displacement, and linear interpreted, left lateral strikeslip components such as the Gira Fault (Rogerson et al., 1987a). The linear faults may represent extensions of rifting in the Woodlark Basin (see later). Importantly, the fault system represents the accretionary structure that sutured ophiolite over the Owen Stanley Metamorphic Complex as long ago as the Paleocene (Davies et al., 1997) or Late Oligocene (Rogerson et al., 1987a).

Wau Basin

The Wau Basin (Figs. 3 & 4) hosts the Bulolo Graben, which transects Miocene granodiorite and Cretaceous slate of the Owen Stanley Thrust Belt. The area may be interpreted as a setting of intra-arc extension on structures such as the Upper Watut and Escarpment Faults, in which gold mineralisation of the Morobe Goldfield is associated with Pliocene felsic subvolcanic units overlain by younger Pliocene sediments (Denwer et al., 1995). Extension on northwest-north to northwest orientated Upper Watut and Wandumi bounding faults, constrained between the Lakekamu Fault to the south and Sunshine Fault to the north, facilitated graben formation.

3.4 Islands to the east and northeast

Papuan Islands Terrane

The Papuan Islands Terrane (Fig. 4) represents the eastward extension of the Papuan Peninsula (extension of Eastern Fold Belt geology offshore) and includes the islands of the D'Entrecasteaux Island Group (Goodenough, Fergusson and Normanby Islands), the Louisiade Archipelago (Misima, Sudest and Rossel Islands), Woodlark Island and many other smaller islands. The islands lie on two east-southeast trending oceanic highs within the Solomon Sea – the Woodlark Rise to the north and the Pocklington Rise to the south, which are separated by the Woodlark oceanic spreading centre that commenced opening from 5 Ma (Benes et al., 1994; Taylor et al., 1999).

On the 40km long Misima Island, Paleogene basement rocks are the Awaibi Association meta-igneous ophiolite rocks in the west, and the Sisa Association meta-sedimentary suite in the east, which is intruded by many small stocks of the 8.1 ± 0.4 Ma Boiou Granodiorite (Williamson & Rogerson, 1983; Adshead, 1997). The two associations are separated by an original thrust fault with later extensional activation. This is further overlain by alkali agglomerate. Uplift on the north coast to 400m is noted in raised Quaternary coral reefs (Williamson & Rogerson, 1983).

Sudest and Rossel Islands are dominated by monotonous pelitic slate and phyllite of the Owen Stanley Metamorphic Complex? of the Papuan Peninsula, possibly deposited off the rifted margin of continental northern Australia during the Mesozoic (Williamson & Rogerson, 1983). Alternatively, an origin as a remnant of the continent rifted during the opening of the Coral Sea has been considered by some workers. Scattered Tertiary mafic porphyritic intrusions throughout the islands are of unknown provenance.

Most of Woodlark Island is covered by Pleistocene coralline limestone which surrounds a 12km wide 'basement' horst block. The block consists of Eocene age, ocean floor low-K basalts and volcanoclastics of the Lolui Volcanics, overlain by Miocene Wonai Hill Beds (16.5-13 Ma; Smith & Milsom, 1984), volcanic rocks and high-K co-magmatic porphyritic intrusions (Joseph & Finlayson, 1991).

The Trobriand Islands are comprised of Pleistocene to Recent coral atolls. This also includes a number of smaller islands within the Trobriand or Kiriwina Group.

Cretaceous to late Palaeozoic layered and domed gneiss, schist, mylonite and amphibolite, which in most cases are overthrust by unmetamorphosed ultramafics, form basement rocks to the islands of the D'Entrecasteaux Group. These units are intruded by Pliocene to Holocene granodiorite on Fergusson Island, resulting in doming and unroofing possibly in association with the Woodlark Rift spreading centre (Figs. 3 & 5). The calc-alkaline to andesitic island arc intrusive rocks emplaced into the

detachment faults date the core complex activity at 1.2-0.4 Ma on Fergusson Island (Chapple & Ibil, 1997) and 3.2 Ma on Normanby Island (Hill, 1990).

Solomon Sea Plate

On the northern side of the Papuan Islands, the Solomon Sea Plate (Figs. 3 & 5), a remnant sliver of Cretaceous oceanic crust, is constrained between the New Britain Trench subduction zone on the north side, and the more poorly defined south dipping inactive Trobriand Trough to the south. The Solomon Sea Plate is being actively consumed along the New Britain Trench and is regarded as an important influence on Pliocene island arc magmatism within the islands. The South Bismarck Plate lies to the north of the trench (Tregoning et al., 1999).

New Britain Trench

The New Britain Trench (Figs. 2-3, 5) is the deepest trench in the PNG region. It developed in the Pliocene in response to active subduction of the Solomon Sea Plate beneath New Britain. The trench may have been initiated and developed due to jamming of the Kilinailau Trench by the Ontong Java Plateau in mid-Miocene. Both the north dipping New Britain Trench and the southwest dipping trench at the edge of the Australian Craton consume oceanic crust of the Solomon Sea Plate.

Figure 5 shows the boundaries of micro-plates, subduction zones, spreading centres and active volcanoes in the PNG region. The recent volcanoes are mostly related to subduction (Bismarck Volcanic Arc and Papuan Peninsula) and fold-thrust deformation (Papuan Fold Belt).

New Guinea Islands Terrane

This terrane comprises island arcs (Melanesian Arc) (Figs. 3 & 4) that have built up since the Eocene in the hanging wall of the southwest dipping Kilinailau Trench, due to subduction related island arc magmatism. The originally linear island arc chain includes Manus, New Britain, New Hanover, New Ireland, Bougainville, and then on through the Solomon Islands, Vanuatu and Fiji along the Pacific Plate margin. The cessation of magmatism as the subduction zone zipped closed during the Miocene resulted in deposition of extensive limestone on the emerging volcanic edifices. This was overprinted by younger magmatism on New Britain and Bougainville, while the volcanism on the Tabar-Feni chain is viewed as a separate entity (see below).

Manus Island, at 100km long, is the largest of the Admiralty Islands Group in the far north of PNG. Interpreted oceanic basement is overlain by Eocene to Mid-Miocene (47-20 Ma) island arc andesite, basaltic agglomerate, tuffs and breccias up to 2000m thick that cover most of the island (Jaques, 1980). Cessation of the magmatism saw Early to Mid-Miocene bioclastic limestone deposited at the fringes of the volcanic edifice grading to Late Miocene marginal volcanic then calcareous sediments. The Yirri Intrusive Complex represents a later event, comprising multiphased quartz diorite to quartz monzonite intrusions extending from 17.6 Ma to 15.0 Ma (Jaques, 1980).

New Britain is typical of the other Melanesian Island arcs and comprises a thick basal sequence of Late Eocene basaltic to andesitic lava, breccia and associated sediments that are overlain by Oligocene island arc volcanic rocks and 30-22 Ma co-magmatic intrusions (Ryburn, 1975; 1976). The hiatus in volcanism in the Miocene is represented by extensive, locally thick shelf limestone with karst topography, which is in turn overlain by Pliocene volcanoclastic sedimentary rocks.

Bougainville and Buka Islands are geologically similar to other islands of Melanesian arc magmatism (Hilyard & Rogerson, 1989). Much of the Eocene-Oligocene submarine basaltic to andesitic volcanism and associated sediments are overlain by Miocene neritic limestone grading to Pliocene sediments, containing conglomerates indicative of active syn-deformational faulting. On Bougainville, Late Miocene to Pliocene intrusives host the Panguna porphyry Cu-Au mineralisation. Several latest Pliocene and Quaternary andesitic stratovolcano complexes overlie the older rocks and locally interfinger with shallow water marine sediments.

Renewed magmatism in the Pliocene, within the New Guinea Islands terrane, resulted in development of volcanic edifices as two separate chains and also overprinted existing island arcs. One arc extends for 1000km from close to the north coast of PNG, eastward as the Schouten Islands Group (Manam, Karkar, Bagabag, Long and Umboi or Rooke Islands), and then along the north coast of New Britain as the Mt Andewa and Mt Schrader stratovolcanoes to the Willaumez Peninsula, Mt Pago and Mt Uluwan, through into the recently active volcanism at Rabaul (East New Britain) and then southwards through Bougainville (Fig. 5). Many of these volcanoes remain active. Mt Andewa and Mt Schrader have collapsed northwards in a Mt St Helens style event.

The second arc is represented by the 250km long NW-trending Tabar-Lihir-Tanga-Feni island chain of Pliocene to Recent volcanoes that lies offshore to the northeast of New Ireland, possibly exploiting an earlier crustal discontinuity. Individual islands (Lihir) and island groups (Tabar) display a north-south elongation. The arc is inferred to have been derived from magmatism associated with subduction of the Solomon Sea Plate into the New Britain Trench, under New Britain and New Ireland (Lindley, 1988; Shatwell, 1987). Many workers have discussed the relationship between shoshonitic magmatism and gold mineralisation on these islands (Heming, 1979; Wallace et al., 1983; Moyle et al., 1990).

Kilinailau Trench

The Kilinailau Trench (Figs. 2 & 3) developed as a Paleogene, south dipping intra-plate subduction zone limiting the oceanic Pacific Plate to the northeast from its dismembered margin in which the Melanesian Arc formed by island arc magmatism. The trench was the locus of Pacific Plate subduction below the Australian Craton from the Paleocene, but became jammed by a thick segment of oceanic plate, the Ontong Java Plateau, and ceased to be inactive by the Middle Miocene (Bruns et al., 1989).

In response to jamming of the Kilinailau Trench, it is thought that a southeast dipping subduction zone developed at the Trobriand Trench located well to the south west of the Solomon Sea Plate, close to the strike continuation of the trench lying north of the Maramuni Arc (Rogerson et al., 1987a, b). The Trobriand Trench system failed in the Middle Miocene and northward directed subduction was initiated along a new northward-dipping New Britain Trench, south of New Britain, and extending towards the Solomon Islands.

Bismarck Sea Plates

The Bismarck Sea Plates (Figs. 3 & 5) contain the New Britain Island Arc formed in the hanging wall to the New Britain Trench, and also the Manus Basin back arc style spreading centres. These spreading centres are separated by a series of northwest-trending transform faults, one of which continues onshore on the north-eastern tip of New Britain at the Gazelle Peninsula (Fig. 5). The North and South Bismarck Plates are separated by a series of transform and strikeslip faults that trend east-west, from New Ireland through to the Manus spreading centre and onto mainland PNG (Fig. 5).

4.0 GEOLOGICAL EVOLUTION

Figure 6 shows the history of accretion of terranes. Without taking into account the Palaeozoic Australian Craton that underlies most of mainland PNG, the rest of the material that make up the geology of PNG are of Late Cretaceous age or younger.

Beginning in the Late Cretaceous, the Irian Jaya (now West Papua) volcanic arc collided with the continent (Fig. 6a). This has resulted in emplacement of major ophiolites. Sometime later, in Paleocene, the East Papua volcanic arc collided with the Owen Stanley terrane (Fig. 6b).

The Coral Sea opened in the Paleocene. The Kami and Uyaknji small ocean basins may have opened at the same time, as a northwesterly extension of the Coral Sea (Davies et al., 1997). Also in the Paleocene, the East Papua composite terrane (EPCT) formed by collision of the East Papua volcanic

arc and the Owen Stanley terrane. The Border terrane (Davies et al., 1997) (Fig. 6b) may have been sutured to the Craton at this time or may be a salient of the Australian Craton.

In the Eocene saw the development of the Sepik (Salumei) volcanic arc due to north-dipping subduction zone (Fig. 6c). Other developments during this time included an early Eocene Kami event, the approach of East Papua composite terrane, and the Eocene-Oligocene Ombura Formation in a foredeep environment. The Uyaknji small ocean basin closed in the Late Paleocene or Early Eocene and the Schrader, Marum, Jimi, Bena Bena, Kubor and Pale terranes were sutured to the Craton. The Sepik volcanic arc was active in the Middle Eocene (Davies et al., 1997) (Fig. 6c).

The Salumei volcanic arc collided with the continent in the Late Eocene and Oligocene to form the Sepik terrane (Davies, 1983). The Uyaknji small ocean basin closed and the EPCT was accreted to the Craton after collision, towards the end of the Oligocene (Davies et al., 1997). The Finisterre volcanic arc developed in the mid-Oligocene (Fig. 6d).

The Finisterre arc collided with the Craton in the Early Miocene (Fig. 6e). Evidence for this is from the unconformity observed in the rock record. The Ramu-Markham Basin developed in the foreland as collision progressed. Magmatic activity within the Orogen (Maramuni volcanic arc) may have been triggered by collision, rather than subduction.

The Bismarck volcanic arc collided with the Craton in the Pliocene (Fig. 6f), resulting in the development of thrust faults within the Finisterre terrane and in the foreland of the Australian Craton (Papuan Fold Belt) (Davies et al., 1997). Evidence for the Bismarck arc-continent collision is from seismic and seismicity data. Palaeomagnetic studies show that most or all terranes were rotated anti-clockwise during the Pliocene, presumably in response to east-west left-lateral strikeslip movements.

Present day overall configuration of PNG is a convergent margin (Fig. 6g), which developed since Late Cretaceous. The collision with the Bismarck volcanic arc continues and causes crustal shortening across the Orogen with active thrust faulting in the Finisterre Range, and the Papuan Fold Belt and the transpressional faulting in-between.

5.0 SEISMICITY

The plate tectonic setting in the PNG region has produced a complex seismicity pattern. This results from the continued oblique convergence of the Indo-Australian and Pacific Plates, which interact with micro-plates located within the region. The micro-plates are the Solomon Sea Plate (south), and North and Bismarck Plates (north) (Figs. 3 & 5). Most of the seismicity of the region occurs at the plate boundaries (Fig. 7).

Figure 7 shows the complex nature of seismicity in the region, and also the deepest earthquakes that occur in the New Britain Trench. The intense shallow seismicity occurs at plate boundaries. The New Britain Trench accommodates the deepest earthquakes.

The main concentration of seismicity is at the northern and northeastern margins of the Solomon Sea, where the Solomon Sea Plate subducts beneath the South Bismarck Plate and the Pacific Plate, respectively. Seismicity in this area has been described as the most intense in the world (Ripper & McCue, 1983; Cooper & Taylor, 1989). From this area the seismicity continues towards the southeast through the Solomon Islands, and towards the northwest under the northern part of mainland PNG and West Papua. The other main belts of seismicity in the PNG region are across the southern margin of the Solomon Sea, across the Bismarck Sea, and an arc north of Manus Island and New Ireland.

Most of the seismicity is at shallow depth, less than 40km, but there is significant deeper seismicity with some earthquakes at depths of about 600km. If one takes the 142°E meridian (Fig. 7) and follows from north to south, three main zones of seismicity can be recognised.

The shallow seismicity in the southern part represents activity in the Papuan Fold Belt on high-angle thrust faults. The intermediate seismicity in the central part reflects the presence of the westward

extension of the Solomon Sea Plate, now deeply buried beneath the Indo-Australian Plate (Ripper, 1980, 1982; Cooper & Taylor, 1987). The western part of the Solomon Sea Plate has an arch-like configuration resulting from subduction both to the north and to the south (Cooper & Taylor, 1987; Pegler et al., 1995). A remnant slab of subducted Solomon Sea lithosphere had been interpreted to continue westward beneath the Indo-Australian Plate margin and is the source of intermediate depth seismicity (100-150km) beneath the New Guinea Trench (Cooper & Taylor, 1987; Kawagle & Davies, 2001; Kawagle, 2005). Recent studies, using seismic tomography (Tregoning & Gorbatov, 2004) indicate that the seismicity from 143°E and extending west to 135°E relate to active and oblique subduction of the North Bismarck and Caroline plates beneath the New Guinea Trench.

The shallow and intermediate depth seismicity of the northern part results from oblique collision of the South Bismarck Plate with the Indo-Australian Plate. The transpressional nature of the collision is reflected in the intense high angle strikeslip and thrust faulting in the coastal areas of northern mainland New Guinea.

The northern part of the Solomon Sea and the northern part of the Bismarck Sea reflects seismicity at two plate boundaries. The zone of seismicity that dips northward beneath New Britain is a classical representation of subduction (Fig. 1). In this case the Solomon Sea Plate is subducting beneath the South Bismarck Plate. The Solomon Sea Plate supports seismicity at depths as great as about 600km. The main concentration of shallow seismicity under the Bismarck Sea reflects mainly strikeslip dynamics (and some normal fault activity) at the boundary between the South Bismarck and North Bismarck Plates.

The seismicity towards the east-southeast (eastern Solomon Sea to the Pacific Ocean), reflects the boundary between the Solomon Sea Plate and the Pacific Plate. The northeast dipping zone of seismicity signifies the subduction of the Solomon Plate beneath the Pacific Plate. There is an apparent discontinuity between the dipping zone of seismicity and the deep seismicity. Adjacent seismicity indicates that the Solomon Sea Plate is splintered and contorted at depth (Cooper & Taylor, 1989).

6.0 DISCUSSION

About half of the material that makes up PNG geology is allochthonous, and the other half autochthonous. Margins of the Orogen is composed either of accreted material of volcanic origin (volcanic arc) or oceanic crust (including obducted material). Elsewhere, the material is mostly composed of island arc volcanics.

The cessation of south-dipping subduction at the Kilinailau Trench, due to jamming of the trench by the Ontong Java Plateau, has initiated a north to northeast-dipping subduction at the New Britain Trench. At present the Solomon Sea Plate is doubly subducting beneath New Britain, New Ireland and Bougainville at the New Britain Trench. The South Bismarck Plate is subducting beneath the PNG mainland at the New Guinea Trench (Fig. 2). The Manus and Woodlark Basins are current active spreading centres.

Magmatism-related mineralisation in the PNG region is dominantly porphyry copper-gold and epithermal silver-gold styles. Volcanogenic massive sulphide, exhalative manganese and limestone are also present. Weathering of selected bedrock has resulted in the formation of lateritic nickel-cobalt-chromite and bauxite occurrences. In addition, erosion of hard rock deposits has generated placer deposits of gold, platinum, titaniferous magnetite and chromite.

While the porphyry Cu-Au deposits in PNG are broadly similar to examples of this mineralisation style in other magmatic arcs (e.g. western USA, Chile), the high gold content of PNG porphyry Cu-Au occurrences, relative to copper and molybdenum, is a characteristic typical of many southwest Pacific deposits and is consistent with the influence of oceanic crust.

Volcanogenic massive sulphide deposits hosting Cu, Pb, Zn, Au and Ag occur as stratiform lenses within volcanoclastic and volcanic rocks at Laloki near Port Moresby. Gold is currently being

deposited with sulphides in the black smokers offshore in the Manus Basin, the Woodlark Basin, and offshore from the Tanga-Feni-Lihir-Tabar Island chain.

As indicated in this overview, the geology of PNG is poorly understood, and models for tectonism and mineralisation should be treated as constantly evolving, especially concerning such aspects as the age of igneous rock formation and associated mineralisation. There is certainly no firm consensus among geoscientists on the geological evolution of PNG. For example, there is considerable disagreement among workers about the timing of the collision between the Australian continent and the island arc(s), ranging from Eocene in the Papuan Peninsula (Davies & Smith, 1974), to Oligocene-Early Miocene (Hall, 2002), and Mid-Miocene (Rogerson et al., 1987b), while several workers suggest a history of multiple collision events with varying docking times in different parts of PNG (Pigram & Davies, 1987; Davies et al., 1996).

The present day geological observations of interest in PNG include: transfer structures, ages of intrusions and rate of destruction of micro-plates, particularly, the Solomon Sea Plate.

Transfer structures occur as north-northeast trending lineaments (Fig. 8) and interpreted as deep crustal fractures possibly formed in association with Mesozoic cratonic margin rifting (Dekker et al., 1990). They display protracted histories of activity, localising Pliocene intrusions, mineralisation at Ok Tedi and Porgera (Corbett, 1994; Hill et al., 2002), and volcanoes such as Bosavi (Davies, 1991). The structures also segment the fold-thrust belt into portions, often with varying thrust events (Hill, 1991), and changes in orientation across the transfer structures.

The ages of intrusions on mainland PNG is another interest. The intrusion ages young from north to south, suggesting that PNG may be moving north over hot spots (Davies, 1991).

The Solomon Sea Plate is actively being consumed by the New Britain Trench in the north and subduction beneath the north-northeastern margin of the Australian Craton. The rate and amount of destruction of this oceanic crust is not known at present.

ACKNOWLEDGMENTS

This paper is a contribution from the Papua New Guinean participants on cruise KR10-05. We have been privileged to be part of this deep sea research cruise and are very grateful to the organisers and sponsors, principally the Japan Agency for Marine-Earth Science and Technology (JAMSTEC), who made everything possible to participate on R/V *Kairei* on its KR10-05 voyage. We are also grateful to the other participants for their support and hospitality while onboard as well as on the ground, particularly Dr Seiichi Miura, the onboard Chief Scientist. The technical crew, as well as the ship's crew under Captain Tanaka is greatly appreciated. We hope the joint participation in research involving deep ocean cruises in the Pacific waters such as this; will go a long way into the future.

REFERENCES

- Adshead, N.D., 1997. The setting and characteristics of the Umuna epithermal Au-Ag deposit, Misima Island, Papua New Guinea. In Hancock, G. (ed), Proceedings of the Geology, Exploration and Mining Conference, Madang, Papua New Guinea. Australasian Institute of Mining and Metallurgy, Parkville, 1-7.
- Benes, V., Scott, S.D. & Binns, R.A., 1994. Tectonics of rift propagation into a continental margin: Western Woodlark Basin, Papua New Guinea. *Journal of Geophysical Research* 99, 4439-4455.
- Bruns, T.R., Vedder, J.G. & Culotta, R.C., 1989. Structure and tectonics along the Kilinailau Trench, Bougainville-Buka Island region, Papua New Guinea. In Vedder, J.G. & Bruns, T.R. (eds), *Geology and offshore resources of Pacific Island arcs – Solomon Islands and Bougainville, Papua New Guinea region*. Circum Pacific Council for Energy and Mineral Resources, Earth Science Series 12, 93-123.

- Chapple, K.G. & Ibil, S., 1997. The Gasmeta gold deposit, Fergusson Island, Papua New Guinea. In Hancock, G. (ed), Proceedings of the Geology, Exploration and Mining Conference, Madang, Papua New Guinea. Australasian Institute of Mining and Metallurgy, Parkville, 29-37.
- Cooper, P. & Taylor, B., 1987. Seismotectonics of New Guinea: A model for arc reversal following arc-continental collision. *Tectonics* 6(1), 53-67.
- Cooper, P. & Taylor, B., 1989. Seismicity and focal mechanisms at the New Britain Trench related to deformation of the lithosphere. *Tectonophysics* 164, 25-40.
- Corbett, G.J., 1994. Regional structural control of selected Cu/Au occurrences in Papua New Guinea. In Rogerson, R. (ed), Proceedings of the Geology, Exploration and Mining Conference, Lae, Papua New Guinea. Australasian Institute of Mining and Metallurgy, Parkville, 57-70.
- Davies, H.L., 1982. Mianmin 1:250 000 geological map and explanatory notes, Sheet SB/54-3. Geological Survey of Papua New Guinea.
- Davies, H.L., 1983. Wabag 1:250 000 geological map and explanatory notes, Sheet SB/54-8. Geological Survey of Papua New Guinea.
- Davies, H.L., 1991. Tectonic setting of some mineral deposits in the Papua New Guinea region. In Rogerson, R. (ed), Proceedings of the Geology, Exploration and Mining Conference, Rabaul, Papua New Guinea. Australasian Institute of Mining and Metallurgy, Parkville, 49-57.
- Davies, H.L., 1992. Mineral and petroleum resources of Papua New Guinea, with notes on geology and history. Department of Geology, University of Papua New Guinea.
- Davies, H.L., 2009. Geology of New Guinea. Proceedings CD of the 2009 PNG Mining Conference, Port Moresby, Papua New Guinea. PNG Chamber of Mines and Petroleum.
- Davies, H.L., Perembo, R.C.B., Winn, R.D. & KenGemar, P., 1997. Terranes of the New Guinea Orogen. In Hancock, G. (ed), Proceedings of the Geology, Exploration and Mining Conference, Madang, Papua New Guinea. Australasian Institute of Mining and Metallurgy, Parkville, 61-66.
- Davies, H.L. & Smith, I.E., 1974. Tufi-Cape Nelson 1:1250 000 geological map and explanatory notes, Sheet SC/55-8,4. Bureau of Mineral Resources, Australia & Geological Survey of Papua New Guinea.
- Davies, H.L., Winn, R.D. & KenGemar, P., 1996. Evolution of the Papuan Basin – a view from the orogen. In Buchanan, P.G. (ed), Petroleum exploration, development and production in Papua New Guinea. Proceedings of the Third PNG Petroleum Convention, Port Moresby, Papua New Guinea. PNG Chamber of Mines and Petroleum, 53-62.
- Dekker, F., Balkwill, H., Slater, A., Herner, R. & Kampschuur, W., 1990. A structural interpretation of the onshore eastern Papuan Fold Belt, based on remote sensing and fieldwork. In Carman, G.J. & Z. (eds), Petroleum Exploration in Papua New Guinea: Proceedings of the First PNG Petroleum Convention, Port Moresby. PNG Chamber of Mines and Petroleum, 319-336.
- Denwer, K.P., Leach, T.M. & Mowat, B.A., 1995. Mineralisation of the Morobe Goldfield, Morobe Province, Papua New Guinea. In Proceedings of the Pacific Rim Congress 95, Auckland, New Zealand. Australasian Institute of Mining and Metallurgy, Carlton South, 181-186.
- Dow, D.B., 1977. A geological synthesis of Papua New Guinea. Bureau of Mineral Resources, Geology and Geophysics, Australia Bulletin 201.
- Findlay, R.H., 2003. Collision tectonics in northern Papua New Guinea: key field relationships in the Finisterre, Sarawaged and Adelbert Mountains and New Britain demand a new model. Geological

- Society of Australia Special Publication 22 & Geological Society of America Special Paper 372, 291-305.
- Findlay, R.H., Arumba, J., Kagl, J., Mosusu, N., Rangin, C. & Pubellier, M., 1997. Revision of the Markham 1:250 000 Sheet, Papua New Guinea: what is the Finisterre Terrane? In Hancock, G. (ed), Proceedings of the Geology, Exploration and Mining Conference, Madang, Papua New Guinea. Australasian Institute of Mining and Metallurgy, Parkville, 87-97.
- Hall, R., 2002. Cenozoic geological and plate tectonic evolution of SE Asia and the SW Pacific: computer-based reconstructions, model and animations. *Journal of Asian Earth Sciences* 20, 353-431.
- Heming, R.F., 1979. Undersaturated lavas from Ambittle Island, Papua New Guinea. *Lithos* 12, 173-186.
- Hill, E.J., 1990. The nature of shear zones formed in Eastern Papua New Guinea. In Proceedings of the Pacific Rim Congress 90, Gold Coast, Queensland. Australasian Institute of Mining and Metallurgy, Parkville, 537-548.
- Hill, E.J., 1991. Structure of the Papuan Fold Belt, Papua New Guinea. *American Association of Petroleum Geologists Bulletin* 75, 857-872.
- Hill, K.C. & Hall, R., 2002. Mesozoic-Cenozoic evolution of Australia's New Guinea margin in a west Pacific context. *Geological Society of Australia Special Publication 22 & Geological Society of America Special Paper 372*, 265-290.
- Hill, K.C., Kenrick, R.D., Crowhurst, P.C. & Gow, P.A., 2002. Copper-gold mineralisation in New Guinea: tectonics, lineaments, thermochronology and structure. *Australian Journal of Earth Sciences* 49, 737-752.
- Hilyard, D. & Rogerson, R., 1989. Revised stratigraphy of Bougainville and Buka Islands, Papua New Guinea. In Vedder, J.G. & Burns, T.R. (eds), *Geology and offshore resources of Pacific Islands arcs – Solomon Islands and Bougainville, Papua New Guinea regions*. Circum Pacific Council for Energy and Mineral Resources, Earth Science Series 12, 87-92.
- Jaques, A.L., 1980. Admiralty Islands 1:250 000 geological map and explanatory notes, Sheets SA/55-10 and SA/55-11. Geological Survey of Papua New Guinea.
- Johnson, R.W. & Jacques, A.L., 1980. Continent-arc collision and reversal of arc polarity: new interpretations from a critical area. *Tectonophysics* 63, 111-124.
- Joseph, L.E. & Finlayson, E.J., 1991. A revised stratigraphy of Muyua (Woodlark Island). In Rogerson, R. (ed), Proceedings of the Geology, Exploration and Mining Conference, Rabaul, Papua New Guinea. Australasian Institute of Mining and Metallurgy, Parkville, 26-33.
- Kawagle, S.A., 2005. The remnant subducted slab of Solomon Sea lithosphere west of the 142°E longitude. Proceedings CD-ROM of the Geology, Exploration and Mining Conference, Lae, Papua New Guinea. PNG Chamber of Mines and Petroleum, Port Moresby & Australasian Institute of Mining and Metallurgy, Parkville.
- Kawagle, S.A. & Davies, H.L., 2001. Seismicity south of the New Guinea Trench. In Hancock, G. (ed), Proceedings of the Geology, Exploration and Mining Conference, Port Moresby, Papua New Guinea. Australasian Institute of Mining and Metallurgy, Parkville, 189-195.
- Lindley, I.D., 1988. Early Cainozoic stratigraphy and structure of the Gazelle Peninsula, East New Britain: an example of extensional tectonics in the New Britain arc-trench complex. *Australian Journal of Earth Sciences* 35, 231-244.

- Milsom, J., Findlay, R. & Kopi, G., 2001. Early nappe deformation in arc-continent collision: gravity evidence from the Huon Peninsula, Papua New Guinea. In Hancock, G. (ed), Proceedings of the Geology, Exploration and Mining Conference, Port Moresby, Papua New Guinea. Australasian Institute of Mining and Metallurgy, Parkville, 275-280.
- Moyle, A.J., Doyle, B.J., Hoogvliet, H. & Ware, A.R., 1990. The Lodalam gold deposit, Lihir Island, Papua New Guinea. In Hughes, F.E. (ed), Geology of the mineral deposits of Australia and Papua New Guinea. Australasian Institute of Mining and Metallurgy Monograph Series 14, 1793-1805.
- Pegler, G., Das, S. & Woodhouse, J.H., 1995. A seismological study of the eastern New Guinea and western Solomon Sea regions and its tectonic implications. *Geophysical Journal International* 122, 961-981.
- Pieters, P.E., 1978. Port Moresby-Kalo-Aroa, Papua New Guinea 1:250 000 Geological Series. Bureau of Mineral Resources, Geology and Geophysics, Australia Record 1979/19.
- Pigram, C.J. & Davies, H.L., 1987. Terranes and the accretion history of the New Guinea orogen. *BMR Journal of Australian Geology and Geophysics* 10(3), 193-212.
- Ripper, I.D., 1980. Seismicity, earthquake focal mechanisms and tectonics of the Indo-Australian /Solomon Sea plate boundary. Geological Survey of Papua New Guinea Report 80/15.
- Ripper, I.D., 1982. Seismicity of the Indo-Australia/Solomon Sea Plate boundary in the Southeast Papua region. *Tectonophysics* 87, 355-369.
- Ripper, I.D. & McCue, K.F., 1983. The seismic zone of the Papuan Fold Belt. *BMR Journal of Australian Geology and Geophysics* 8, 147-156.
- Rogerson, R. & Francis, G., 1983. Owen Stanley metamorphic complex type of initial prograde metamorphism. *Science in New Guinea* 10, 60-64.
- Rogerson, R., Hilyard, D.B., Francis, G. & Finlayson, E.J., 1987a. The foreland thrust belt of Papua New Guinea. In Proceedings of the Pacific Rim Congress 87, Gold Coast, Australia. Australasian Institute of Mining and Metallurgy, Parkville, 579-583.
- Rogerson, R., Hilyard, D.B., Finlayson, E.J., Holland, D.J., Nion, S.T.S., Sumaiang, R.M., Duguman, J. & Loxton, C.D.C., 1987b. The geology and mineral resources of the Sepik headwaters region, Papua New Guinea. Geological Survey of Papua New Guinea Memoir 12.
- Ryburn, R.J., 1975. Talasea-Gasmata, New Britain 1:250 000 Geological Series Explanatory Notes, Sheets SB/56-5 and SB/56-9. Bureau of Mineral Resources, Geology and Geophysics, Australia & Geological Survey of Papua New Guinea.
- Ryburn, R.J., 1976. Cape Raoult-Arawe 1:250 000 Geological Series Explanatory Notes, Sheets SB/55-8 and SB/55-12. Bureau of Mineral Resources, Geology and Geophysics, Australia & Geological Survey of Papua New Guinea.
- Shatwell, D., 1987. Epithermal gold mineralisation and Late Cenozoic magmatism in the Melanesian outer arc. In Proceedings of Pacific Rim Congress 87, Gold Coast, Queensland. Australasian Institute of Mining and Metallurgy, Parkville, 393-398.
- Smith, R.I., 1990. Tertiary plate tectonic setting and evolution of Papua New Guinea. In Carman, G.J. & Z. (eds), Petroleum exploration in Papua New Guinea: Proceedings of the First PNG Petroleum Convention, Port Moresby. PNG Chamber of Mines and Petroleum, 229-244.

Smith, I.E. & Milsom, J.S., 1984. Late Cenozoic volcanism and extension, eastern Papua. In Kokelaar, B.P. & Howell, M.F. (eds), *Marginal basin geology*. Geological Society of London Special Publication 16, 163-171.

Struckmeyer, H.I.M., Yeung, M. & Pigram, C.J., 1993. Mesozoic-Cainozoic plate tectonic and palaeogeographic evolution of the New Guinea region. In Carman, G.J. & Z. (eds), *Petroleum exploration and development in Papua New Guinea: Proceedings of the Second PNG Petroleum Convention, Port Moresby*. PNG Chamber of Mines and Petroleum, 261-290.

Taylor, B., Goodliffe, A.M. & Martinez, F., 1999. How continents break up: insights from Papua New Guinea. *Journal of Geophysical Research* 104, 1497-1512.

Tregoning, P. & Gorbato, A., 2004. Evidence for active subduction at the New Guinea Trench. *Geophysical Research Letters* 31, L13608, doi:10.1029/2004GL020190.

Tregoning, P., Russell, J.L., McQueen, H., Lambeck, K., Stevens, C., Little, R.P., Curley, R. & Rosa, R., 1999. Motion of the South Bismarck Plate, Papua New Guinea. *Geophysical Research Letters* 26, 3517-3520.

Tregoning, P., McQueen, H., Lambeck, K., Jackson, R., Little, R.P., Saunders, S. & Rosa, R., 2000. Motion of the South Bismarck Plate, Papua New Guinea. *Earth Planets Space* 52, 727-730.

Wallace, D.A., Johnson, R.W., Chappell, B.W., Arculus, R., Perfit, M.R. & Crick, I.H., 1983. Cainozoic volcanism of the Tabar, Lihir, Tanga and Feni Islands, Papua New Guinea: geology whole-rock analyses, and rock forming mineral compositions. Bureau of Mineral Resources, Geology and Geophysics, Australia Report 243.

Williamson, A. & Hancock, G., (eds), 2005. *The geology and mineral potential of Papua New Guinea*. Papua New Guinea Department of Mining, 152p.

Williamson, A. & Rogerson, R., 1983. Geology and mineralisation of Misima Island, Papua New Guinea. Geological Survey of Papua New Guinea Report 83/12.

FIGURES

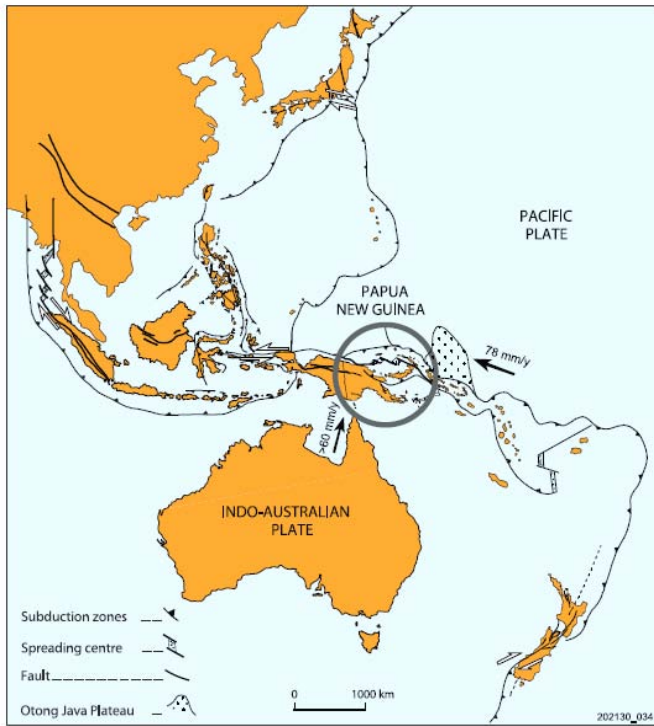


Figure 1. PNG, its position in the Pacific ‘Rim of Fire’ (after Williamson & Hancock, 2005). Arrows indicate rate of movement and direction of the Indo-Australian and Pacific Plates.

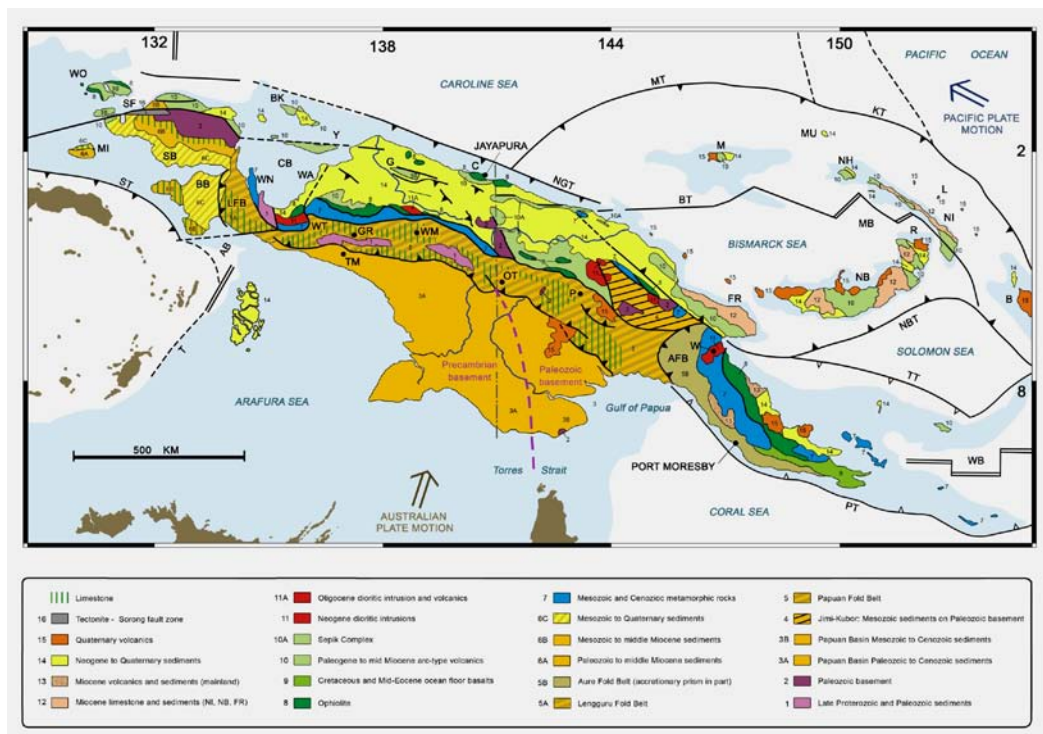


Figure 2. Geology of the New Guinea region (after Davies, 2009). Abbreviations for the PNG section. NGT New Guinea Trench, BT Bismarck Transform, MT Manus Trench, KT Kilinailau Trench, M Manus Is, MB Manus Basin, MU Mussau Is, NH New Hanover, NI New Ireland, L Lihir mine, B Bougainville, NB New Britain, NBT New Britain Trench, TT Trobriand Trough, WB Woodlark Basin, PT Pocklington Trough, AFB Aure Fold Belt (Aure Deformation Zone), W Wafi prospect, FR Finisterre Range, P Porgera mine, OT Ok Tedi mine. The pink line separates the Pre-Cambrian basement (west) from the Palaeozoic basement (east).

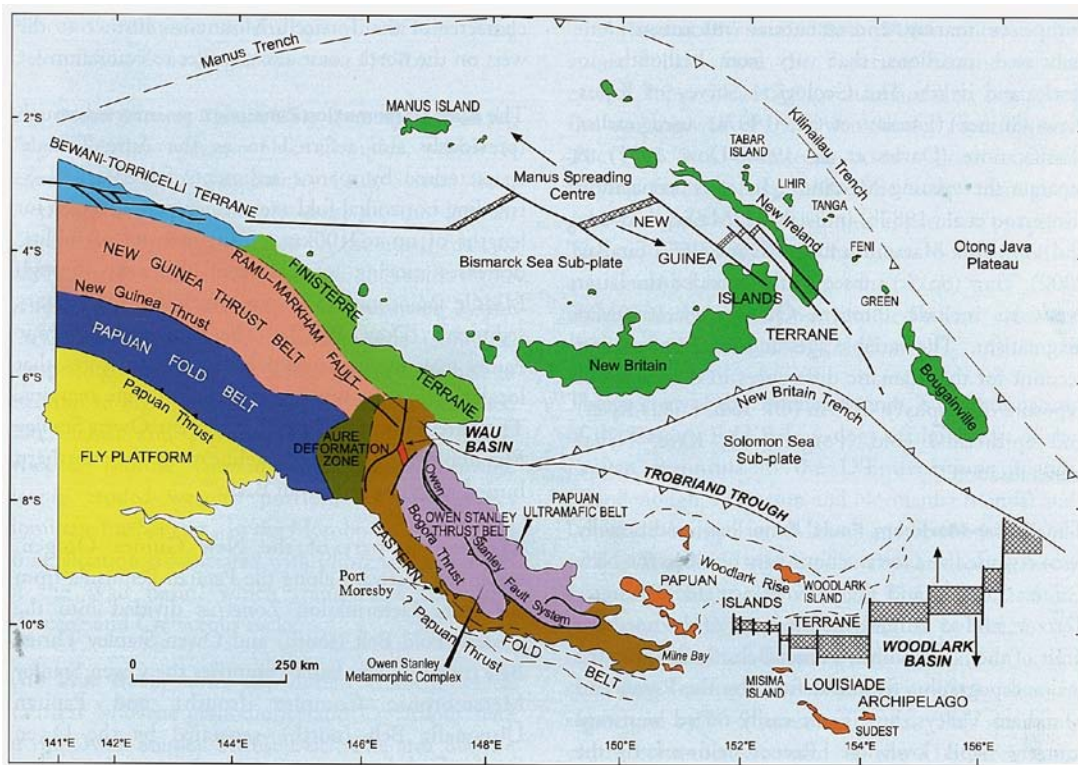


Figure 3. Geological framework of Papua New Guinea (after Williamson & Hancock, 2005).

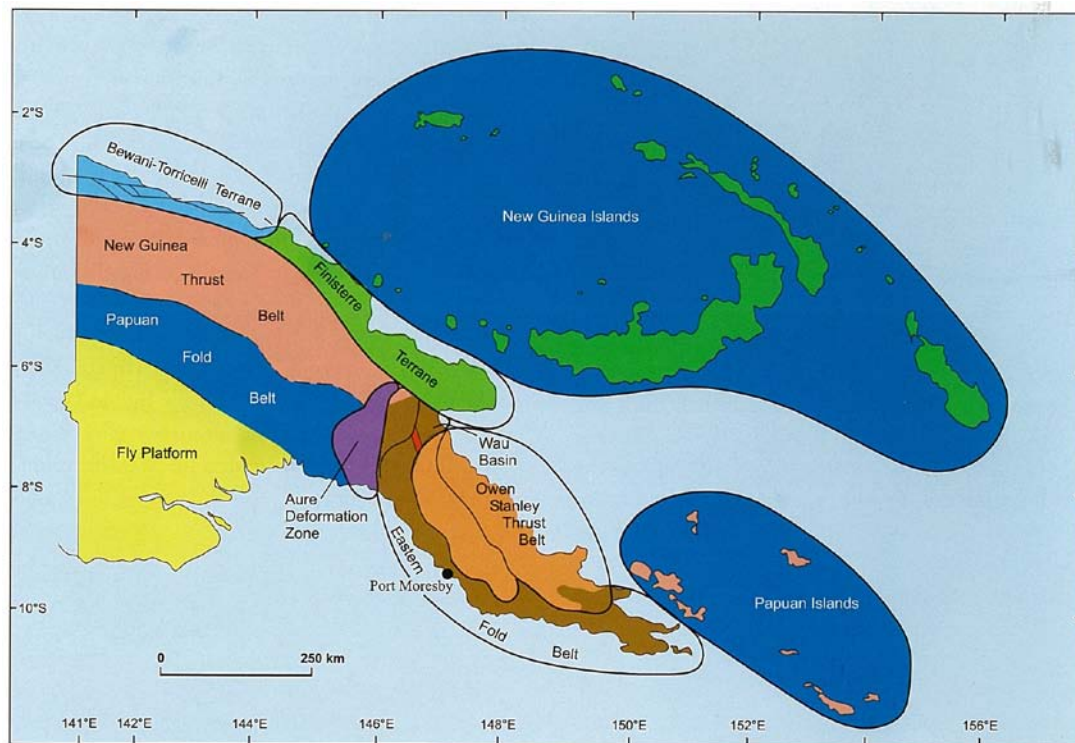


Figure 4. Geological terranes of Papua New Guinea (after Williamson & Hancock, 2005).

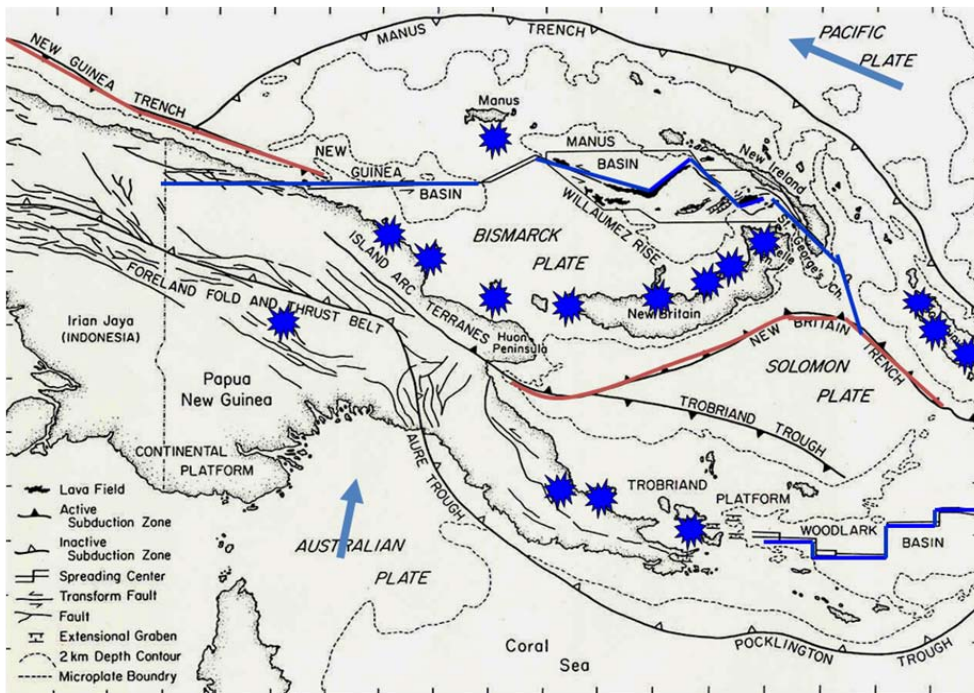
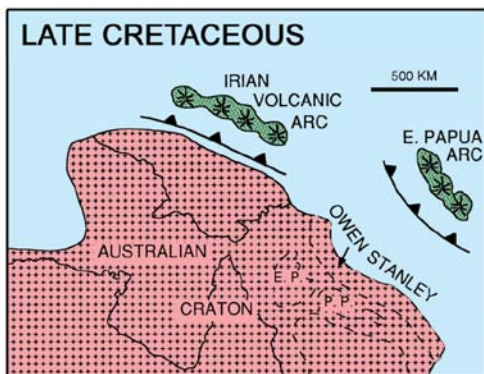
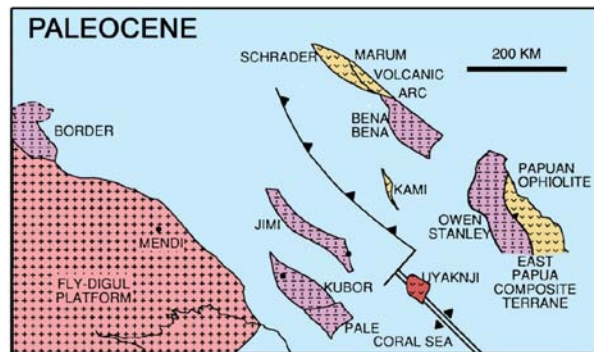


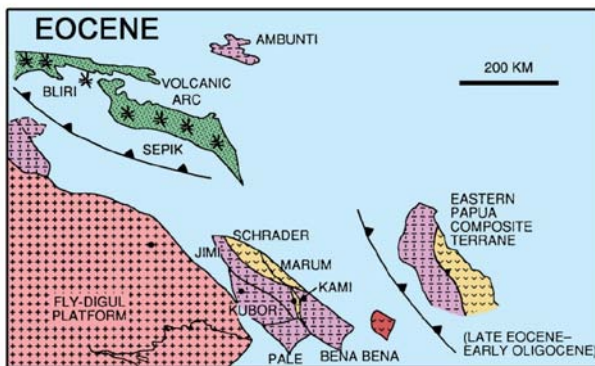
Figure 5. Micro-plates, subduction zones and active volcanoes in the PNG region (after Davies, 2009). Stars show recent volcanoes. Arrows indicate direction of major plate motion. Blue lines indicate strikeslip and transform fault systems.



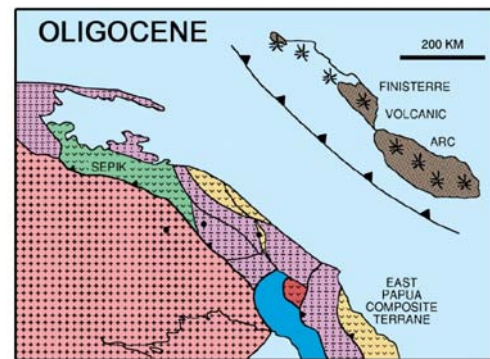
(a)



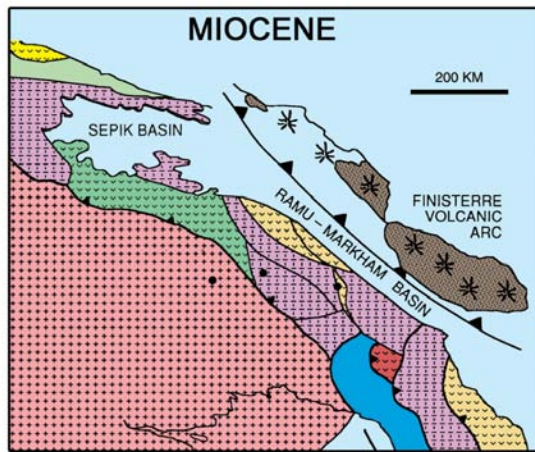
(b)



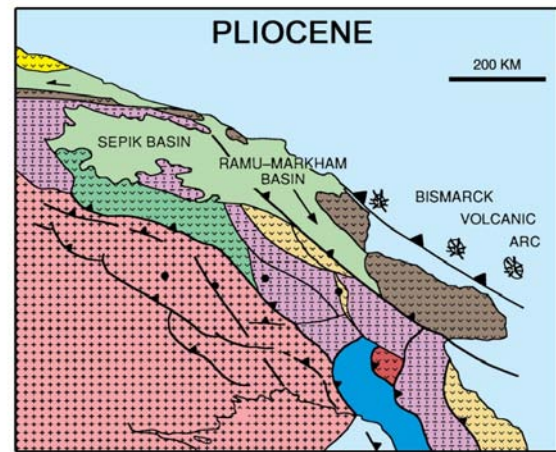
(c)



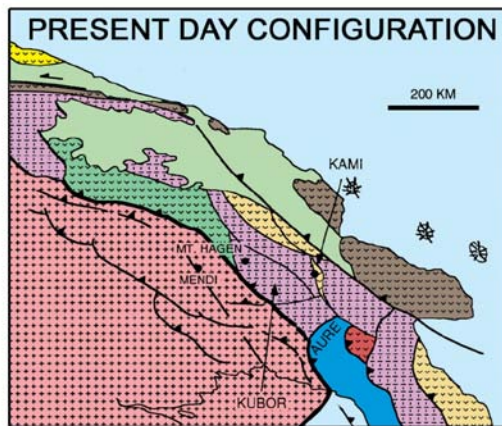
(d)



(e)



(f)



(g)

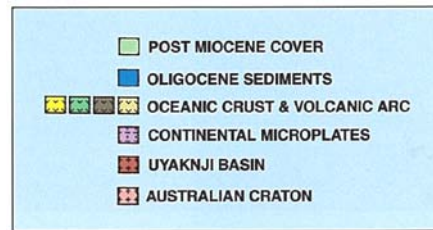


Figure 6. History of accretion of terranes. (a) Late Cretaceous, 68-61 Ma; (b) Paleocene, 66-55 Ma; (c) Eocene, 55-34 Ma; (d) Oligocene, 34-23.8 Ma; (e) Miocene, 23.8-5.5 Ma; (f) Pliocene, 5.5-2.0 Ma; (g) Present day configuration, 2.0-0.0 Ma (after Williamson & Hancock, 2005; Davies, 2009).

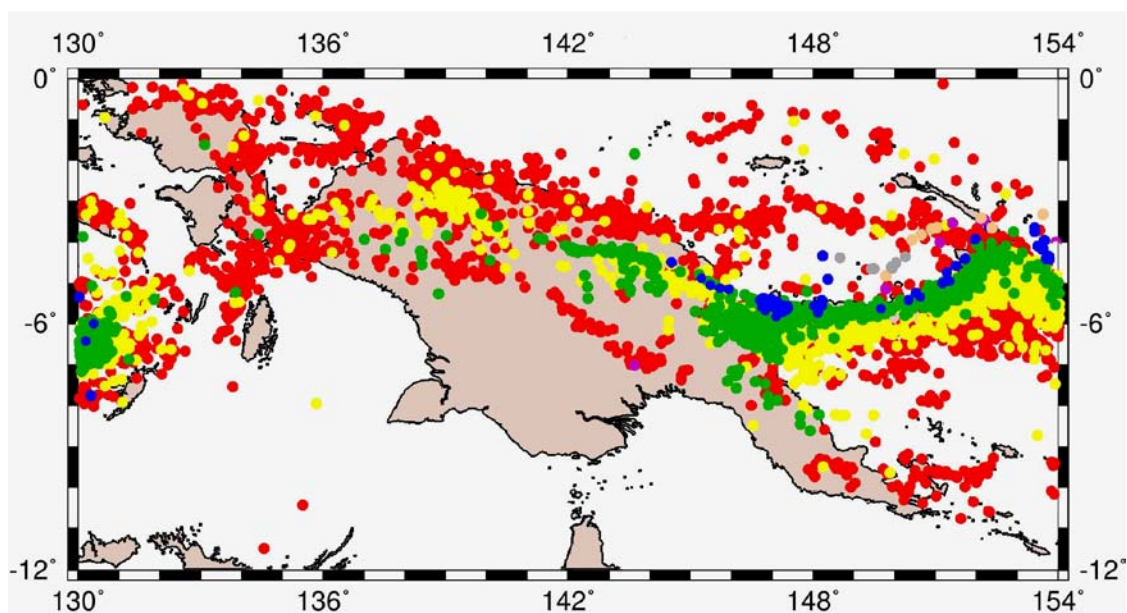


Figure 7. Seismicity map of the New Guinea region showing earthquakes with M5, 1963-2004 (after Davies, 2009). Red - crustal level depth (<50km); yellow/green - intermediate depth (<300km); blue - deep earthquakes (>300km).

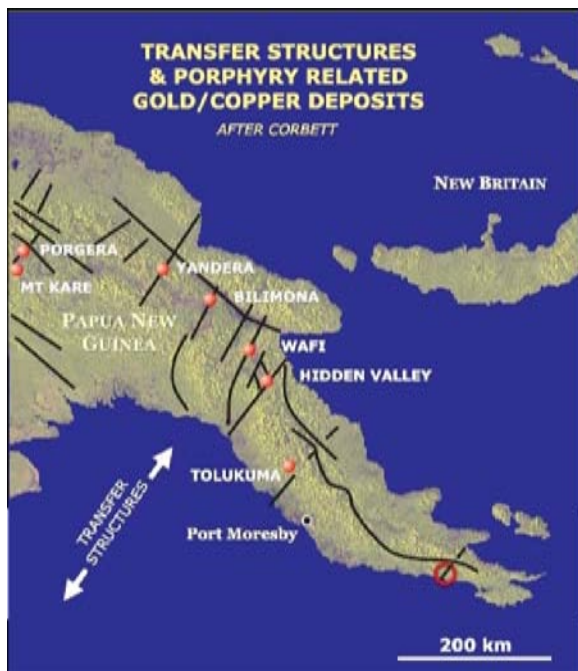


Figure 8. Transfer structures and porphyry related gold-copper deposits on mainland PNG (after Corbett, 1994).